Microplastic and nanoplastic analysis in drinking water and indoor air with Raman micro-spectroscopy

Maurizi, Luca

DOI (link to publication from Publisher):
10.54337/aau617106604

Publication date:
2023

Document Version
Publisher's PDF, also known as Version of record

MICROPLASTIC AND NANOPLASTIC ANALYSIS IN DRINKING WATER AND INDOOR AIR WITH RAMAN MICRO-SPECTROSCOPY

BY
LUCA MAURIZI

DISSERTATION SUBMITTED 2023

AALBORG UNIVERSITY
DENMARK

Microplastic and nanoplastic analysis in drinking water and indoor air with Raman micro-spectroscopy

Ph.D. Dissertation

Luca Maurizi

AALBORG UNIVERSITY
DENMARK

Dissertation submitted July, 2023

Dissertation submitted: September 2023

PhD supervisors: Associate Professor Asbjørn Haaning Nielsen
Aalborg University

Professor Jes Vollertsen
Aalborg University

PhD committee: Associate Professor Morten Lykkegaard Christensen
Aalborg University, Denmark (chair)

Researcher Stefania Federici
University of Brescia, Italy

Assistant Professor Agnieszka Dąbrowska
University of Warsaw, Poland

PhD Series: Faculty of Engineering and Science, Aalborg University

Department: Department of the Build Environment

ISSN (online): 2446-1636
ISBN (online): 978-87-7573-623-2

Published by:
Aalborg University Press
Kroghstræde 3
DK – 9220 Aalborg Ø
Phone: +45 99407140
aauf@forlag.aau.dk
forlag.aau.dk

Printed in Denmark by Stibo Complete, 2023

Af alle latterlige Ting forekommer det mig
at være det allerlatterligste at have travlt

(Of all ridiculous things, it seems to me
the most ridiculous to be busy)

S. Kierkegaard
Enten - Eller, "Diapsalmata", SKS bd. 2, s. 33 / SKS-E

Curriculum Vitæ

Luca Maurizi

Education

2020 - 2023	*PhD of Civil Engineering (H2020 ITN MONPLAS 860775)* Aalborg University (Denmark)
2017 - 2018	*Erasmus+ Internship* Aalborg University (Denmark)
2016 - 2018	*Master of Chemical Sciences for Clinical, Forensic and Sport Chemistry* University of Turin (Italy)
2013 - 2016	*Bachelor of Chemical Sciences for Industrial Chemistry* University of Rome "La Sapienza" (Italy)

Scientific dissemination

Conferences

15^{th} - 19^{th} May 2022
SETAC Europe 32nd Annual Meeting, Copenhagen (Denmark)
Micro Raman analysis of micro and nanoplastics in drinking water: from number to mass (Poster)

25^{th} - 28^{th} September 2022
3rd International Conference on Microplastic Pollution in the Mediterranean Sea (III µMed), Naples (Italy)
A comparison between FTIR microscopy and Raman microscopy applied to microplastic analysis in drinking water (Oral)

14^{th} - 18^{th} November 2022
MICRO 2022, online and Aalborg (Denmark)
Study and comparison of a new substrate compatible with µFTIR and µRaman (Oral, chair, and local node organization)

30^{th} April - 4^{th} May 2023
SETAC Europe 33rd Annual Meeting, Dublin (Ireland)
µRaman analysis of airborne indoor microplastics down to 1 µm - should facemasks be recommended? (Oral)

List of scientific papers

I. **L. Maurizi**, L. Iordachescu, I.V. Kirstein, A.H. Nielsen, J. Vollertsen, Do drinking water plants retain microplastics? An exploratory study using Raman micro-spectroscopy, Heliyon, 9, 6, e17113 (2023), https://doi.org/10.1016/j.heliyon.2023.e17113

II. **L. Maurizi**, L. Iordachescu, I.V. Kirstein, A.H. Nielsen, J. Vollertsen, It matters how we measure - Quantification of microplastics in drinking water by µFTIR and µRaman (under review)

III. **L. Maurizi**, L. Simon-Sánchez, A. Vianello, A.H. Nielsen, J. Vollertsen, Every breath you take: high concentration of breathable microplastics in indoor environments (under review)

English abstract

In a report published in June 2022, the OECD (Organization for Economic Co-operation and Development) predicts that world plastic production will triple by 2060, increasing from the current 460 million tonnes to around 1321. Specifically, the developing countries in Asia and Africa will be the major contributors to this growth, which will also be reflected in greater anthropic environmental pressure at the level of the various ecosystems. However, over the past 80 years, the mass production and incorrect disposal of plastics have already led to the accumulation of two new pollutants in the environment, the microplastics (MPs) and nanoplastics (NPs).

By convention, MPs are defined as fragments of plastic material ranging from 1 µm to 5 mm in size, while NPs represent the size fraction smaller than 1 µm. They basically derive from the disintegration of plastic macro-objects in the environment, caused by the action of the UV radiation from the sunlight, meteorological phenomena, and mechanical friction against the surfaces. It follows, therefore, that the generation of MPs and NPs has to be ascribed to complex chemical-physical processes subject to a high number of environmental and extra-environmental variables. The plastic particles deliberately produced and used in numerous cosmetic and personal hygiene products (e.g. toothpastes) for their exfoliating function also fall into the MP and NP categories. It should also be considered that, once introduced into the environment, MPs and NPs undergo a progressive aging and bio-compatibility process which renders them chemically different from the original polymer. Finally, MPs and NPs themselves can act as vectors for other micropollutants (e.g. PCBs and heavy metals) and pathogens such as bacteria and viruses. These peculiarities make MPs, and even more so NPs, complex analytes to treat on a theoretical and practical level, which translates to the current absence of standard operational definitions and shared analysis protocols.

The present PhD study focuses on analytical methods capable of providing new scientific knowledge about the presence of MPs and NPs in two environmental matrices vital for human survival: drinking water and air. The aim of the research is thus twofold: on the one hand, to study if the current

technical solutions for the treatment of drinking water are effective against MPs down to 1 µm and to what extent human activity contributes to indoor airborne MP pollution ; on the other hand, to estimate the intake of MPs from these two matrices as a consequence of contact with humans.

The MP filtration efficiency of a drinking water treatment plant was studied over a five-day period by comparing the MP concentration at the inlet with that at the outlet. The chosen plant is located in Denmark and is fed by an aquifer at a depth of about 90 m; the raw water is treated only with sand filtration, as commonly happens in the rest of the country. The water is pumped through poly-ethylene (PE) pipes inside the structure and, after filtration, it remains for a few hours in two storage tanks before being sent to the users. For each sample, about 1 m^3 of water was filtered through 1 µm sintered steel filters by means of a device built at the Department of The Built Environment of Aalborg University. It consists of four "arms", each terminating with a filter holder, which is in turn connected to a flowmeter. After a mild pre-treatment aimed at concentrating the particles retained on the filter in a pre-filtered alcoholic matrix, the samples were first analyzed by Raman micro-spectroscopy (µRaman) and then by Fourier-Transform IR micro-spectroscopy (µFTIR).
The µRaman analysis was carried out quantitatively down to 1 µm and the MPs were quantified according to the MP counts and estimated mass. Hence it could be shown that MPs up to 5 µm were released in the section between the inlet and outlet of the facility, with consequent enrichment of the treated water destined to the public network. Nonetheless, the mean counts concentration of MPs at the inlet (2.5 ± 2.0 counts/L) was lower than that of the outlet (1.4 ± 1.3 counts/L), although the efficiency of the plant proved to decrease with decreasing MP size. Furthermore, the fraction of NPs between 0.45 and 1 µm was qualitatively analysed, highlighting also in this case the presence of plastic particles. Overall, it was estimated that an average consumer could intake 1533 MPs/year from the studied drinking water.
The second study on µFTIR aimed at comparing this analytical technique with µRaman when applied to the analysis of MPs in drinking water. Approximately 96% of the MPs analyzed by µRaman were not detected by µFTIR as the rate of false negatives started increasing already below 50 µm, well above the nominal size limit of 6.6 µm. Furthermore, by combining the morphological frequency data of the two studies, it was found that the MP frequency in the analysed water samples decreases with increasing MP length according to a third-power function. Consequently, the counts average concentrations of MPs obtained with the µFTIR data were significantly lower than those of the µRaman study (inlet 31.9 ± 17.2 counts/m^3, outlet 5.0 ± 2.1 counts/m^3), although they were in line with previous works employing µFTIR. This investigation, in addition to proposing for the first time a quan-

titative comparison between the two most used spectroscopic techniques for the analysis of MPs in drinking water, also highlighted how the estimates of human exposure to MPs depend on the analytical technique used, which necessarily provides only a partial photograph of a larger picture. Hence the estimation of human MP intake from the µFTIR data was approximately 5 MPs/year, 332 times lower than the result from the µRaman analysis. In both studies, the MP concentration was also quantified as mass per volume of water by applying an ellipsoidal shape factor to the analysed particles. Therefore, it was possible to determine the efficiency of the plant by applying the mass conservation law, which takes into account possible breaking processes of the MPs in the inlet-outlet section.

The third study focuses on MP pollution in the atmosphere of two workplaces and two private apartments. The sampling system employed consisted of a vacuum pump with adjustable flow connected to a steel funnel, at the bottom of which is placed a silicon filter with 1 µm pores. The sampling events were carried out both during the working days and on weekends to account for the different level of human activity in the selected locations. Furthermore, each sample was taken in two sampling sessions - with and without a surgical facemask applied to the sampling system - to evaluate its efficiency in retaining airborne MPs. No pre-treatment of the sample was performed, in order to preserve the non-plastic particles and, at the same time, provide an analytical protocol potentially applicable to the environmental monitoring of indoor air. The µRaman analysis was directly carried out on the filters used during the sampling on particles down to 1 µm, by adopting a semi-randomized approach. Thus, it was also possible to quantify the fraction of MP below 10 µm, which seems to be able to overcome the clearance mechanisms of the upper airways and, if sized between 1 - 5 µm (breathable range), penetrate the cellular tissue. The MP concentration of the investigated locations (58 - 684 counts/m^3) was generally higher than that of previous works, which didn't consider the airborne MPs below 10 µm. Specifically, the value of MP concentration in the indoor environments depended on the level of human activity and the MP composition on the location (i.e. the *type* of human activity). Overall, the filtration efficiency of the surgical facemask was approximately 85% for the indoor airborne MPs, however for the 1 - 5 µm fraction it dropped to 57%. Hence the samples taken with the surgical facemask presented a higher fraction of 1 - 5 µm MPs than those taken without the facemask. Overall, approximately 3415 MPs/day on average may be intaken by a human in the investigated indoor locations, of which 1504 MPs/day between 1 - 5 µm. Wearing a surgical facemask like the one employed in the study may lower the total intake to around 283 MPs/day, of which 201 MPs/day (71%) in the range 1 - 5 µm. Due to the current lack of research on the toxicity of environmental airborne MPs in the breathable

range, the usage of further preventive measures to prevent the related human intake should be carefully evaluated.

Dansk resumé

I en rapport offentliggjort i juni 2022 forudsiger OECD (Organisationen for Økonomisk Samarbejde og Udvikling), at verdens plastproduktion vil tredobles i 2060 fra de nuværende 460 millioner tons til omkring 1321. I særdeleshed vil de udviklingslande i Asia og Afrika være de største bidragydere til denne vækst, der nødvendigvis også vil reflekteres sig i en større antropisk miljømæssigt pres på de forskellige økosystemer. Alligevel har plastiksmassproduktionen og den ukorrekt bortskaffels af plastik allerede bragt i de sidste 80 år til akkumuleringen af to nye forunende stoffer, de mikroplastiker (MPs) og nanoplastiker (NPs).

MPs defineres konventionelt som plastik stykker med størrelsen fra 1 µm til 5 mm, mens NPs repræsenterer den dimensionelle fraktion under 1 µm. De udleder primært fra opløsningen af plastik makro-objekter i miljøet, hvilket forårsages af lysstrålernes UV radiation, vejret, og mekanik aktionen på overfladerne. MP og NP oprettelse skal altså forårsages af nogle komplekse kemiske og fysiske processer, der kommer an på et højt tal af miljømæssige og ekstra-miljømæssige variabler. Der findes også i MP og NP kategori de plastik partikler, der bevidst produceres og bruges i mange kosmetikker og hygiejneprodukter på grund af deres eksfolierende funktion. Der skal også overvejes, efter at MPs og NPs indfører sig i miljøet, at de lider en gradvis ældnings- og biokompatibiliseringsproces, der gør dem kemisk anderledes end den originelle polymer. Til sidste kan MPs og NPs selv virke som vektorer til andre forunende stoffer (f.eks. PCBs og metaller) og patogener som virusser og bakterier. Disse karakteristikker gør MPs, og endnu mere NPs, analytter komplekse til at behandle på et teoretisk og praktisk niveau, hvilket oversættes i den nuværende mangel af standard definitioner og fælles analyseprotokoller.

Denne PhD fokuserer om analysemetoder, der kan udstyre en ny videnskabe omkring MPs and NPs tilstedeværelse i to miljømessige matricer vitale til menneskernes overlevelse: drikkevanden og luften. Så forskningens mål er dobbelt: på en side at bedømme, om de nuværende tekniske løsninger for drikkevandets behandling er effektive mod MPs indtil 1 µm, og i hvilket om-

fang bidrager menneskelig aktiviteten til indendørs luftbårne MP forureningen, på den anden side at estimere MP indtag fra disse to matricer som konsekvens af kontakten med mennesket.

Filtreringseffektiviteten mod MPs af et drikkevandsanlæg blev studeret i fem dage, og MP koncentration på indtægten blev sammenlignet med den på udgangen. Det vælge drikkevandsanlæg ligger i Danmark og næres med grundvanden i 90 m cirka dybde. Grundvandet behandles kun med sandfiltreringen, hvilket også er almindeligt i resten af landet. Vandet pumpes op gennem nogle røre af poly-ætylen (PE) i strukturen, og efter filtreringen forbliver den i to bassiner før at blive afsendt til husstande. For hver prøve blev 1 m^3 cirka vandet filtreret på et filter af sintret metal på 1 µm ved hjælp af et apparat bygget i det By, Byggeri, og Miljø Institut af Aalborg Universitet. Det består af fire "arme", og hver af dem afslutter med filterholderen, der forbindes til en flowmeter. Efter en mild behandling for at koncentrere partiklerne på filtrene i en pre-filtreret alkoholisk matrix, blev prøverne analyseret før med Raman mikroskopi (µRaman) og bagefter med Fourier-Transform IR mikroskopi (µFTIR).
µRaman analysen blev kvantitavt føregået indtil 1 µm, og MP blev kvantificeret ifølge de MP tæller og den estimerede masse. Derfor blev MP op til 5 µm frigjort i stregen mellem anlæggets indtægt og udgang med en følgende berigning af det behandlede vand bestemt til husstande. Ikke desto mindre blev MP gennemsnitlig nummerisk koncentration på indtægten (2.5 $\pm$ 2.0 counts/L) fundet lavere end den på udgangen (1.4 $\pm$ 1.3 counts/L), selvom anlæggets effektivitet formindskede for mindre MPs. Den NP fraktion fra 0.45 til 1 µm blev også kvalitativt analyseret, og tilstedeværelsen af plastik partikler blev fremhævet. Alt i alt blev det estimeret, at en gennemsnitsforbruger kunne indtage 1533 MP/år fra det undersøgte drikkevand.
Det andet studie med µFTIR havde som mål at sammenligne denne analyseteknik med µRaman, når de anvendes på MP analyse i drikkevandet. 96% cirka af MPs opdagede af µRaman blev ikke fundet af µFTIR, for antallet af falske negativer steg allerede under 50 µm, meget over den nominelle størrelsesgrænse af 6.6 µm. Desuden blev data af morfologisk frekvens fra de to studier forenet, og der blev fundet ud af, at MP frekvens i de analyserede vandeprøver aftager mod længden ifølge en power funktion. Som konsekvens er gennemsnitlige nummeriske koncentrationer, der blev fundet med µFTIR, meget lavere end de opnåede i det µRaman studie (indtægt 31.9 $\pm$ 17.2 counts/m^3, udgang 5.0 $\pm$ 2.1 counts/m^3), selvom i overensstemmelse med de andre studier brugende µFTIR. Denne undersøgelse, der foreslår for den første gang en kvalitativ sammenligning imellem de to mest brugte spektroskopiske tekniker for MP analyse i drikkevandet, fremhævede også, at estimaterne af menneskernes udsættelse for MPs kommer an på den valgte analyseteknik, der nødvendigvis kun giver en partiel billede af en bredre

ramme. Derfor var det menneskelige MP indtag fra μFTIR datene 5 MP/år cirka, 332 gange lavere end resultaten fra den μRaman analyse.
I begge studier blev MP koncentrationer også kvantificeret som masse ved hjælpen af en ellipsoidefaktor, der blev anvendt til de analyserede MPs. Det tillod også at bestemme anlæggets effektivitet med massefredningslovet, der overvejer mulige brudprocesser af MPs i stregen intægt-udgang.

Det tredje studie handler om MP forunening i atmosfæren af to arbejdspladser og to boliger. Det brugte prøveudtagningssystem består af en vakuumpumpe med et justebart flow forbundet til en tragt af stål, hvortil enden et filter af silicium på 1 μm ligger. Prøveudtagninger blev lavet både på arbejdsdage og i weekenden for at tage hensyn til det forskellige aktivitetsniveau i de valgte områder. Desuden blev hver prøve udtaget dobbelt: uden og med en kirurgisk mundbind anvendt til prøveudtagningssystemet for at vurdere dens effektivitet til at holde tilbage de luftbårne MPs. Der blev ikke lavet nogen prøvebehandling for at beskytte de ikke-plastik partikler og på den samme tid at udstyre en analyseprotokol for miljøovervågningen. Den μRaman analyse blev straks lavet på filtrene brugte for prøveudtagningen på pårtiklerne ned til 1 μm med en semi-randomiseret strategi. Så det var også muligt at kvantificere den MP fraktion under 10 μm, der synes at kunne overgå høje luftvejenes eliminationsmekanismer og, hvis mellem 1 - 5 μm (åndbar rækkevidde), trænge ind i cellevævet. Den MP koncentration (58 - 684 counts/m^3) var generalt højere på de undersøgte områder end i tidligere undersøgelser, der ikke overvejede de luftbårne MPs under 10 μm. I særdeleshed kom den MP koncentrations værdi i de indendørs områder an på graden af menneskelig aktiviteten og lokaliteten (dvs *slags* af menneskelig aktivitet). I alt var filtreringseffektiviteten til kirurgisk mundbinden 85% cirka for de indendørs luftbårne MPs, alligevel faldt den ned til 57% for den 1 - 5 μm fraktion. De prøver udtagne med den kirurgiske mundbind vist derfor en højere fraktion af de 1 - 5 μm MPs end de prøver udtagne uden mundbinden. Alt i alt kunne 3415 MP/dag cirka indtages af en person i de undersøgte indendørs områder, og 1504 MP/dag kunne være mellem 1 - 5 μm. At have en kirurgisk mundbind på som den brugte i studiet kunne reducere det totale indtag til 283 MP/dag cirka, og 201 MP/dag (71%) kunne være mellem 1 - 5 μm. På grund af den nuværende mangel af forskningen om giftigheden af de miljømæssige luftbårne MPs i den andbåre rækkevidde bør brugen af yderligere forebyggende forholdsregel for at forhindre menneskeligt indtaget vurderes forsigtigt.

Riassunto italiano

In una relazione pubblicata nel giugno 2022, l'OECD (Organizzazione per la Cooperazione e Sviluppo Economico) prospetta che la produzione mondiale di plastica triplicherá entro il 2060, passando dalle attuali 460 milioni di tonnellate a circa 1321. Nello specifico, saranno i Paesi in via di sviluppo in Asia e Africa i maggiori contributori a tale crescita, che si rifletterá necessariamente anche in una maggiore pressione ambientale antropica a livello dei diversi ecosistemi. Tuttavia, la produzione di massa e lo scorretto smaltimento della plastica ha già portato, nel corso degli ultimi 80 anni, all'accumulo nell'ambiente di due nuovi inquinanti, le microplastiche (MP) e nanoplastiche (NP).

Per convenzione, le MP sono definite come frammenti di natura plastica di dimensioni comprese tra 1 µm e 5 mm, mentre le NP rappresentano la frazione dimensionale inferiore a 1 µm. Esse derivano fondamentalmente dalla disgregazione di macro-oggetti in plastica nell'ambiente, causata dall'azione della radiazione UV dei raggi solari, dai fenomeni meteorologici e dall'azione meccanica contro le superfici; ne deriva, perciò, che la generazione di MP e NP è da ascrivere a complessi processi chimico-fisici soggetti a un elevato numero di variabili ambientali ed extra-ambientali. Rientrano nelle categorie di MP e NP anche le particelle di plastica deliberatamente prodotte e impiegate in numerosi prodotti cosmetici e per l'igiene personale (e.g. dentifrici) per la loro funzione esfoliante. Si consideri, inoltre, che una volta introdotte nell'ambiente, le MP e NP subiscono un progressivo processo di invecchiamento e bio-compatibilizzazione che le rende chimicamente diverse rispetto al polimero di partenza. Infine, le stesse MP e NP possono agire da vettori per altri microinquinanti (e.g. PCB e metalli pesanti) e agenti patogeni quali virus e batteri. Queste peculiarità rendono le MP, e a maggior ragione le NP, analiti complessi da trattare a livello teorico e pratico, il che si traduce nell'attuale assenza di definizioni operative standard e protocolli d'analisi condivisi.

Il presente studio di dottorato si focalizza su metodi analitici in grado di fornire nuove conoscenze scientifiche circa la presenza di MP e NP in due

matrici ambientali vitali per la sopravvivenza umana: l'acqua potabile e l'aria. Lo scopo della ricerca è così duplice: da un lato, studiare se le attuali soluzioni techniche per il trattamento dell'acqua potabile siano efficaci contro le MP fino a 1 µm e in che grado l'attività umana contribuisce all'inquinamento da MP nell'atmosfera di ambiente confinato; dall'altro, stimare l'assunzione di MP da queste due matrici quale conseguenza del contatto con l'uomo.

L'efficienza di filtrazione delle MP di un impianto di trattamento dell'acqua potabile è stata studiata per un periodo di cinque giorni, confrontando la concentrazione di MP in entrata con quella in uscita. L'impianto scelto è localizzato in Danimarca ed è alimentato da una falda acquifera a circa 90 m di profondità; l'acqua grezza viene sottosposta soltanto a filtrazione a sabbia, come comunemente accade nel resto del Paese. L'acqua viene pompata attraverso condutture di polietilene (PE) all'interno della struttura e, dopo la filtrazione, permane per alcune ore in due vasche di accumulo prima di essere spedita all'utenza. Per ogni campione, circa 1 m^3 d'acqua è stato filtrato su filtri in acciaio sinterizzato da 1 µm per mezzo di un dispositivo costruito nel Dipartimento di Ingegneria Civile di Aalborg. Esso consta di quattro "braccia", ciascuna terminante con l'alloggio per il filtro, che è a sua volta collegato con un flussimetro. Dopo un mite pretrattamento volto a concentrare le particelle trattenute sul filtro in una matrice alcolica pre-filtrata, i campioni sono stati analizzati dapprima tramite microscopia Raman (µRaman) e poi con microscopia IR a Trasformata di Fourier (µFTIR).
L'analisi al µRaman è stata condotta quantitativamente fino a 1 µm e le MP sono state quantificate in numero e massa. È stato così evidenziato il rilascio di MP fino a 5 µm nel tratto tra l'entrata e l'uscita dell'impianto, con conseguente arricchimento dell'acqua trattata destinata alla rete pubblica. Ciò nonostante, la concentrazione numerica media di MP in entrata (2.5 ± 2.0 counts/L) è risultata inferiore a quella in uscita (1.4 ± 1.3 counts/L), sebbene l'efficienza dell'impianto diminuisse al decrescere della dimensione delle MP. Inoltre, la frazione delle NP tra 0.45 e 1 µm è stata analizzata qualitativamente, evidenziando anche in questo caso la presenza di particelle di tipo plastico. Complessivamente, è stato stimato che un consumatore medio potrebbe assumere 1533 MP/anno dall'acqua potabile analizzata.
Il secondo studio al µFTIR ha invece avuto come obiettivo il confronto di questa tecnica analitica con il µRaman quando applicati all'analisi delle MP nell'acqua potabile. Circa il 96% delle MP analizzate dal µRaman non sono state identificate dal µFTIR in quanto il tasso di falsi negativi aumentava già al di sotto di 50 µm, ben al di sopra del limite nominale di risoluzione spaziale di 6.6 µm. Inoltre, unendo i dati di frequenza morfologica dei due studi, è stato appurato che la frequenza delle MP nei campioni d'acqua analizzati decresce con la lunghezza secondo una potenza di terzo grado. Per

conseguenza, le concentrazioni numeriche medie di MP ottenute con i dati µFTIR sono risultate fortemente inferiori a quelle dello studio con il µRaman (entrata 31.9 $\pm$ 17.2 counts/m^3, uscita 5.0 $\pm$ 2.1 counts/m^3), benché in linea con i lavori precedenti utilizzanti il µFTIR. Questa investigazione, oltre che proporre per la prima volta un confronto quantitativo tra le due tecniche spettroscopiche più utilizzate per l'analisi delle MP nelle acque potabili, ha anche evidenziato come le stime di esposizione umana alle MP siano dipendenti dalla tecnica analitica utilizzata, che necessariamente fornisce solo una fotografia parziale di un quadro più vasto. Perciò, la stima di assunzione umana delle MP dai dati µFTIR è stata circa 5 MP/anno, 332 volte più bassa del risultato dell'analisi µRaman.
In entrambi gli studi, la concentrazione delle MP è stata quantificata anche come massa applicando un fattore di forma ellissoidale alle particelle analizzate. Ciò ha permesso di determinare l'efficienza dell'impianto applicando anche la legge di conservazione di massa, che tiene conto di eventuali processi di rottura delle MP nel tratto entrata-uscita.

Il terzo studio verte sull'inquinamento da MP nell'atmosfera di due luoghi di lavoro e due abitazioni private. Il sistema di campionamento utilizzato consta di una pompa a vuoto a flusso regolabile collegata a un imbuto in acciaio, sul cui fondo è posto un filtro in silicio con pori da 1 µm. I campionamenti sono stati effettuati sia durante la settimana lavorativa che nei fine settimana per tenere conto del diverso livello di attività umana nelle sedi selezionate. Inoltre, ogni campione è stato preso in duplicato - con e senza una mascherina chirurgica applicata al sistema di campionamento - per valutare l'efficacia della stessa a trattenere le MP aeree. Non si è ricorsi ad alcun pre-trattamento del campione al fine di preservare anche le particelle non plastiche e, al tempo stesso, fornire un protocollo d'analisi potenzialmente applicabile a monitoraggi di aria in ambiente confinato. L'analisi al µRaman è stata condotta direttamente sui filtri utilizzati in fase di campionamento su particelle fino a 1 µm, adottando un approccio semi-randomizzato. È stato così possibile quantificare anche la frazione di MP al di sotto di 10 µm, che sembrano essere in grado di superare i meccanismi di eliminazione delle vie aeree superiori e, se comprese tra 1 - 5 µm (intervallo di respirabilità), penetrare nel tessuto cellulare. La concentrazione di MP negli ambienti investigati (58 - 684 counts/m^3) era generalmente maggiore che negli studi precedenti, i quali non avevano considerato le MP aeree al di sotto di 10 µm. Nello specifico, il valore della concentrazione delle MP negli ambienti interni è dipesa dal grado di attività umana e la composizione polimerica dal luogo (i.e. dal *tipo* di attività umana). Nel complesso, l'efficienza di filtrazione della mascherina chirurgica è stata circa 85% per le MP aeree, tuttavia per la frazione 1 - 5 µm calava a 57%. Quindi i campioni prelevati con la mascherina chirurgica presentavano una frazione più elevata di MP 1 - 5 µm rispetto a quelli

senza mascherina. Conseguentemente, circa 3415 MP/die potrebbere essere assunte in media da un soggetto negli ambienti studiati, di cui 1504 MP/die tra 1 - 5 µm. Indossare una mascherina chirurgica come quella impiegata nello studio potrebbe diminuire l'assunzione totale a circa 283 MP/die, di cui 201 MP/die (71%) nell'intervallo 1 - 5 µm. A causa dell'attuale mancanza di ricerca sulla tossicità delle MP ambientali aeree nell'intervallo di respirabilità, il ricorso a misure preventive addizionali per prevenirne l'assunzione umana dovrebbe essere attentamente valutato.

Preface

This thesis has been submitted in partial fulfillment of the PhD degree. As part of the assessment, co-author statements have been made available to the assessment committe and are also available at the Faculty.

This PhD project was granted by H2020 ITN MONPLAS 860775 and was carried out at Aalborg University, Department of Civil Engineering, Division of Water and Environment, in the period from August 2020 to July 2023. The PhD included two abroad stays in the United Kingdom from November 2021 to April 2022, the first hosted by Renishaw plc UK and the second by Severn Trent Water.

The present thesis is based on one published scientific paper (**Paper I**) and two scientific papers currently under review (**Paper II** and **Paper III**). Contents of the papers are briefly discussed in the extended summary of the thesis. Additional details are given in the relevant chapters where the papers are presented.

Luca Maurizi
Aalborg University, August 9, 2023

Acknowledgements

I won't spend many words on how challenging doing a PhD may be, especially if compared with other things populating the human existence. During the last three years, we as individuals have experienced a pandemic first, and then a war in the very hearth of Europe; two events we used to think belonging to the dark ages. So being here in Denmark to do my research work, was after all a comfortable activity, like sitting on a chair in the eye of a tornado: as long as it keeps moving, you are not going to fall to the ground.

I learnt that one of the most important and unexpected aspects of a PhD, and of academic jobs in general, is the constitutive value of networking. I had the greatest chance to explore it during my PhD project: with my colleagues throughout the last three years at Aalborg University and in the MONPLAS consortium, but also with many other people I happened to know at conferences or during my abroad stays. Some of these characters were very "pecualiar", but I guess this is what we commonly call *humanity*, isn't it? I cannot help but sincerely thank those who supported me during this journey, with an advice, a joke or just a smile. We share many funny memories together, and thanks to you I really felt part of something wider yet deeply human, I felt *home*. I won't make a tedious list with names, because it's not my style to rank people and I want to cut it short. And also because it'd be a bit painful.
However, I must explicitly express my gratitude to my supervisors Asbjørn and Jes for their superhuman strength to always find time to help me with wise recommendations and sense of humor.

A huge thank to my friends from my previous life for supporting me through many life journeys, last but not least this one: Mattia, Salah, Ronald "McSacchetto" Field, Fabio "Er pignolo" Lutzu, and Giuseppe "Er pigna" Pignatelli.

Grazie anche ai miei genitori, che hanno mostrato la sensibilitá e la forza necessarie a sopportare che il loro unico figlio si trasferisse in un altro Paese per ricominciare da zero. Siete una fonte di ispirazione constante.

Finally, thank to those who didn't believe in me. Thank to those who found me unrrespectful and impatient because I didn't want to stay silent. Because

I wanted to bear the responsibility of my conscience and act according to my principles. Thanks to you, I figured out what I didn't want to become. This PhD is also for you.

Table of contents

List of Figures

List of Tables

Part I

Summary of the dissertation

Chapter 1

Introduction

1 The plastic age and microplastic pollution

About 60 years ago, the mass production of plastic opened the so-called "plastic age", which is still lasting nowadays (Thompson *et al.* 2009). Plastic has indeed revolutionised the human society by offering cheap and ready-to-use materials, which in turn led to several advantages in terms of health, safety, energy saving, and material conservation (Andrady and Neal 2009). However, the drawbacks of plastic mass consumption have also followed, of which plastic pollution is undoubtedly a significant consequence (Horton 2022). The threat for the environment represented by mismanaged plastic is essentially associated with one of the most celebrated quality of these materials: the durability over time and across different environmental conditions. Research is also on the rise in order to comprehend how to tackle the multiple risks associated with the uncontrolled release of plastic in the environment, and scientists are increasingly asking for the attention of national and international bodies (Lanzarote Declaration MICRO 2022).

In 1993 Ryan and Moloney wrote a brief article (Ryan and Moloney 1993) where they described how marine litter was increasing at an exponential rate even in regions not inhabitated by humans, and 80% of these residuals were of plastic nature. Since then, especially after Thompson's article on plastic pollution in the North Sea (Thompson *et al.* 2004), plastic pollution was addressed as a major environmental issue by environmental scientists. The term *microplastic* (MP) was coined by Thompson himself to describe the small plastic fragments he and his collaborators observed during their sampling campaigns. Altough no standard definitions are currently available, it is generally accepted to name microplastics the plastic debris between 1 µm and 5 mm in size (Frias and Nash 2018). Plastic particles below 1 µm show a colloidal behaviour and were consequently termed *nanoplastics* (NPs) as op-

posed to larger plastic fragments (Gigault *et al.* 2018, Figure 1.1). Regardless their size, it is customary to classify MPs and NPs in two categories according to their origin (Cole *et al.* 2011a): primary and secondary. Primary MPs are purposedly manufactured of microscopic size to be used in cosmetics (Fendal and Sewell 2009), as drug vectors (Patel *et al.* 2009), and scrubbers to remove rust and paint (Derraik 2002). Secondary MPs are the result of the breakdown of larger plastic items in the environment due to multiple physical, chemical, and biological processes (Browne *et al.* 2007); in particular, the UV radiation seems to be the main responsible for plastic oxidation, which leads to the cleavage of chemical bonds (Moore 2008). The indirect sources of secondary MPs are virtually infinite, spanning from wastewater treatment plants (Chand *et al.* 2021), stormwater runoff (Liu *et al.* 2019), washing machines (De Falco *et al.* 2019), to ship paints (Gaylarde *et al.* 2021) and even plastic cutting boards (Yadav *et al.* 2023) and disposable drink cups (Zhou *et al.* 2023).

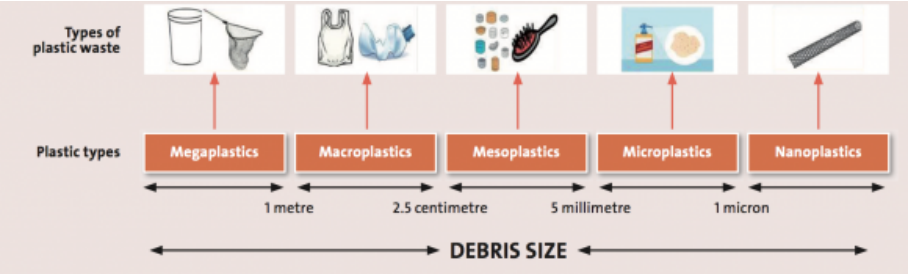

Fig. 1.1: MP and NP classification according to the size (graphic slightly modified from Chatterjee and Sharma 2019).

The various plastic types are distinguished according to the chemical structure of the molecular chains, which leads to densities between 0.8 and >2 g/cm^3 for the pristine materials. However, since the environmental MPs and NPs undergo a process of *aging*, their chemical and physical characteristics can become quite different than the original ones (Zha *et al.* 2022). Moreover, environmental MPs can act as vectors for other micropollutants such as heavy metals (Brennecke *et al.* 2016), pesticides (Zhang *et al.* 2015), unreacted monomers and additives (Swan 2008) and serve as a substrate for biopatogens (Bowley *et al.* 2021). It is also worth reporting that the MPs and NPs found in environmental samples are usually covered with a bio-corona mostly composed of proteins and lipids, which increases the cellular uptake of these particles (Wright and Kelly 2017).

In summary, the MP/NP pollution issue is an eminently multi-disciplinary

issue, involving the efforts of many environmental scientists with backgrounds in biology, chemistry, physics, and engineering just to name a few. The current lack of standardised and validated protocols for the MP sampling and analysis does not facilitate the information sharing among these different disciplines, and the results in the literature should be contextualised according to the experimental design. Recently, there has been some isolated attempts to tackle this substantial lack of reproducibility (Schymanski *et al.* 2021a) by employing multi-laboratorial approaches. However, general guidelines for the MP and NP analysis in different environmental matrices and with different analytical methods are yet far to come. This is even more problematic in the light of the increased speed with which national and international bodies are keen to address MP pollution: in this year 2023, for example, the new Europen requirements for drinking water quality came into force, and they explicitly state that MP levels have to be monitored besides those of other well-known pollutants (Directive EU 2020/2184). The European Commission also funded many research projects aiming at improving the state-of-the-art of MP science through H2020, like the ITN MONPLAS 860775 to which this PhD belongs.

The MP analysis of an environmental sample generally comprises the following three steps: sampling, sample preparation, and analysis. Sampling and sample preparation are tailored to the matrix to be investigated, and the number of the steps to be performed is directly proportional to the matrix complexity (e.g. sludge, soils, biological samples). The goal of the sample preparation is to render the sample ready to be analysed with the analytical method of choice. Different analytical methods provide different information on the MPs in the sample, which lastly affects the type of answer resulting from the study. Currently, the MP science field is shifting its attention to the study of the 1 - 10 µm MPs and NPs in various environmental systems, hence the tendency is to employ analytical techniques capable of detecting such small particles in a reliable way.

2 Sampling techniques

When investigating a system for MP occurrence, the sampling strategy to be adopted needs to address the two following critical points:

- It has to employ the appropriate equipment to sample the chosen matrix
- The amount of each sample and the number of samples for each location (replicates) need to be enough to guarantee the representativity of the results

Being the first step of any investigation targeting environmental samples, the sampling is of pivotal importance. A poor sampling strategy can jeopardise the entire investigation, since it affects the accuracy and representativity of the final result. The sampling strategy also needs to take into account the size of the MPs to be analysed, as this affects not only the equipment to be utilised when taking the samples, but also the subsequent sample preparation and the choice of the analytical technique. Further, the time and costs employed for the sampling have to optimised, especially in the case of routine monitoring. Unfortunately, these key aspects are still subject to either the literature conventions or the operator's expertise, since no standardised sampling protocol is available for the MP analysis of environmental matrices. The ISO/FDIS 24187 "Principles for the analysis of microplastics present in the environment" is currently still under development, but, as stated in the draft, it only aims at providing a "pool" of general recommendations.

The sampling methods applicable for the MP analysis can be grouped into three main categories: selective sampling, volume-reduced sampling, and bulk sampling (Hidalgo-Ruz *et al.* 2012). Selective sampling *in situ* consists of manual extraction of items that are recognizable by the naked eye, for example on the surface of sediments. This sampling strategy is obviously not applicable to the MPs invisible to the naked eye, so approximately below 100 µm.
If the entire bulk sample is taken during the sampling with no further reduction during the operation, a bulk sampling is being performed. The bulk sampling is the strategy of choice for solid matrices like soils and sediments, although the amount of sample which can be taken is limited by the size of the containers employed.
Finally, in the volume-reduced sampling, the volume of the bulk sample is reduced during the procedure, and only the part containing the MPs is preserved. This strategy is usually employed for liquid matrices such as drinking and marine water, but also for air. The majority of works employing this strategy reports using filters or meshes to isolate the particles from the matrix (Stock *et al.* 2019). However, it must be noticed that the mesh size employed

during the sampling does not automatically represent the size limit of the MPs found in the samples: it is quite common, indeed, that particles smaller than the filter's pores get stopped on the filter's surface, thus ending in the samples to be analysed. Nonetheless, for quantitative results, it is customary not to consider particles below the filters mesh.

Contamination from the external environment occurs upon sampling and handling the sample in the lab. The phenomenon is unavoidable, and, although depending to a certain extent on the sampling protocol (Buteler *et al.* 2023), must be taken into account, otherwise overestimations will be made. Apart from avoiding using plastic items during the sampling and sample treatment, it is generally recommended to include procedural blanks in the experimental design. Since the major source of MP contamination in environmental samples is indoor air, air-blanks should be collected in parallel with the field samples and handled with the same procedure. However, there is no consensus whether the MPs detected in the blanks should be subtracted from the results of the field blanks. As a general practice, whether or not contamination is negligible relates to the concentration in the sample and not to the specific matrix. Hence sometimes the contribution from the contamination can be ignored, thus avoiding any correction (Molazadeh *et al.* 2023).

The sampling of environmental NPs poses a further challenge related to the small size of these analytes, which also questions the feasibility of the sample preparation without excessive loss of the particles. The current tendency of the scientific community is to avoid the analytical protocols adopted so far for the MPs and try to develop more direct approaches. Surette *et al.* (2023) employed a magnetic flow cell to extract metal-doped PAN NPs (polyacrylonitrile NPs) from synthetic aqueous matrices, by adding magnetic NPs to facilitate the process. In general, the few works focusing on NP detection utilize synthetic NPs with a metallic core to enable single-particle detection with techniques such as SEM-EDX and ICP-MS (Mitrano *et al.* 2019).

2.1 Drinking water

Drinking water is usually sampled with volume-reduced sampling strategies. This is due to the high volume of water needed for each sample to obtain significative results afterwards (Koelmans *et al.* 2019). The MP abundance in drinking water is generally low, despite increasing as smaller MPs are considered (Leusch *et al.* 2023). The investigation may focus either on tap water (and, in turn, on the MP occurrence as a function of the water source and/or the water treatment) or commercial bottled water (Elkhatib and Oyanedel-Craver 2020).
Surface water can be sampled with trawls, bottles or buckets directly *in situ* (Koelmans *et al.* 2019). However, in the majority of works, the drinking wa-

ter source is sampled at the waterworks' inlet by means of closed devices equipped with filters (Mintenig *et al.* 2019, Kirstein *et al.* 2021, Gomiero *et al.* 2021). Then, the MP contamination can also be investigated at the plant's outlet, at domestic taps connected to the chosen network, and during the various stages of the water treatment.
There is no standard classification of the apparati employed for drinking water sampling or consensus on the filter mesh to be used. Weber *et al.* (2021) modified a stainless steel pressure filter housing to sample drinking water with 10 µm steel filters and connected it with silicone hoses at the taps (Figure 1.2).

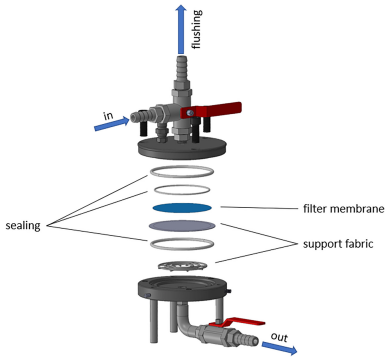

Fig. 1.2: The sampling apparatus adopted by Weber *et al.* (2021).

Kirstein *et al.* (2021) made use of a closed four-lines device capable of sampling replicates in parallel with 5 µm steel filters (Figure 1.3). The apparatus consisted of four modified filter holders connected by stainless steel pipes, and each flow line was equipped with a flowmeter to check the sampled volume of drinking water. The inlet of the device was connected to the sampling points with a flexible stell tube. Moreover, by connecting two filters in series in the same flow line (i.e. a low-mesh glass fiber filter before the steel filter), field blanks could also be obtained.

Fig. 1.3: The sampling apparatus adopted by Kirstein *et al.* (2021) (Credits: Luca Maurizi).

It can also be useful to separate the MPs in size fractions upon sampling, so to have sub-samples destined to different analytical methods. Pittroff *et al.* (2021) used a multi-stage filtration system equipped with three cartridges of decreasing pore size (100, 20, and 5 µm) in series. A stopcock followed by an over pressure valve was installed at the inlet of the apparatus and a flowmeter at the outlet (Figure 1.4).

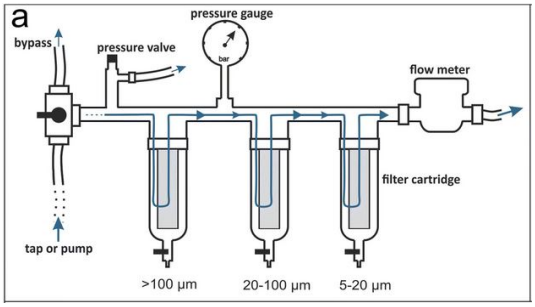

Fig. 1.4: The sampling apparatus adopted by Pittroff *et al.* (2021).

MP analysis of bottled water requires much smaller volumes of sample, typically in the order of 10 L (Praveena and Laohaprapanon 2021). Before any processing, bottled water should be stored dark at 4°C to prevent the formation of organic material and the photooxidation of MPs (Fan *et al.* 2014). After collecting an adequate amount of commercial bottled water, this can be easily filtered in the laboratory with vacuum-assisted filtering systems through the chosen mesh. MPs can occurr in bottled water primarily due to the plastic material of which bottles are composed, even though water distributed in

glass bottles also showed the presence of MPs possibly from the production process (Oßmann *et al.* 2018). Further, the mechanical stress exerted on the bottle's cap upon opening/sealing may also play a role in the MP release (Winkler *et al.* 2019).

2.2 Airborne particulate

Sampling protocols for airborne particulate can be distinguished in two categories: passive and active sampling. Passive sampling is often used to investigate outdoor airborne pollution thank to its simplicity and low-cost, and, in addition, it does not require electricity. These advantages render passive sampling ideal for observations lasting weeks or months, even thoug weather conditions can influence the particle collection (Chen *et al.* 2020). However, with passive sampling protocols is not possible to quantify the concentration of the collected particles, as the volume of the air sampled cannot be registered. The devices employed for passive sampling usually consist of a glass container coupled with a steel funnel (dry passive sampling, Dris *et al.* 2016), which can also be used to sample particles trapped in the rainfall (wet passive sampling, Roblin *et al.* 2020) (Figure 1.5). The fallout of airborne particulate can also be investigated by collecting outdoor or indoor dust with a vacuum cleaner or similar tool (Zhu *et al.* 2022).

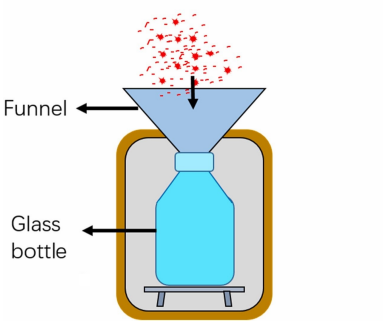

Fig. 1.5: General schematic of a passive sampler (image slightly modified from Shao *et al.* 2022).

In the active sampling methods, pumping devices are employed. The particles are collected on a filter or substrate while the apparatus pumps air at certain flowrate for a given period of time, enabling to quantify the particle concentration. The disadvantage of active sampling methods is the need for electrical power, which hinders their applicability to remote or natural locations. Nonetheless, active sampling is the preferred strategy for studies focusing on human intake of airborne MPs. Li *et al.* (2020) sampled the air in the vicinity of a Chinese campus at different heights, whilst Vianello *et al.*

(2019) employed a thermal manikin simulating the average human breathing rate to estimate the intake of airborne indoor MPs down to 10 µm (Figure 1.6).

Fig. 1.6: The Breathing Thermal Manikin employed by Vianello *et al.* (2019).

3 Sample preparation

The sample preparation stage is needed to extract the MPs from the matrix for the subsequent analysis. Ideally, the sample preparation protocol should completely eliminate the matrix without affecting the original status of the MPs in the sample, and it should have a high recovery. The choice of the preparation protocol also depends on the chosen analytical technique, since some techniques can be more sensitive to (in)organic residuals than others. Although of pivotal importance for the MP analysis of the overall sample, there is no standardised protocol for the different environmental matrices which can be investigated. Nonetheless, researchers agree on some bottom lines regarding the treatments to perform to obtain representative samples.

For drinking water samples, the sample preparation may comprise vacuum filtration, digestion, and density separation, in different combinations according to the characteristics of the matrix (Picó *et al.* 2022). Generally, the filters employed in the first step of the sample preparation are those employed during the sampling (Kirstein *et al.* 2021, Dalmau-Soler *et al.* 2021). The particles concentrated on the filters are extracted by rinsing with mQ or with a mild incubation in a surfactant, and a particle-enriched suspension is obtained. Then, either the same filters (Kirstein *et al.* 2021) or smaller meshes can be utilised for the next steps. Depending on the chosen analytical technique, the particle-enriched filter may also directly be analysed as such (Figure 1.7).

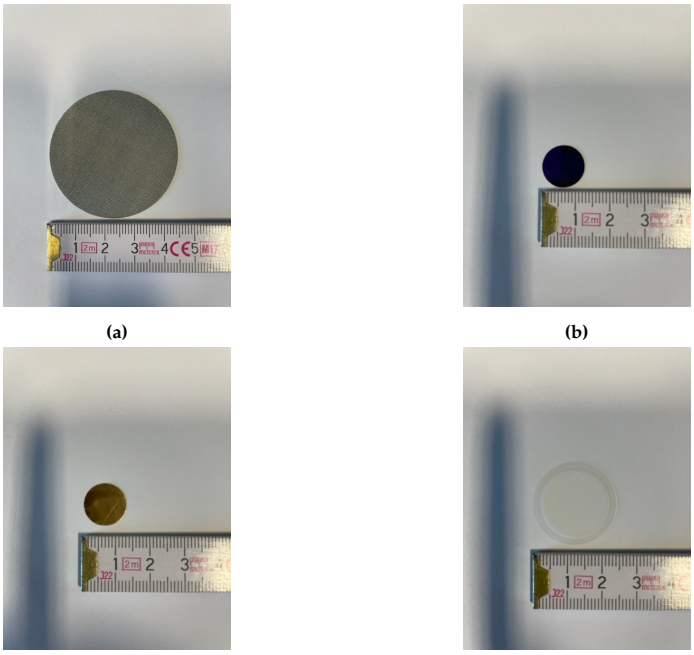

Fig. 1.7: Examples of filters used during the sample preparation: (a) 1 µm sintered steel filter (Ø 46 mm); (b) 1 µm Silicon filter (Ø 13 mm); (c) 0.8 µm gold-coated polycarbonate filter (Ø 13 mm); (d) 0.2 µm aluminum-oxide filter (Ø 25 mm) (Credits Luca Maurizi).

Rinsing of filtering apparati is usually performed with ethanol or the anionic surfactant sodium dodecyl sulphate (SDS) to maximise the particle recovery on the filter. The area of the filter onto which the particles are concentrated depends on the diameter of the funnel employed during the filtration (Figure 1.8).

Fig. 1.8: Filtration of an SDS suspension (Credits Luca Maurizi).

Inorganic content can be eliminated from the matrix by employing a solution with a density higher than that of the plastic polymer to be recovered, and, at the same time, lower than that of the particles to be discharged. As final result, the sample is split into two phases, where the lower one contains the inorganic content and the upper one the MPs. The operation is called density separation and is performed inside separating funnels. The correct density of the separating medium can be achieved by employing salts and depends on the quantity of salt dissolved in the water matrix of the medium (Stock *et al.* 2019). Since inorganic particles generally have densities higher than 1.8 g/cm^3 (Tirkey *et al.* 2021), the density of the separating medium should be around this value to maximise the recover of MPs while excluding the undesidered components of the matrix. Table 1.1 lists some of the most common salts utilised in the density separation stage (Stock *et al.* 2019, Tirkey *et al.* 2021).

Salt	Max Density (g/cm^3)	Disadvantages
NaCl	1.3	PVC, PET not separated
NaI	1.8	Costly, blackens filters
$ZnCl_2$	1.8	Hazardous, corrosive
$ZnBr_2$	1.7	Hazardous, expensive
Sodium polytungstate (SPT)	1.8	Costly, may crystallize

Table 1.1: The most commonly employed salts for density separation. The densities reported are those most used for the separation of MPs.

The next step (if needed) is the oxidation of the organic matter in the MP-enriched mixture (digestion), after filtering out the salt used for the density separation. In the past, acidic and alkaline solutions were utilised to oxidise the organic components of the sample, however their efficiency was quite low. Cole *et al.* (2014b) compared acidic, alkaline, and enzimatic digestions at different conditions and demonstrated that the enzymatic treatment was the most performing in preserving the MP while digesting the organic residues. Nowadays, the digestion is normally performed with hydrogen peroxide (H_2O_2) 30 - 50% or the Fenton's reagent (Koelmans *et al.* 2019) for not more than 48 hours (wet peroxidation), followed by an enzymatic treatment. Air samples may also need to undergo sample preparation as described for drinking water samples (Mbachu *et al.* 2020). The final outcome of the sample preparation is to concentrate the MPs previously in the sample onto a substrate or into a matrix of choice for the subsequent analysis and quantification.

4 Microplastic analysis and quantification

Table 1.2 shows the most common techniques employed for the visualisation, analysis and quantification of the MPs in environmental samples. The choice of the analytical method has to take into account the advantages and drawbacks of each technique and the story to be drawn upon the analysis results. Typically, several techniques are combined to fully characterise the MPs and NPs of the sample.

Method	Output
Visual spectroscopy	Number, Morphology
Thermochemical methods	Mass, Chemical ID
FTIR spectroscopy	Number, Morphology, Chemical ID
Raman spectroscopy	Number, Morphology, Chemical ID
Fluorescence spectroscopy	Number, Chemical ID
O-PTIR spectroscopy	Number, Chemical ID
Atomic Force Microscopy	Morphology, Surface physics/chemistry

Table 1.2: The analytical methods used for MP visualisation, analysis and quantification.

This PhD thesis focuses on the application of Raman and FTIR micro-spectroscopy to the MP analysis of drinking water and indoor air, hence these two techniques are discussed in detail in the following of this chapter.

4.1 Molecular spectroscopy

The analytical techniques based on molecular spectroscopy exploits the interaction bewteen the electromagnetic radiation and matter to acquire information on the chemical structure of the sample (Guo *et al.* 2022). The spectroscopic techniques are classified according to the radiation used to perform the analysis, which, in the case of MP analysis, spans from the visible to the IR (Figure 1.9).

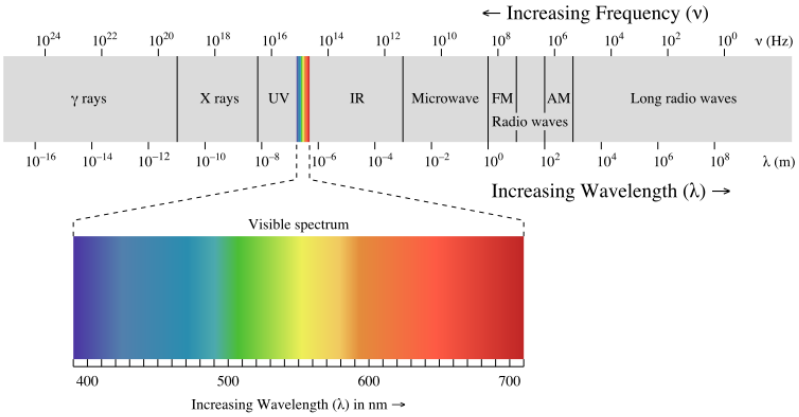

Fig. 1.9: The electromagnetic spectrum (UC Davis ChemWiki, CC-BY-NC-SA 3.0).

FTIR spectroscopy

Fourier-Transform InfraRed (FTIR) spectroscopy represents an evolution of the previous dispersive IR spectrophotometers and is historically a major analytical technique for several types of samples (Berthomieu and Hienerwadel 2009). The radiation employed by FTIR is midIR (1000 - 4000 cm^{-1}), whose energy is compatible with molecular vibrations along the chemical bonds (stretching) and variations of the chemical bond angles (bending). In order to be IR active, a vibration must cause a change in the dipole moment of the molecule: hence, only either polar molecules (e.g. water) or asymmetric vibrations of apolar molecules (e.g. the asymmetric stretching of the oxygen atoms in the CO_2 molecule) can be detected during an IR analysis. The energy associated with the molecular vibration depends on the mass of the atoms involved and the strength of the chemical bond, thus double and triple bonds vibrate at higher frequencies than single bonds. IR spectroscopy can be employed for gas, liquid and solid samples, provided that the signal from the H_2O and CO_2 in the atmosphere is eliminated. The result of an IR analysis is represented by an IR spectrum, which shows either the Transmittance (% of IR radiation passed through the sample) or the Absorbance (% of IR radiation absorbed by the sample) against the frequency, normally expressed as wavenumber (cm^{-1}). Each peak in the spectrum corresponds to a molecular vibration, hence each molecule is represented by a characteristic set of signals (chemical fingerprint) easily recognizable with a reference library.
The usage of Fourier-Transform instruments permitted to strongly shorten the acquisition time required to obtain an IR spectrum. Further, the advance of computer technology allowed for computing an increasing amount of data per analysis, leading to a wide application of FTIR to environmental analysis

(Simonescu 2012). The core of an FTIR spectrophotometer is the Michelson interferometer (Figure 1.10).

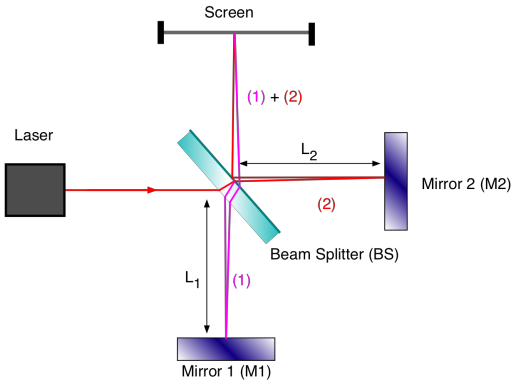

Fig. 1.10: Schematic of a Michelson interferometer (Boeglin 2022).

The Michelson interferometer is fundamentally a device constituted of three mirrors: a beam splitter at 45° normally in KBr, a static mirror (M2 in Figure 1.10) and a moving mirror (M1 in Figure 1.10). The IR radiation emitted from the laser source is splitted by the beam splitter towards the two mirrors, and, in particular, the moving mirror travels at constant velocity back and forth along L1. The IR radiation is reflected by the two mirrors and is recombined by the beam splitter, which forwards it to the sample and, eventually, to the detector. When the IR beams recombine at the beam splitter, they can interfere either constructively or destructively, depending on the distance travelled by the beam reflected by M1. Thus, during the analysis, all the wavelengths of the employed IR range can be covered and registered by the detector. However, the outcome is not an IR spectrum, but an interferogram, a diagram showing the frequency variation against time. The conversion of the raw interferogram to an identifiable spectrum is performed with a function called Fourier Transform, which is nowadays automatically implemented in the software of these machines.
IR analyses are traditionally performed in transmission mode, which means that the IR radiation absorbed by the sample is sourced. When coupled with an IR microscope (FTIR microscopy or µFTIR) and a Focal-Plane-Array (FPA) detector, it is possible to map quite extended areas with a spatial resolution of approximately 10 µm (Figure 1.11). In this case, a chemical map of the sample is obtained, and each point cointains a single IR transmission spectrum. The application of FPA-µFTIR to MP analysis dates back to 2004 and it has so far been the most fruitful for the advancement of the field (Veerasingam *et al.* 2021). The analysis can be run either on filters (Primpke *et al.* 2017a) or windows transparent to midIR (Chand *et al.* 2021) on a wide range of en-

vironmental matrices. ATR-FTIR is also largely employed in environmental monitoring of MPs above 100 µm (Simon *et al.* 2021).

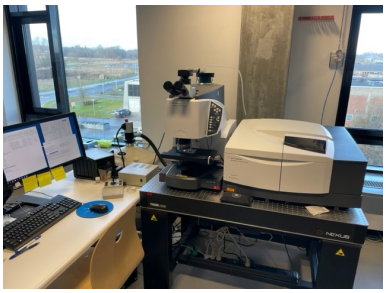

Fig. 1.11: An FPA-µFTIR (Credits Luca Maurizi).

FTIR-based methods can be employed only on perfectly dried samples, due to the strong IR absorption characterising water. Moreover, the spatial resolution limit of the technique does not allow to analyse MPs below 10 µm and NPs, which somehow puts the method aside the most recent advancements of the field. Finally, the amount of data produced in a single FPA-µFTIR analysis is significative and requires *ad-hoc* technical solutions for the chemical identification of the spectral maps (Primpke *et al.* 2020b).

Raman spectroscopy

Raman spectroscopy is an analytical method probing the radiation scattered by the sample when it is irradiated with a monochromatic source (Smith and Dent 2019). When interacting with matter, radiation can scatter either elastically (Rayleigh scattering) or anelastically (Raman scattering), besides other phenomena such as absorption (on which IR spectroscopy is based). In particular, the radiation anelastically scattered by the sample can have a frequency (energy) either higher than the incident light, which is called anti-Stokes scattering, or lower (Stokes scattering). The probability of the anti-Stokes scattering is much lower than that of the Stokes scattering, since anti-Stokes involves the release of energy from the first excited molecular vibrational state. On the contrary, when Stokes occurs, it is the incident light to pass energy to the ground vibrational state, which is more populated at room temperature (Figure 1.12). Hence, Raman spectroscopy focuses on the detection of Raman Stokes signals. However, it must be noticed that Raman scattering is generally a weak spectroscopic phenomenon involving one photon per 10^6 - 10^7 Rayleigh scattered photons.

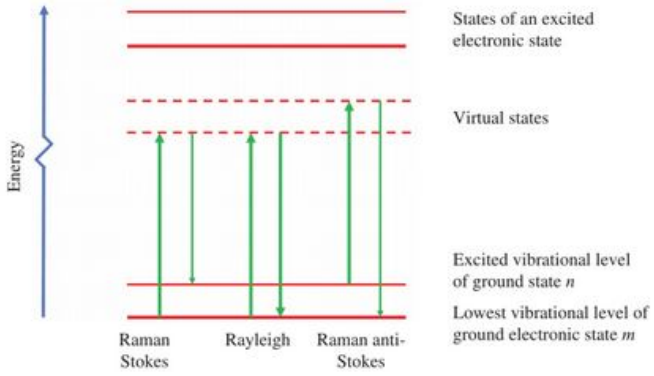

Fig. 1.12: Jabloski plot of light scattering (Smith and Dent 2019).

The electric field of the incident ligth polarizes the electronic cloud surronding the atomic nuclei of the molecule and "electronic virtual states" are generated. As already said, the radiation is normally elastically scattered, although, when nuclear motion also occurs, a change in the polarizability of the molecule may happen. The polarizability is a parameter indicating how easily the distribution of the electronic cloud can be distorted by an electromagnetic radiation: hence, if the two atoms involved do not differ very much in electronegativity, the polarizability of the molecular system is high. On the contrary, if the delta in electronegativity is significant, the polarizability is low, because the electronic cloud cannot be distorted much more than it already is. Consequently, the most active molecular vibrations in Raman spectroscopy do not involve a change in the dipolar moment, as opposed to what happens in IR spectroscopy (indeed, it is often said that IR and Raman spectroscopy are two complementary techniques). For instance, water is a weak Raman scatterer, whilst the symmetric vibration of the oxygen atoms in the CO_2 molecule has a clear Raman signal. A Raman spectrum summarizes the Raman fingerprint of the sample by showing the counts of Stokes photons against the Raman shift (energy of the incident radiation minus energy of the emitted radiation) in cm^{-1}.
Raman microscopy (µRaman) is the hyphenation of a confocal optic microscope with a Raman spectrophotometer. There are two important differences between µRaman and µFTIR:

1. The microscope of a µRaman system mounts optic objectives because it employs visible radiation, as opposed to the Cassegrain objectives of a µFTIR. Hence, the quality of the visible image is higher with µRaman;

2. µRaman systems normally have a dispersive geometry, Fourier-Transform µRaman (FT-µRaman) still being a technology under development.

Figure 1.13 shows the internal optics of a dispersive µRaman system.

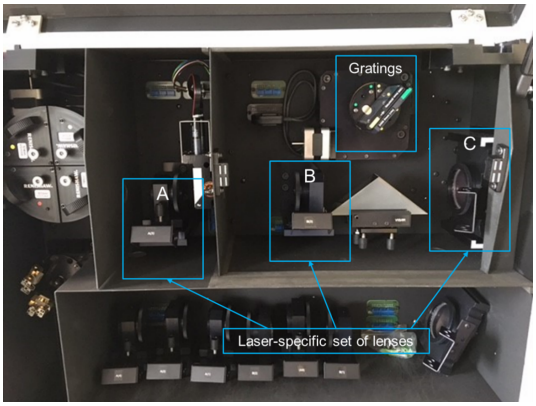

Fig. 1.13: The internal optics of a dispersive µRaman (Credits Luca Maurizi).

The radiation sources of a µRaman emit in the visible region, and normally the system is equipped with three laser sources (once helium sources, nowadays solid-state) emitting at around 530, 630 and 785 nm. The chosen laser impinges on the sample through the microscope's objective, and the scattered radiation is recollected by the microscope and sent to the optics of the spectrophotometer. First of all, the Rayleigh radiation is filtered out, then the Raman Stokes scattering is decomposed in its constituting wavelengths by the gratings. The gratings are reflective substrates with a given groove density (expressed in lines per mm, ll/mm) and they can be selected upon starting the analysis. Finally, the Raman scattering is registered by the detector, typically a Charge-Coupled Device (CCD) cooled at -60°C through Peltier effect. The laser-specific lens set shown in Figure 1.13 has to be manually changed upon setting the laser wavelenght, however modern µRaman systems are fully automatised. Despite some works reporting the manual selection of MPs to be analysed with µRaman (Lenz *et al.* 2015), the current approach involves a "point and shoot" automatic mapping. Briefly, the sample is concentrated onto a filter or substrate and a visible picture (montage) of the area is taken. The visible montage is then analysed by a dedicated function of the software, which can locate single items of the montage by constrast and calculate their morphological features. Next, the laser is automatically driven onto each item and its Raman spectrum is aquired. In most of the studies, the µRaman mapping is performed onto selected sub-areas of the sample, and the total MP abundance is calculated by assuming the MPs to be homogeneously distributed (Schymanski *et al.* 2018b, Oßmann *et al.* 2018).
The spatial resolution limit of a µRaman system is below 1 µm and can po-

tentially reach 100 nm, enabling to analyse NPs (Sobhani *et al.* 2020) despite with a decreased spectral quality. Thus, µRaman systems are being coupled with Atomic Force microscopes (AFM) to obtain a system capable of performing Tip-Enhanced Raman Spectroscopy (TERS, Figure 1.14). Briefly, in TERS the laser is focused onto a tip of nanometric size, which enhances the electric field of the radiation by several orders of magnitude (Bailo and Deckert 2008). This allows to acquire high-quality Raman spectra of nanometric items even though smaller than the spot size of the original laser. However, it must be noticed that TERS is a demanding technique in terms of know-how and costs, and at the moment it does not seem applicable for routine monitoring of MP pollution.

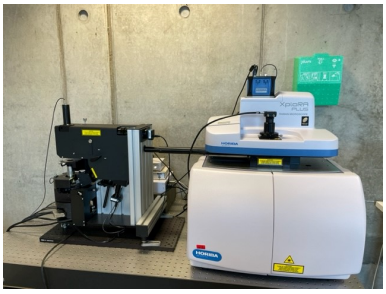

Fig. 1.14: An AFM-Raman (Credits Luca Maurizi).

To summarise, µRaman appears a promising technique for the analysis of small MPs and NPs, however it is not exempt from drawbacks. Running a µRaman analysis generally requires more experience than µFTIR: setting a too long aquisition time can provoke the burning of the sample under the laser, and the analysis is typically hampered by fluorescence, which is a competitive phenomenon to Raman scattering.

5 MP pollution in drinking water

In 2019 the World Health Organization (WHO 2019) issued a report addressing MP pollution in fresh and drinking water, as well as the possible sources of contamination and the MP removal performance of drinking water plants. The overall conclusion of the study was that more data were needed to develop a comprehensive overview of MP occurrence and fate in drinking water. Further, the WHO advocated for an effort to standardise the analytical procedures, given the scarce comparability of the published studies and, consequently, of the results.
In most cases, the raw drinking water is supplied by freshwater, whilst the usage of seawater is still hampered by the high cost associated with desalination

(Shen *et al.* 2020). Freshwater sources comprise rivers, lakes, water reservoirs, and groundwater, with the vast majority of works investigating the MP occurrence in surface-water derived drinking water. Freshwater environments are reportedly affected by MP pollution, which is generally influenced by the location, vicinity to human activity, and weather conditions. In particular, surface waters prove to be particularly exposed to the phenomenon, as a consequence of wastewater disharges (Hartline *et al.* 2016), environmental decomposition of macroplastics (Lambert *et al.* 2014), and atmospheric deposition (Free *et al.* 2014). Despite being a more isolated environment, in the case of groundwaters, MP contamination is associated with the downwards transport through the soil pores (Blaäsing and Amelung 2018). The MP tranportation dynamics towards the groundwater reeservoirs is mostly influenced by the soil granularity and fracture network (Zhu 2020), dry/wet cycles (O'Connor *et al.* 2019), and the aging of MPs (Ren *et al.* 2021). However, surface waters generally present higher MP loads than groundwaters, especially in the case of non-Karst aquifers (Oladoja and Unuabonah *et al.* 2021).

Despite the majority of studies indicating that 1 - 100 µm MPs are efficiently removed from the raw water during the water treatment (Xue *et al.* 2022), only three studies (Pivokonsky *et al.* 2018a, Pivokonsky *et al.* 2020b, Wang *et al.* 2020) investigated the MP removal performance down to 1 µm and found values above 80%. However, the MP abundance in the treated water was in the order of thousands per liter, with the majority of MPs being sized 1-10 µm. It must also be noticed that the sampling volume in Pivokonsky *et al.* 2018a, Pivokonsky *et al.* 2020b and Wang *et al.* was as low as 1 L and the investigated plants operated different types of water treatment. In general, the MP removal efficieny is expected to increase if more treatment steps are performed: thus, a conventional waterworks (train coagulation-flocculation, sand filtration, and disinfection) is likely less efficient than advanced facilities equipped with Active Aarbon (AC) or membrane filtration (Xue *et al.* 2022). Nonetheless, the increased complexity of advanced treatment trains can lead to the release of additional MPs in the treated water sent to the network. Dalmau-Soler *et al.* (2021) detected poly-tetrafluorethylene (PTFE) and epoxy resins after the treatment, and Wang *et al.* (2020) demonstrated that the coagulant aid PAM could be traced in drinking water. On the other hand, the usage of ozonation did not prove to provide any additional benefits to the MP removal (Pivokonsky *et al.* 2018a, Pivokonsky *et al.* 2020b, Wang *et al.* 2020, Dalmau-Soler *et al.* 2021). Furthermore, the MP shape also seems to play a role, as shown by Wang *et al.* (2020), who quantified the removal of MP fibres by GAC as 45% against the 82% of MP spheres. As can be seen, drinking water plants can contribute to the MP occurrence in the environment and MP human intake by inefficiently retaining the MPs (especially

the 1 - 10 µm fraction) from the water source and possibly releasing additional particles during the treatment (Mintenig *et al.* 2019). Overall, there is a pressing need to deepen the understanding of the MP removal efficiency of drinking water plants under different conditions and to what extent these facilities may contribute to the MP occurrence during the various stages of the water treatment. As already discussed throughout this chapter, the lack of standardization in the MP research field hinders the comparison among the different studies. Hence it proves difficult to draw a coherent picture of the state-of-the-art of MP occurrence in drinking water. This deficiency of well-established rules also applies to the choice of the analytical method, whose technical characteristics determine the outcome of the investigation. The two main analytical techniques so far employed for the MP analysis in drinking water are µFTIR and µRaman (Nirmala *et al.* 2023), nonetheless a quantitative comparison between these two methods is still lacking. Assessing to what extent the outcomes from these two methods differ, would be useful to put into perspective the current knowledge on MP occurrence in drinking water.
NP analysis in drinking water is still an open challenge (Mortensen *et al.* 2021), whilst there is no direct knowledge of the removal rate for NPs during the water treatment. Devi *et al.* (2022) hypothesized that current technologies for nanoparticle remediation in drinking water may apply to NPs as well, despite recognizing that much more studies are needed to (at least) indicate suitable analytical methods for NP detection. As of today, there exist a few studies reporting on the NP characterization in drinking water (e.g. Huang *et al.* 2022, Li *et al.* 2022, Zhang *et al.* 2023), but they employ complex and expensive methods such as TD-GC/MS, FTIR-AFM, and SERS. Hence it would be a step forward to find a technique not too demanding in terms of required know-how and cost and capable of detecting plastic particles in the sub-micron range with minor intervention from the operator.

Drinking water is potentially the most important pathway for MP human dietary intake (Sánchez *et al.* 2022), according to the estimations by Cox *et al.* (2019). Assuming that tap water presents a concentration of 4.23 MP/L, the daily intake for an adult male would be 16 MPs/day (corresponding to 6000 MPs/year). It is although difficult to put in perspective these values, due to poor knowledge on MP absorption and excretion rates *in vivo*, the lack of research on NP occurrence in drinking water, and the occasionality in protocols focusing on MP and NP toxicity (Zhang *et al.* 2022).

6 Airborne MP pollution

Atmospheric diffusion is one of the most important route through which MPs could spread in different environments over great distances (Sridharan

et al. 2022). Indeed, MPs could also be found in isolated regions such as the high Himalayas and the Poles (Bergmann *et al.* 2019). Investigating airborne MP diffusion is a matter of particular concern also due to the possible implications for human health related to the MP intake *via* breathing in outdoor (Abbasi *et al.* 2019) and indoor environments (Wright *et al.* 2019). According to Shao *et al.* (2022), airborne MPs can lead to the "fiber paradigm" (increased bioreactivity due to a fibrous shape) and constitute a not negligible fraction of $PM_{2.5}$, the breathable particulate.

Airborne MPs may predominantly have a fibre shape (Moreno *et al.* 2014), hence clothing textile can be considered a major source of airborne MP fibres in indoor environments. Nonetheless, the composition of indoor atmosphere is also affected by the antropogenic activity occurring outdoor, such as industrial emissions, landfills, traffic and waste incineration (Shao *et al.* 2022). It is also worth noting that the majority of MPs detected in the atmosphere were not primary, suggesting that MPs generated from plastic macro-objects can diffuse through different habitats (Auta *et al.* 2017). The human intake of airborne MPs down to 10 µm can be as high as 272 MPs per day (Vianello *et al.* 2019), however information on the occurrence of smaller airborne MPs (so called "breathable MPs") in indoor environments is almost not present in the literature. Hence investigating the occurrence of small airborne MPs in indoor environments and seeking the link with human activity would be extremely helpful to estimate the related human intake. Further, it may also be necessary to explore possible ways to tackle human exposure to brethable MPs, given their higher risk to affect human health. Alexander *et al.* (2016) indeed demonstrated that 0.1 - 10 µm MPs were able to translocate from the lungs into organs and could cross the blood-brain barrier, potentially resulting in inflammation, cellular necrosis and tissue tearing (Enyoh *et al.* 2019). Besides these inherent toxic effects, MPs below 10 µm can cause oxidative stress in human cells by facilitating the production of Reactive Oxygen Species (ROS) (Schirinzi *et al.* 2017), and desorbing pollutants such as polycyclic aromatic hydrocarbons (PAHs) (Akhbarizadeh *et al.* 2021) and heavy metals (Wang *et al.* 2020) from their porous surface.

Chapter 2

Aim and objectives of the study

The research described in this thesis focuses on analytical methods applicable to the microplastic and nanoplastic quantification in drinking water and indoor air to estimate the human intake from these two matrices. There is a lack of scientific knowledge regarding the fate and occurrence of small MPs (1 - 10 µm) and NPs in drinking water, how water treatment affects them, on their occurrence in indoor air, and how the latter depends on the type and degree of human activity. Hence, the main aim of this PhD is to develop new analytical protocols for the quantification of the smallest fraction of MPs and NPs, given their supposedly higher bio-toxicity.

To address this aim, the study was divided into three main research questions, and each was addressed to complete the relevant objective.

Research question 1: *How efficient is a conventional drinking water plant to retain microplastics down to 1 µm? Is it possible to employ Raman micro-spectroscopy to analyse NPs in drinking water?*
To answer this, a conventional drinking water plant was studied over a period of five days with regard to the fate and occurrence of the MPs in the facility's inlet and outlet, in order to evaluate the MP retainment efficiency. An analytical protocol was also developed for the NP analysis of the related drinking water samples.

Research question 2: *How does the choice of a certain spectroscopic technique influence the MP quantification in drinking water and the subsequent estimation of MP human intake?*
To address this, the drinking water samples studied to answer RQ1 were analysed with µFTIR, and the results obtained were compared with those of

μRaman.

Research question 3: *Do the type and degree of human activity in indoor environments influence the fate and occurrence of small airborne MPs? Is it possible to reduce the related human exposure somehow?*
To answer this, the atmosphere of four indoor locations was sampled during workdays and weekends, and the filtering efficiency of a commercial type of surgical facemask was investigated.

Chapter 3

Methodology

This PhD study was carried out focusing on the topics addressed by the 3 research questions outlined in Chapter 2:

1. Occurrence, formation and fate of microplastics above 1 µm in a Danish conventional drinking water plant during routine activity
2. Comparison of the outcomes from Raman micro-spectroscopy and FTIR micro-spectroscopy applied to the analysis of the same set of drinking water samples
3. Influence of location and human activity on the occurrence of indoor airborne MPs above 1 µm and effect of a commercial type of surgical facemask on the potential human intake of indoor airborne MPs

The three topics were addressed adopting matrix-specific protocols and customised sampling devices, as described in the following of Chapter 3. The sample preparation procedures and the analytical techniques employed were consistent with the state-of-the-art of the field at the time the experiments were conducted and also represent the methodological developments of the field itself.

1 Occurrence, formation and fate of microplastics above 1 µm in a Danish conventional drinking water plant during routine activity

This study investigated the occurrence of MPs down to 1 µm in the raw and treated drinking water produced by a Danish conventional waterworks over a period of five days. The MP concentration in the samples was quantified according to the MP number (counts) and the MP mass to take into account possible breaking processes involving the MPs during the treatment process. Hence, the MP removal efficiency was calculated, and the time variation of each identified polymer was investigated. Finally, based on the outcome of the study, the yearly MP human intake from the studied drinking water was estimated. The research aimed at studying to what extent a conventional drinking water plant can retain MPs above 1 µm, the possible source of contamination of the threated water sent to the network, and how the previous two findings can affect the human consumption of MPs from drinking water. In addition, a qualitative proof-of-concept for the analysis of environmental NPs was presented. The study was organised following the methodological steps described in Chapter 1 (sampling, sample preparation and analysis).

1.1 Sampling

The drinking water samples were collected over a period of five days (Monday - Friday, September - October 2021) at the inlet and outlet of a conventional drinking water plant located in Denmark. A simplified scheme of the plant is shown in Figure 3.1.

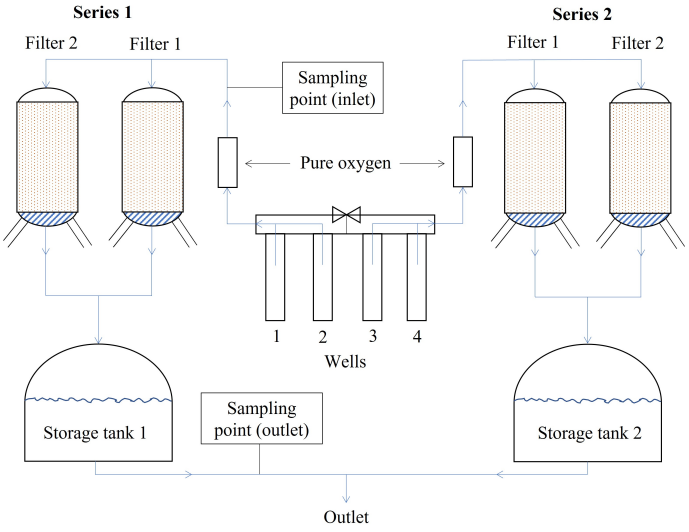

Fig. 3.1: Simplified scheme of the investigated drinking water plant (Maurizi *et al.* 2023).

The waterworks was fed with groundwater from a limestone aquifer 92 m deep. The groundwater underwent sand filtration and was stored in two storage tanks placed ahead of the outlet before being sent to the distribution network. The samples were taken in triplicate in parallel by means of two custom-made devices, and approximately 1 m^3 of water was filtered through a 1 µm sintered steel filter for each triplicate. The sampling procedure and preparation of the recovery samples are described in detail in **Paper I**.

1.2 Sample preparation

After the sampling, the 1 µm sintered steel filters were stored in Petri dishes. Each filter was incubated at 50°C for 24 hours in 5% SDS, then the incubation medium was filtered through the filter with a vacuum filtration system. The particles on the filter were recovered in 1 mL of ∼99.5% ethanol into a 10 mL vial, then 25 µL were deposited on 10×10 mm Silicon substrates through a funnel of 2 mm in diameter. After drying each deposited sample at 55°C overnight, the particles were concentrated into a circular area of approximately 2 mm in diameter. A detailed description of the sample preparation protocol is available in **Paper I**.

1.3 Sample analysis

The sample analysis was conducted at Renishaw plc UK (New Mills, UK) between November 2021 and February 2022 with an InVia Raman microspectro-

scope (Renishaw plc UK). For each sample, the analytical protocol depicted in Figure 3.2 was followed.

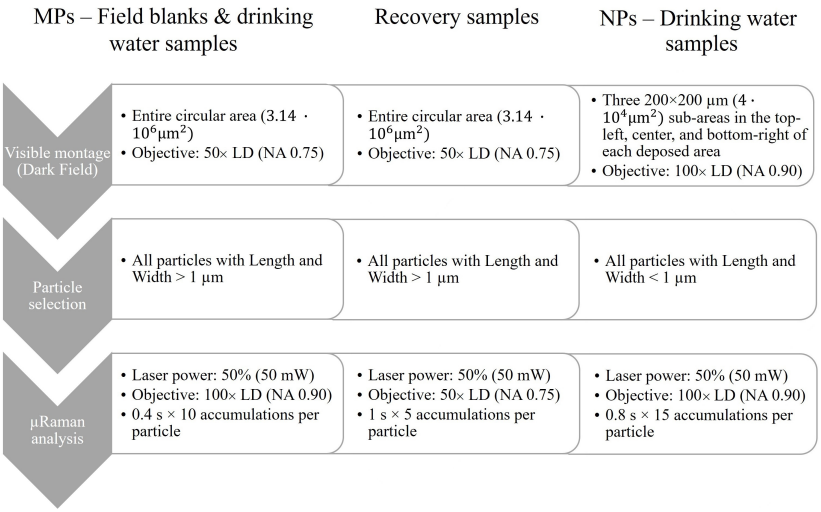

Fig. 3.2: The analytical protocol of the µRaman analysis (Maurizi *et al.* 2023).

In brief, a visible montage of the circular area was acquired in Dark Field (DF) with a long-distance 50× objective (Leica, Germany) before the analysis of the recovery samples and drinking water samples and with a 100× objective (Leica, Germany) before analysing the NPs. For the NP qualitative analysis, three 200×200 µm sub-areas were selected at the top-left, centre, and bottom-right of the circular area, whilst for the MPs the entire area was considered. The visible montages were analysed with the software "Particle Analysis" (Renishaw plc UK) to extract the position and morphological parameters of each item shown in the pictures, then the objects were virtually filtered setting proper values of "Length" and "Width" in the software. Specifically, all the MPs with length and width above 1 µm in the circular area were considered for the analysis, whilst in the three sub-areas only the objects having length and width below 1 µm were selected. The µRaman analysis of the selected objects automatically followed with the parameters shown in Figure 3.2. The spectral recognition was performed in "Particle Analysis" by comparing the experimental spectra with Renishaw Polymer library version 2.2. Further, the MP mass was estimated by modeling the particles as ellipsoids, the morphological parameters being given by the visible image analysis and the density being assigned according to the chemical identification from the µRaman analysis. A more comprehensive description of the sample analysis can be found in **Paper I**.

2 Comparison of the outcomes from Raman micro-spectroscopy and FTIR micro-spectroscopy applied to the analysis of the same set of drinking water samples

The outcome from **Paper I** was compared with the results provided by µFTIR on the same set of drinking water samples. The aim of the study was to fill a knowledge gap of the field by putting in perspective the findings of the previous works based on µFTIR, as analytical techniques with finer spatial resolution such as µRaman are gaining popularity. Further, by merging the datasets from the two methods, a formal description of the frequency variation across the different MP length ranges was proposed. The work also contributed to clarify how the human MP intake estimations generally depend on the technique chosen for the MP analysis. The study was organised in two steps: sample preparation and sample analysis.

2.1 Sampling

The samples from **Paper I** were employed, so no further sampling was necessary (see also **Paper II**).

2.2 Sample preparation

After the µRaman analysis, the samples were dried under gentle nitrogen flow in a water bath at 55°C and reconstituted with 5 mL of ∼50% ethanol. For each sample, 1000 µL were deposited onto 2 mm tick Zinc Selenide (ZnSe) windows of 13 mm diameter by means of a compression cell. The deposited sample was dried at 55°C overnight, producing an area of approximately 10 mm in diameter on the window. Further details are available in **Paper II**.

2.3 Sample analysis

A Focal Plane Array (FPA) – FTIR was utilised to analyse the enriched ZnSe windows in transmission mode. The system was equipped with a Cary 620 FTIR microscope hyphenated with a Cary 670 IR spectroscope (Agilent Technologies, USA). Specifically, a 25× Cassegrain objective was mounted on the microscope, producing a resolution of 3.3 µm pixels on a 128×128 mercury cadmium telluride (MCT) FPA detector. The detector was constantly cooled at 80K by means of liquid nitrogen, which was automatically pumped into the FPA dewar (Norhof, The Netherlands). A spectral range of 3750 – 850 cm^{-1} at 8 cm^{-1} resolution was selected for all scans, and 30 co-added scans

were applied for the enriched ZnSe windows. Before each sample's analysis, a background tile was collected from a clean ZnSe window by co-adding 120 scans and it was automatically subtracted during the sample's scan. A chemical image of the sample's active area was thus obtained, where each pixel contained an IR background-corrected spectrum. The spectral recognition was performed with the software siMPle, which compared the raw and first derivative of the experimental spectra with a custom-made library of µFTIR polymer references (Figure 3.3). In **Paper II** the description of the entire procedure can be found.

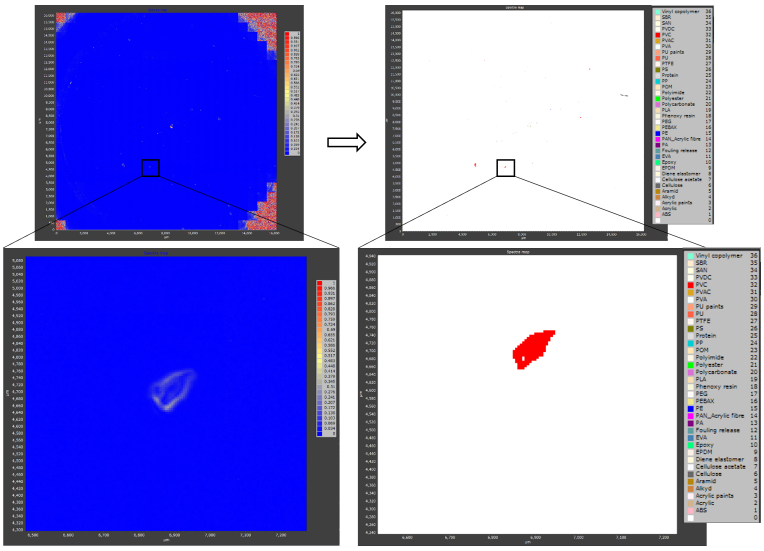

Fig. 3.3: Example of application of the siMPle software on an experimental chemical map. The particle shown was identified as PVC.

3 Occurrence of indoor breathable microplastics and filtering efficiency of a commercial surgical facemask

In this study, the indoor atmosphere of four locations in Aalborg (Denmark) was sampled during workdays and weekends to investigate the effect of human activity on the occurrence and formation of airborne MPs down to 1 µm. In addition, replicates of the samples were taken by mounting a type IIR surgical facemask on the sampling setup to quantify the MP retainment operated by this medical device. The goal of this work was to propose a straightforward analytical protocol employing µRaman for the monitoring of MP pollution in indoor air, as well as estimate the human MP intake of small airborne MPs when everyday tasks are performed. The study was organised in two main methodological steps, sampling and sample analysis.

3.1 Sampling

The locations selected were a workshop, a meeting room, an apartment located in the Northern part of Aalborg in a renewed building of the late XIX century (first floor), and an apartment in a building from 2014 (eighth floor) located in the city centre. For each sampling session, a vacuum pump (Lab Logistics Group GmbH, Germany) was connected to a metallic funnel (EMD Millipore Corporation, USA) hosting a 1 µm Silicon filter at its bottom, and the air flow was adjusted to 2 L/min by means of the pump's flowmeter. The sampling events took 24 hours each at an average breathing height of 1.60 m during workdays and weekends, and each sample was taken in two sampling sessions: without facemask, and putting a surgical facemask at the inlet of the funnel. Since a PTFE o-ring of 10 mm diameter was put on top of the filter to protect it from the metallic funnel, the airborne particles were concentrated onto the area delimited by the inner perimeter of the o-ring (approximately 10 mm in diameter). Figure 3.4 shows the sampling setup in the four investigated locations.

Fig. 3.4: The four investigated locations: (a) workshop; (b) meeting room; (c) apartment in the XIX century building; (d) apartment in the building from 2014.

After the sampling, the filters were stored in closed glass Petri dishes until the µRaman analysis was performed (**Paper III** reports in detail on the sampling procedure).

3.2 Sample analysis

The analysis of the air samples was conducted with an XPlora Nano Raman microscope (Horiba Sas, France). The system was equipped with a Peltier-cooled CCD detector and three solid-state laser sources emitting at 532, 638, and 785 nm. Briefly, each filter was analysed according to a semi-randomised approach: all the particles in the active area with a diameter above 10 µm were scanned, while 10% of the particles with a diameter between 1 and 10 µm were randomly selected on the whole area with the dedicated function of the instrument's software. The 638 nm laser was employed for both size fractions at 100% power (40.2 mW, grating 600 ll/mm), and the analysis was

performed at 50× magnification with a short-distance objective (Olympus, Japan) in the spectral range 0 - 3500 cm^{-1}. The spectral recognition was performed with the siMPle software as described in **Paper III**, which also reports in detail on the analysis protocol. The composition of the surgical facemasks was checked with FTIR-ATR (Cary 630 FTIR ATR, Agilent, USA) in the spectral range 600 - 4000 cm^{-1} by comparing the experimental spectra with Agilent Polymer Handheld ATR library (as described in **Paper III**).

Chapter 4

Research outcomes

This PhD study represents a collection of three distinct studies, having as a common goal to advance the state-of-the-art of the MP science field by providing new insights on the occurrence, formation, and fate of small MPs and NPs in drinking water and indoor air. The research carried out during the PhD underlined the pivotal role of spectroscopic methods in the MP analysis of environmental matrices, and three scientific papers were produced based on the outcomes described in the following of this chapter.

1 Occurrence, formation and fate of microplastics above 1 µm in a Danish conventional drinking water plant during routine activity

The study provided new insights on the influence of the MP size on the retainment performance of a conventional drinking water plant. In addition, it showed the application of the mass conservation law to small MPs from Raman spectroscopic data. Hence the MP concentration at the plant's inlet and outlet was calculated according to two complementary parameters: the MP counts per liter (N/L) and MP mass in picograms per liter (pg/L) (Figure 4.1).

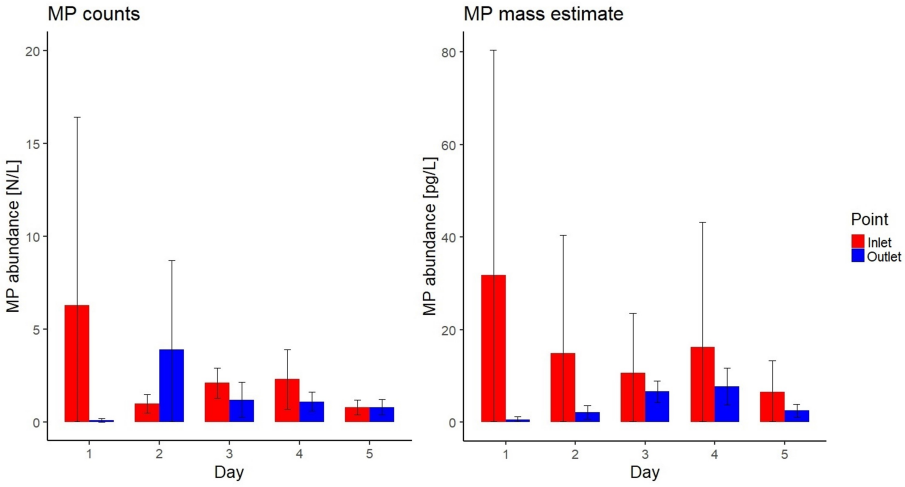

Fig. 4.1: MP abundance in counts per liter (N/L) and estimated mass per liter (pg/L) at the plant's inlet and outlet over the five investigated days (Maurizi *et al.* 2023).

The mean values of MP concentration found at the two sampling points (inlet: 2.5 ± 2.0 N/L, 16.0 ± 8.5 pg/L; outlet: 1.4 ± 1.3 N/L, 4.0 ± 2.7 pg/L) were generally higher than in previous works if the MP counts are considered (Pitroff *et al.* 2022, Mintenig *et al.* 2019). However, it must also be considered that most of the works published so far relied on spectroscopic techniques with a coarser spatial resolution (typically µFTIR), which does not allow for efficiently detecting MPs below 10 µm. The overall MP retainment efficiency of the plant was obtained by cumulating the MP abundance at the inlet and outlet for each investigated day, and it was 43.2 ± 45.9% in terms of MP counts and 75.1 ± 28.2% in terms of MP mass. These values of MP removal were comparable with those found in the literature for more advanced facilities (Enfrin *et al.* 2019, Cherniak *et al.* 2022) and, in the case of the current study, were associated to the release of 1 - 5 µm MPs from the plastic elements of the facility. On day 2 of the investigated period, the MP counts at the outlet (3.9 ± 5.6 N/L) were approximately 4 times higher than at the inlet (1.0 ± 0.6 N/L), and for the remaining three days the MP counts at the outlet showed close values regardless of the MP counts at the inlet (Figure 4.1). This was not the case for the MP mass concentration, which proved to be lower at the outlet on all investigated days. Hence it was hypothesized that a release of small-sized MPs occurred during the water treatment between inlet and outlet, as they did not hold a large mass altogether.
The study of the polymer composition suggested that the released MPs were mostly poly-amide (PA), this being the most common polymer according to

the MP counts and the second most frequent according to the MP mass. The retainment efficiency was also calculated according to the MP size, which showed that the 1 - 5 µm MPs were the least retained during the treatment (41.1%), as opposed to the larger MPs (above 70%). This finding was in good accordance with previous works modeling the dynamics of deep bed filtration (e.g. Zamani *et al.* 2009), which is characterised by a drop in the performance for particles roughly sized 1 µm. Based on these outcomes, an intake of 1533 N/(year·capita) (4.4 ng/(year·capita)) was estimated for a male subject drinking the water treated by the investigated plant. Despite this estimation being still lower than those from other pathways such as food (1.42 - $1.54 \cdot 10^5$ N/(year·capita), Bai *et al.* 2022) and air ($2.38 \cdot 10^6$ N/(year·capita), Vianello *et al.* 2019), it was nonetheless several orders of magnitude higher than that of Kirstein *et al.* (2021).
The qualitative exploration of the NP fraction in the drinking water samples provided 621 plastic-like Raman spectra for the particles sized 0.45 - 1 µm (Figure 4.2). This proof-of-concept demonstrated the applicability of µRaman to the analysis of environmental NPs, which is a topic of concern increasingly attracting specialised research. Further details are available in **Paper I**.

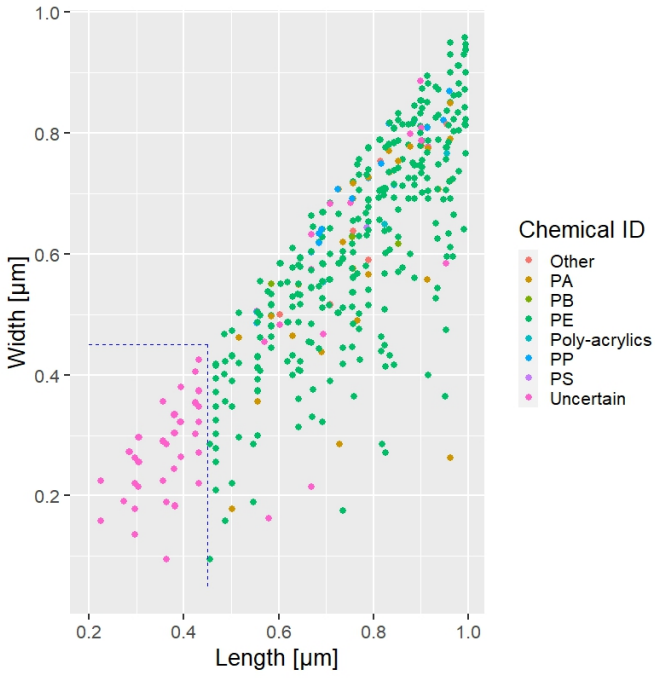

Fig. 4.2: Width *vs* Length for the analysed nanoparticles. The blue dotted line indicates the size limit above which the chemical identification was possible (Maurizi *et al.* 2023).

2 Comparison of the outcomes from Raman micro-spectroscopy and FTIR micro-spectroscopy applied to the analysis of the same set of drinking water samples

The results obtained in **Paper I** were compared to the outcomes from the µFTIR analysis of the same set of drinking water samples. The study aimed at putting in perspective the current state-of-the-art, which has mostly relied on µFTIR, thus neglecting the contribution of small-sized MPs. Overall, the coarser spatial resolution of µFTIR compared to µRaman could justify the outcome from **Paper II**: no MPs below 13.3 µm could be identified in the samples, and the rate of false negatives unexpectedly started increasing already below 50 µm, which led to the loss of roughly 95% of the entire MP population of the samples. The MP diameter datasets from the two techniques were merged to extrapolate the total MP population in the range 1 - 1865.9 µm (the largest MP identified by µFTIR), and it was showed that the MP frequency could be described by a third-power function against the MP size (Kooi and Koelmans 2018). 86% of the MPs was shown bewteen 1 and 5 µm and 9.7% between 5 and 10 µm, hence the total distribution was skewed to the smaller size values (Figure 4.3).

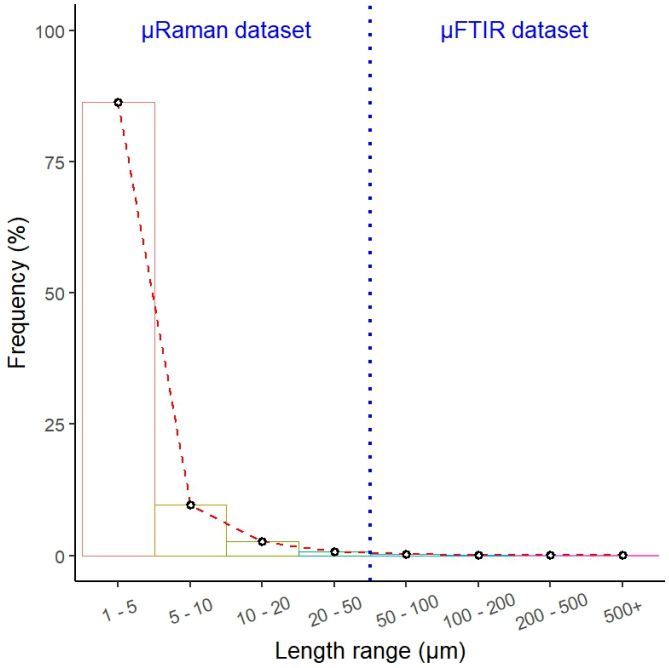

Fig. 4.3: MP frequency by length range in the analysed drinking water samples. For the range 1 - 50 μm, the data from the μRaman analysis were considered, while for the 50 - 1865.9 μm range the results from the μFTIR analysis were employed (**Paper II**).

Consequently, the mean MP counts concentration proved to be significantly lower at the sampling points (inlet 31.9 ± 17.2 N/m^3, outlet 5.0 ± 2.1 N/m^3) than the values from the μRaman analysis (Figure 4.4), as opposed to the mean MP mass concentration (inlet 76.3 ± 106.3 μg/m^3, outlet 2.8 ± 2.8 μg/m^3), which was approximately 10^3 higher (Figure 4.5). Only on day 3 the MP mass concentration at the outlet (8.1 ± 16.0 μg/m^3) was higher than at the inlet (0.3 ± 0.5 μg/m^3), hence the MP removal efficiency proved to be higher than that calculated from the μRaman data (MP counts 78.1 ± 49.7%, MP mass 98.7 ± 11.1%). Importantly, these values of MP removal were in good accordance with the outcome from **Paper I** for the 10+ μm MPs. The estimated MP human intake was 5 N/(year·capita) (1.9 μg/(year·capita)), which was roughly 332 times lower than the outcome from μRaman, although in line with the result of Kirstein *et al.* (2021). For further details, see **Paper II**.

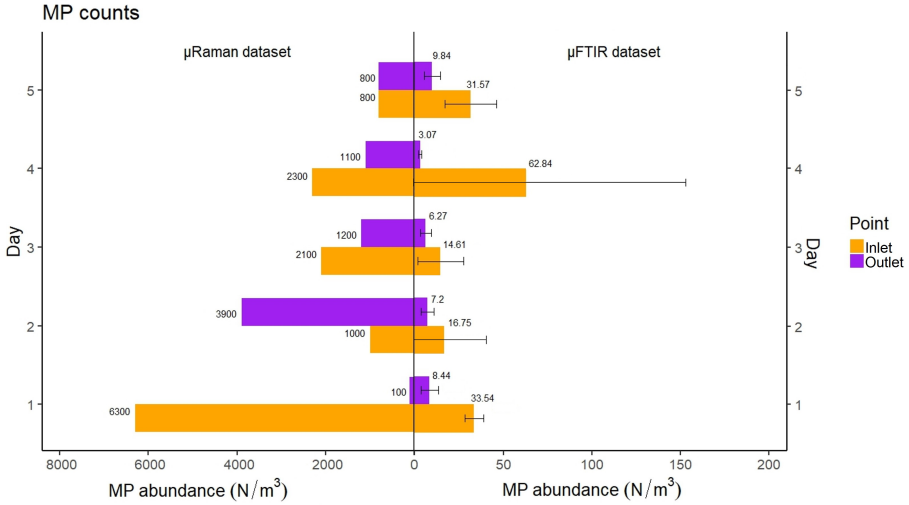

Fig. 4.4: MP counts abundance according to µFTIR and µRaman at the plant's inlet and outlet over the five investigated days (**Paper II**).

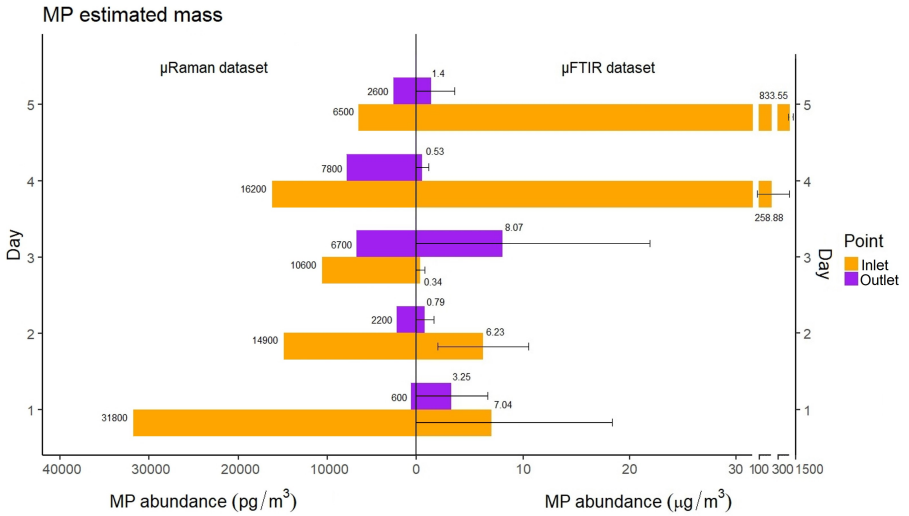

Fig. 4.5: MP estimated mass abundance according to µFTIR and µRaman at the plant's inlet and outlet over the five investigated days (**Paper II**).

3 Occurrence of indoor breathable microplastics and filtering efficiency of a commercial surgical facemask

The study addressed the source and occurrence of indoor airborne MPs sized 1 - 10 µm, which are suspected to cause more adverse health effects on humans due to their higher translocation rate (Wieland *et al.* 2022). In addition, the potential use of surgical facemasks to limit the human intake of airborne indoor MPs was investigated in locations where different human activities were performed. Regarding the samples taken without the surgical facemask, the median MP concentration (counts of MPs per cubic metre, N/m^3) was 212 ± 233 N/m^3, proving to be higher than that in previous works (Vianello *et al.* 2019, Perera *et al.* 2022). To explain the difference between the MP concentration in the investigated locations on workdays and weekends, the type and degree of human activity had to be considered, as well as the building characteristics of the indoor environments. In general, the MP concentration was expected to be higher in the high-activity periods (workdays for the workplaces and weekends for the apartments). However, the meeting room and the apartment in the XIX century building presented an inverted tendency, which could be explained by considering that air currents occurred in these locations when humans were active. The MP concentrations obtained from the samples taken with the facemask were generally lower (4 - 196 N/m^3), showing that a filtering effect occurred (Figure 4.6).

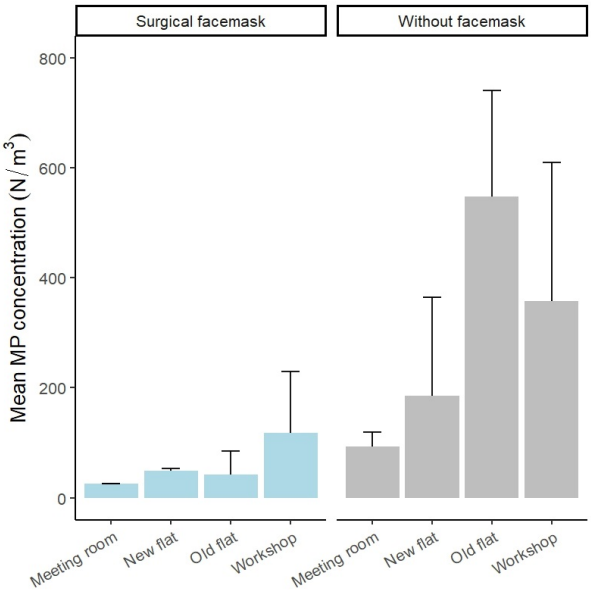

Fig. 4.6: Mean MP concentration with and without the surgical facemask in the investigated indoor locations (**Paper III**).

The analysed MPs were classified into two morphotypes, fragments and fibres, according to their Diameter/Width ratio as previously done by Vianello *et al.* (2019). Specifically, the MPs with a Diameter/Width ratio below 3 were considered fragments, otherwise fibres. Fragments represented the majority (99%) of the analysed MPs, which conflicted with the common observation of prevailing presence of fibres in indoor atmosphere (Jenner *et al.* 2021, Choi *et al.* 2022). The polymer composition of the samples was mostly affected by the location (i.e. type of human activity), and PA was the most common polymer detected during the µRaman analysis.
The samples taken with the surgical facemask showed a higher frequency of the 1 - 5 µm MPs (74.1%) than the samples taken without the facemask (45.2%, Figure 4.7). Although the overall filtering efficiency for the MPs > 1 µm was 85.4 ± 3.9%, the 1 - 5 µm fraction (breathable MPs) was the least retained (57.6%), whilst for the larger MPs values above 80% were found. This outcome matched well with the study of Tcharkhtchi *et al.* (2021), who calculated for commercial surgical facemasks a filtering efficiency around 50% for airborne particles below 5 µm.

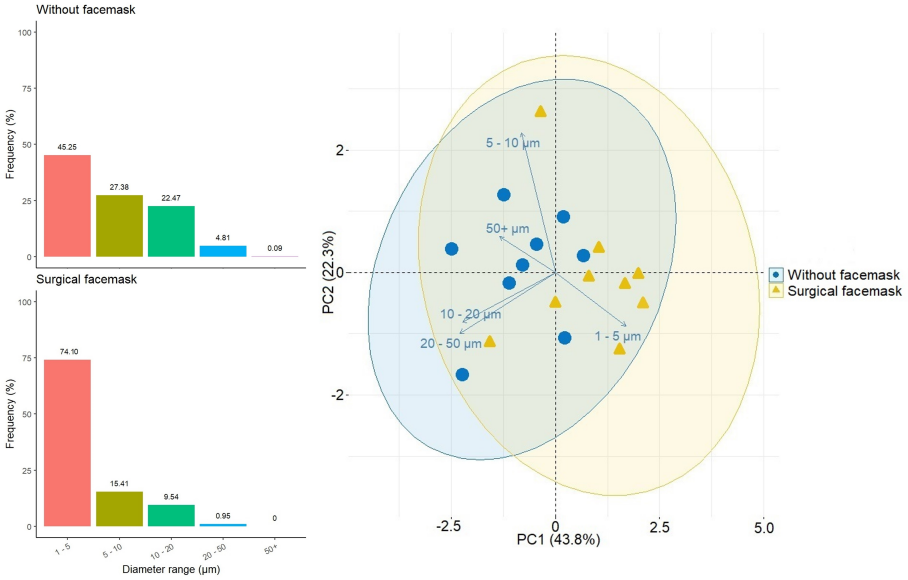

Fig. 4.7: MP diameter frequency with and without the surgical facemask (**Paper III**).

The human exposure to indoor airborne MPs was estimated for the four locations during the high-activity periods. A mean value of 3415 ± 2881 N/(day·capita) was obtained for a male subject not wearing the surgical facemask and 283 ± 317 N/(day·capita) for one with the facemask on. The estimated intake for an unprotected subject was dramatically higher than in previous works (Cox *et al.* 2019, Soltani *et al.* 2021), since this study was the first one ever performed on indoor airborne MPs down to 1 µm with an automatised analytical protocol. Although the usage of a surgical facemask would decrease the intake by roughly 10 times, the persisting prevalence of 1 - 5 µm MPs in the filtered particulate questions the utility of such a hygienic measure in the everyday life.

Chapter 5

Conclusions

This PhD study was divided into the following three research questions, which were addressed following the established objectives. The conclusions drawn for each question are hence reported.

Research question 1: *How efficient is a conventional drinking water plant to retain microplastics down to 1 µm? Is it possible to employ Raman micro-spectroscopy to analyse NPs in drinking water?*
The retainment efficiency of a conventional drinking water plant depends on the MP size taken into consideration. The smaller the MPs, the lower the efficiency of the plant in removing them from the raw water, the 1 - 5 µm range being the most critical one. In addition, a drinking water plant can be a hotspot for MP release *per se*, due to the ageing process undergone by the plastic elements of the facility. This further hinders the MP retainment, as additional plastic particles are added during the drinking water treatment. Hence the smaller fraction of MPs should be extensively monitored to obtain more accurate values of MP retainment and human exposure, while a deeper knowledge on the risk associated to the human intake of small MPs should be achieved.
Raman micro-spectroscopy proved to be a useful tool to analyse NPs in drinking water, which is important as NPs are likely much more numerous than MPs in the environment. Hence conventional drinking water plants may prove less efficient in retaining NPs, given their small size and abundance. Finally, NPs may also be released by aged plastic components of a waterworks in a similar fashion to MPs, hence posing further questions on the related human exposure.

Research question 2: *How does the choice of a certain spectroscopic technique influence the MP quantification in drinking water and the subsequent estimation of MP human intake?*

The coarser the spatial resolution of the technique employed, the fewer the MPs that can be identified. This is due to the major abundance of small-sized MPs (below 10 µm) when compared to larger MPs in the environment, here included drinking water sources and treated drinking water. Importantly, besides the nominal size resolution of a spectroscopic technique, there is also an experimental size resolution limit, which can be obtained by comparing two complementary methods such as µRaman and µFTIR. With this approach, it can be seen that the experimental size resolution of µFTIR is higher than the nominal one, hence much more MPs than expected are missed with this technique. By comparing µFTIR and µRaman, it clearly emerged that small sized MPs carry most of the information of a sample and they must necessarily be included in the quantification process to obtain a more accurate picture of the studied system.

Research question 3: *Do the type and degree of human activity in indoor environments influence the fate and occurrence of small airborne MPs? Is it possible to reduce the related human exposure somehow?*
When humans operate in indoor environments, they produce airborne MPs, most of which fall in the breathable range. Hence, as seen for drinking water, the smaller, the more abundant MPs are, and proper analytical protocols have to be employed to quantify them. Being a kind of airborne particulate, indoor airborne MPs may also be subjected to the same diffusion dynamics, which depend on the degree of air exchange and the architectural characteristics of the investigated locations. Reducing the human exposure to breathable MPs (without reducing the time spent indoors) by means of respirators would be impractical (or useless in the case of surgical facemasks). However, more research on the toxicological effects of breathable MPs should be conducted to decide on the appropriateness of preventive hygienic measures.

Chapter 6

Main contributions to the science field and future perspectives

Microplastic pollution has increasingly gained the attention of scientists and public opinion due to its pervasivity in natural and anthropogenic environments. The multi-disciplinary approach requested to perform the microplastic analysis of environmental matrices boosted the development of technical solutions *ad hoc* and the collaboration among several specialists with different backgrounds, often not limited to the hard sciences. Providing reliable and reproducible results is the only way to understand the extent of the microplastic threat to ecosystems and humans, and this requires awareness of the advantages and drawbacks associated with the analytical techniques employed in the microplastic science field. Further, pushing the limits of the instrumental apparati shows how much research is still needed to address the next level of the plastic pollution challenge, the nanoplastics.
This PhD study addressed these aspects, putting into perspective the current state-of-the-art on MP pollution in drinking water and indoor air with the provision of new knowledge based on scientifically accurate data. The results reported do not aim to be definitive, but they rather demonstrate how much effort should be devoted to compose a more complete picture of the microplastic problem. Overall, the main aim of this PhD was to advance the MP science field by proposing novel strategies to characterise small microplastics and nanoplastics in environmental systems associated with human exposure. Hence this study fully embodies the transition currently occurring in the microplastic science field, where research focusing on small microplastics and nanoplastics is increasingly growing.

The result from **Paper I** demonstrated the multi-faceted nature of microplastic pollution in drinking water, which depends both on the particulate dynamics involving microplastics during the drinking water treatment and the ageing process of the plastic elements of waterworks. The study represented a successful application of the mass conservation to small-sized microplastics from purely spectroscopic data, thus overcoming the sensitivity of classical thermochemical methods. The not negligible presence of small microplastics in the treated water led to a more realistic intake estimation than those of previous studies, which were affected by the technical limitations of the methods employed. Further, for the first time, the nanoplastic fraction found in the samples was qualitatively explored, which represented an important step forward to address the nanoplastic issue with an already existing technology.

Paper II experimentally showed how the choice of the analytical method influences the results provided by the same samples, hence the message told by the study can radically change. Results of past works should be put into perspective in the light of the new technological advances in the field of spectroscopy, where novel radiation sources and system geometries are being developed. **Paper II** is the first one to address this issue in these terms for the microplastic analysis of drinking water. This especially applies to small microplastics and nanoplastics, whose reliable quantification has already become a pressing need and cannot be ignored anymore.

Paper III is a first-time investigation on indoor airborne microplastics in the breathable range. It also shows the flexibility of the current commercial spectroscopic systems, which can be applied to quite different matrices and still provide accurate data on microplastic occurrence and fate. This work will hopefully initiate further effort to improve the state-of-the-art of the topic, creating more data relevant for assessing human health impacts.

References

Abbasi S., Keshavarzi B., Moore F., Turner A., Kelly F.J., Dominguez A.O., Jaafarzadeh N., Distribution and potential health impacts of microplastics and microrubbers in air and street dusts from Asaluyeh County, Iran, Environ. Pollut., 244, 153-164 (2019), ISSN 0269-7491, https://doi.org/10.1016/j.envpol.2018.10.039

Akhbarizadeh R., Dobaradaran S., Torkmahalleh M.A., Saeedi R., Aibaghi R., Ghasemi F.F., Suspended fine particulate matter (PM2.5), microplastics (MPs), and polycyclic aromatic hydrocarbons (PAHs) in air: Their possible relationships and health implications, Environmen. Res. 192, 110339 (2021), ISSN 0013-9351, https://doi.org/10.1016/j.envres.2020.110339

Alexander J., Ard L.B., Bignami M., Ceccatelli S., Lundebye A.K., Presence of microplastics and nanoplastics in food, with particular focus on seafood, EFSA J. 14, 4501 (2016), 10.2903/j.efsa.2016.4501

Andrady A.L., Neal M.A., Applications and societal benefits of plastics, Phil. Trans. R. Soc., B3641977–1984 (2009), http://doi.org/10.1098/rstb.2008.0304

Auta H.S., Emenike C.U., Fauziah S.H., Distribution and importance of microplastics in the marine environment: A review of the sources, fate, effects, and potential solutions, Environ. Int. 102, 165-176 (2017), ISSN 0160-4120, https://doi.org/10.1016/j.envint.2017.02.013

Bai C., Liu L., HuY., Zeng E.Y., Guo Y., Microplastics: A review of analytical methods, occurrence and characteristics in food, and potential toxicities to biota, Sci. of The Tot. Environ., 806, 1, 150263 (2022), ISSN 0048-9697, https://doi.org/10.1016/j.scitotenv.2021.150263

Bailo E., Deckert V., Tip-enhanced Raman scattering, Chem. Soc. Rev. 37, 921-930 (2008), DOI: 10.1039/B705967C

Bergmann M., Mützel S., Primpke S., Tekman M.B., Trachsel J., Gerdts G., White and wonderful? Microplastics prevail in snow from the Alps to the Arctic, Sci. Adv. 5, 8 (2019), DOI: 10.1126/sciadv.aax1157

Berthomieu C., Hienerwadel R., Fourier transform infrared (FTIR) spectroscopy, Photosynth. Res. 101, 157–170 (2009), https://doi.org/10.1007/s11120-009-9439-x

Bläsing M., Amelung W., Plastics in soil: Analytical methods and possible sources, Sci. of The Total Environ., 612, 422-435 (2018), ISSN 0048-9697, https://doi.org/10.1016/j.scitotenv.2017.08.086

Bowley J., Baker-Austin C., Porter A., Hartnell R., Lewis C., Oceanic Hitchhikers – Assessing Pathogen Risks from Marine Microplastic, Tr. in Microbiol., 29, 2, 107-116 (2021), ISSN 0966-842X, https://doi.org/10.1016/j.tim.2020.06.011

Brennecke D., Duarte B., Paiva F., Caçador I., Canning-Clode J., Microplastics as vector for heavy metal contamination from the marine environment, Estuar., Coast. and Shelf Sci., 178, 189-195 (2016), ISSN 0272-7714, https://doi.org/10.1016/j.ecss.2015.12.003

Browne M.A., Galloway T., Thompson R., Microplastic–an emerging contaminant of potential concern?, Integrated Environmental Assessment and Management, 3, 4, 559-561 (2007), 10.1002/ieam.5630030412

Buteler M., Fasanella M, Alma A.M., Silva L.I., Langenheim M., Pablo Tomba J.P., Lakes with or without urbanization along their coasts had similar level of microplastic contamination, but significant differences were seen between sampling methods, Sci. of The Total Environ., 866, 161254 (2023), ISSN 0048-9697, https://doi.org/10.1016/j.scitotenv.2022.161254

Chand R., Rasmussen L.A., Tumlin S., Vollertsen J., The occurrence and fate of microplastics in a mesophilic anaerobic digester receiving sewage sludge, grease, and fatty slurries, Sci. of The Total Environ., 798, 149287 (2021), ISSN 0048-9697, https://doi.org/10.1016/j.scitotenv.2021.149287

Chatterjee S., Sharma S., Microplastics in our oceans and marine health, FACTS Reports, 19, 54-61 (2019)

Chen G., Fu Z., Yang H., Wang J., An overview of analytical methods for detecting microplastics in the atmosphere, TrAC Trends in Anal. Chem. 130, 115981 (2020), ISSN 0165-9936, https://doi.org/10.1016/j.trac.2020.115981

Cherniak S.L., Almuhtaram H., McKie M.J., Hermabessiere L., Yuan C., Roch man C.M., Andrews R.C., Conventional and biological treatment for the removal of microplastics from drinking water, Chemosphere, 288, 132587 (2022), ISSN 0045-6535, https://doi.org/10.1016/j.chemosphere.2021.132587

Choi H., Lee I., Kim H., Park J., Cho S., Oh S., Lee M., Kim H., Comparison of Microplastic Characteristics in the Indoor and Outdoor Air of Urban Areas of South Korea, Water Air Soil Pollut. 233, 169, (2022), https://doi.org/10.1007/s11270-022-05650-5

a. Cole M., Lindeque P., Halsband C., Galloway T.S., Microplastics as contaminants in the marine environment: A review, Mar. Pollut. Bull., 62, 12, 2588-2597 (2011), ISSN 0025-326X, https://doi.org/10.1016/j.marpolbul.2011.09.025

b. Cole M., Webb H., Lindeque P.K., Fileman E.S., Halsband C., Galloway T.S., Isolation of microplastics in biota-rich seawater samples and marine organisms, Sci. Rep. 4, 4528 (2014), DOI: 10.1038/srep04528

Cox K.D., Covernton G.A., Davies H.L., Dower J.F., Juanes F., Dudas S.E., Human Consumption of Microplastics, Environ. Sci. Technol., 53, 12, 7068–7074 (2019), https://doi.org/10.1021/acs.est.9b01517

Dalmau-Soler J., Ballestros-Cano R., Boled M., Paraira M., Ferrer N., Lacorte S., Microplastics from headwaters to tap water: occurrence and removal in a drinking water treatment plant in Barcelona Metropolitan area (Catalonia, NE Spain), Environ. Sci. Pollut. Res. 28, 59462–59472 (2021), https://doi.org/10.1007/s11356-021-13220-1

De Falco F., Di Pace E., Cocca M., Avella M., The contribution of washing processes of synthetic clothes to microplastic pollution., Sci. Rep., 9, 6633 (2019), https://doi.org/10.1038/s41598-019-43023-x

Derraik J.G.B., The pollution of the marine environment by plastic debris: a review, Mar. Pollut. Bull., 44, 9, 842-852 (2002), ISSN 0025-326X, https://doi.org/10.1016/S0025-326X(02)00220-5

Devi M.K., Karmegam N., Manikandan S., Subbaiya R., Song H., Kwon E.E., Sarkar B., Bolan N., Kim W., Rinklebe J., Govarthanan M., Removal of nanoplastics in water treatment processes: A review, Sci. of The Total Environ., 845, 157168 (2022), ISSN 0048-9697, https://doi.org/10.1016/j.scitotenv.2022.157168

Dris R., Gasperi J., Saad M., Mirande C., Tassin B., Synthetic fibers in atmospheric fallout: A source of microplastics in the environment?, Mar. Pollut. Bull. 104, 1–2, 290-293 (2016), ISSN 0025-326X, https://doi.org/10.1016/j.marpolbul.2016.01.006

Ebere Enyoh C.E., Verla A.W., Verla E.N., Ibe F.C., Amaobi C.E., Airborne microplastics: a review study on method for analysis, occurrence, movement and risks, Environ. Monit. Assess. 191, 668 (2019), https://doi.org/10.1007/s10661-019-7842-0

Elkhatib D., Oyanedel-Craver V., A Critical Review of Extraction and Identification Methods of Microplastics in Wastewater and Drinking Water, Environ. Sci. Technol. 54, 12, 7037–7049 (2020), https://doi.org/10.1021/acs.est.9b06672

Enfrin M., Dumée F. L., Lee J., Nano/microplastics in water and wastewater treatment processes – Origin, impact and potential solutions, Water Res. 161, 621-638 (2019), https://doi.org/10.1016/j.watres.2019.06.049

Fan Y., Zheng J., Ren J., Luo J., Cui X., Ma L.Q., Effects of storage temperature and duration on release of antimony and bisphenol A from polyethylene terephthalate drinking water bottles of China, Environ. Pollut. 192, 113-120 (2014), ISSN 0269-7491, https://doi.org/10.1016/j.envpol.2014.05.012

Fendall L.S., Sewell M.A., Contributing to marine pollution by washing your face: Microplastics in facial cleansers, Mar. Pollut. Bull., 58, 8, 1225-1228 (2009), ISSN 0025-326X, https://doi.org/10.1016/j.marpolbul.2009.04.025

Free C.M., Jensen O.P., Mason S.A., Eriksen M., Williamson N.J., Boldgiv B., High-levels of microplastic pollution in a large, remote, mountain lake, Mar. Pollut. Bull., 85, 1, 156-163 (2014), ISSN 0025-326X, https://doi.org/10.1016/j.marpolbul.2014.06.001

Frias J.P.G.L., Nash R., Microplastics: Finding a consensus on the definition, Mar. Pollut. Bull., 138, 145-147 (2019), ISSN 0025-326X, https://doi.org/10.1016/j.marpolbul.2018.11.022

Gaylarde C.C., Neto J.A.B., da Fonseca E.M., Paint fragments as polluting microplastics: A brief review, Mar. Pollut. Bull., 162, 111847 (2021), ISSN 0025-326X, https://doi.org/10.1016/j.marpolbul.2020.111847

Gigault J., ter Halle A., Baudrimont M., Pascal P., Gauffre F., Phi T., Hadri H., Grassl B., Reynaud S., Current opinion: What is a nanoplastic?, Environ. Pollut., 235, 1030-1034 (2018), ISSN 0269-7491, https://doi.org/10.1016/j.envpol.2018.01.024

Gomiero A., Øysæd K.B., Palmas L., Skogerbø G., Application of GCMS-pyrolysis to estimate the levels of microplastics in a drinking water supply system, J. of Hazard. Mater. 416, 125708 (2021), ISSN 0304-3894, https://doi.org/10.1016/j.jhazmat.2021.125708

Guo X., Lin H., Xu S., He L., Recent Advances in Spectroscopic Techniques for the Analysis of Microplastics in Food, J. Agric. Food Chem. 70, 5, 1410–1422 (2022), https://doi.org/10.1021/acs.jafc.1c06085

Hartline N.L., Bruce N.J., Karba S.N., Ruff E.O., Sonar S.U., Holden P.A., Microfiber Masses Recovered from Conventional Machine Washing of New or Aged Garments, Environ. Sci. Technol. 50, 21, 11532–11538 (2016), https://doi.org/10.1021/acs.est.6b03045

Hidalgo-Ruz V., Gutow L., Thompson R.C., Thiel M., Microplastics in the Marine Environment: A Review of the Methods Used for Identification and Quantification, Environ. Sci. Technol., 46, 6, 3060–3075 (2012), https://doi.org/10.1021/es2031505

Horton A.A., Plastic pollution: When do we know enough?, J. of Hazard. Mater., 422, 126885 (2022), ISSN 0304-3894, https://doi.org/10.1016/j.jhazmat.2021.126885

Huang Y., Wong K.K., Li W., Zhao H., Wang T., Stanescu S., Boult S., van Dongen B., Mativenga P., Li L., Characteristics of nano-plastics in bottled drinking water, J. of Hazard. Mater., 424, C, 127404 (2022), ISSN 0304-3894, https://doi.org/10.1016/j.jhazmat.2021.127404

Jenner L.C., Sadofsky L.R., Danopoulos E., Rotchell J.M., Household indoor

microplastics within the Humber region (United Kingdom): Quantification and chemical characterisation of particles present, Atmos. Environ., 259, 118512 (2021), ISSN 1352-2310, https://doi.org/10.1016/j.atmosenv.2021.118512

Kirstein I.V., Hensel F., Gomiero A., Iordachescu L., Vianello A., Wittgren H.B., Vollertsen J., Drinking plastics? – Quantification and qualification of microplastics in drinking water distribution systems by µFTIR and Py-GCMS, W. Res. 188, 116519 (2021), ISSN 0043-1354, https://doi.org/10.1016/j.watres.2020.116519

Koelmans A.A., Nor N.H.M., Hermsen E., Kooi M., Mintenig S.M., De France J., Microplastics in freshwaters and drinking water: Critical review and assessment of data quality, W. Res., 155, 410-422 (2019), ISSN 0043-1354, https://doi.org/10.1016/j.watres.2019.02.054

Kooi M., Koelmans A. A., Simplifying Microplastic via Continuous Probability Distributions for Size, Shape, and Density, Environ. Sci. & Technol. Lett. 6 (9), 551-557 (2019), doi: 10.1021/acs.estlett.9b00379

Lambert S., Sinclair C., Boxall A., Occurrence, Degradation, and Effect of Polymer-Based Materials in the Environment, Reviews of Environmental Contamination and Toxicology 227. Springer, Cham. (2014), https://doi.org/10.1007/978-3-319-01327-51

Lenz R., Enders K., Stedmon C.A., Mackenzie D.M.A., Nielsen T.G., A critical assessment of visual identification of marine microplastic using Raman spectroscopy for analysis improvement, Mar. Pollut. Bull. 100, 1, 82-91 (2015), ISSN 0025-326X, https://doi.org/10.1016/j.marpolbul.2015.09.026

Leusch F.D.L., Lu H., Perera K., Neale P.A., Ziajahromi S., Analysis of the literature shows a remarkably consistent relationship between size and abundance of microplastics across different environmental matrices, Environ. Pollut., 319, 120984 (2023), ISSN 0269-7491, https://doi.org/10.1016/j.envpol.2022.120984

Li Y., Shao L., Wang W., Zhang M., Feng X., Li W., Zhang D., Airborne fiber particles: Types, size and concentration observed in Beijing, Sci. of The Total Environ. 705, 135967 (2020), ISSN 0048-9697, https://doi.org/10.1016/j.scitotenv.2019.135967

Li Y., Wang Z., Guan B., Separation and identification of nanoplastics in tap water, Environ. Res., 204, B, 112134 (2022), ISSN 0013-9351, https://doi.org/10.1016/j.envres.2021.112134

Liu F., Olesen K.B., Borregaard A.R., Vollertsen J., Microplastics in urban and highway stormwater retention ponds, Sci. of The Total Environ., 671, 992-1000 (2019), ISSN 0048-9697, https://doi.org/10.1016/j.scitotenv.2019.03.416

Maurizi L., Iordachescu L., Kirstein I.V., Nielsen A.H., Vollertsen J., Do drinking water plants retain miroplastics? An exploratory study using Raman

micro-spectroscopy, Heliyon, 9, 6, e17113 (2023), https://doi.org/10.1016/j.heliyon.2023.e17113

Mbachu O., Jenkins G., Pratt C., Kaparaju P., A New Contaminant Superhighway? A Review of Sources, Measurement Techniques and Fate of Atmospheric Microplastics, Water Air Soil Pollut. 231, 85 (2020), https://doi.org/10.1007/s11270-020-4459-4

MICRO 2022. (2022, November 25). Lanzarote Declaration, MICRO 2022 for the UN Treaty on Plastic Pollution. MICRO 2022, Online Atlas Edition: Plastic Pollution from MACRO to nano (MICRO 2022), https://doi.org/10.5281/zenodo.7359316

Mintenig S.M., Löder M.G.J., Primpke S., Gerdts G., Low numbers of microplastics detected in drinking water from ground water sources, Sci. of The Total Environ. 648, 631-635 (2019), ISSN 0048-9697, https://doi.org/10.1016/j.scitotenv.2018.08.178

Mitrano D.M., Beltzung A., Frehland S., Schmiedgruber M., Cingolani A., Schmidt F., Nat. Nanotechnol. 14, 362–368 (2019), https://doi.org/10.1038/s41565-018-0360-3

Molazadeh M., Liu F., Simon-Sánchez L., Vollersten J., Buoyant microplastics in freshwater sediments – How do they get there?, Sci. of The Total Environ., 860, 160489 (2023), ISSN 0048-9697, https://doi.org/10.1016/j.scitotenv.2022.160489

Moore C.J., Synthetic polymers in the marine environment: A rapidly increasing, long-term threat, Environ. Res., 108, 2, 131-139 (2008), ISSN 0013-9351, https://doi.org/10.1016/j.envres.2008.07.025

Moreno T., Rivas T., Bouso L., Viana M., Jones T., Àlvarez-Pedrerol M., Alastuey A., Sunyer J., Querol X., Variations in school playground and classroom atmospheric particulate chemistry, Atmos. Environ. 91, 162-171 (2014), ISSN 1352-2310, https://doi.org/10.1016/j.atmosenv.2014.03.066

Mortensen N.P., Fennell T.R., Johnson L.M., Unintended human ingestion of nanoplastics and small microplastics through drinking water, beverages, and food sources, NanoImpact, 21, 100302 (2021), ISSN 2452-0748, https://doi.org/10.1016/j.impact.2021.100302

Nirmala K., Rangasamy G., Ramya M., Shankar V.U., Rajesh G., A critical review on recent research progress on microplastic pollutants in drinking water, Environ. Res., 222, 115312 (2023), ISSN 0013-9351, https://doi.org/10.1016/j.envres.2023.115312

O'Connor D., Pan S., Shen Z., Song Y., Jin Y., Wu W., Hou D., Microplastics undergo accelerated vertical migration in sand soil due to small size and wet-dry cycles, Environ. Pollut. 249, 527-534 (2019), ISSN 0269-7491, https://doi.org/10.1016/j.envpol.2019.03.092

Oladoja N.A., Unuabonah I.E., The pathways of microplastics contamination

in raw and drinking water, J. of W. Process Eng. 41, 102073 (2021), ISSN 2214-7144, https://doi.org/10.1016/j.jwpe.2021.102073

Oßmann B.E., Sarau G., Holtmannspötter H., Pischetsrieder M., Christiansen S.H., Dicke W., Small-sized microplastics and pigmented particles in bottled mineral water, W. Res. 141, 307-316 (2018), ISSN 0043-1354, https://doi.org/10.1016/j.watres.2018.05.027

Patel M.M., Goyal B.R., Bhadada S.V., Bhatt J.S., Amin A.F., Getting into the Brain, CNS Drugs 23, 35–58 (2009). https://doi.org/10.2165/00232102-200923010-00003

Perera K., Ziajahromi S., Nash S.B., Manage P.M., Leusch F.D.L., Airborne Microplastics in Indoor and Outdoor Environments of a Developing Country in South Asia: Abundance, Distribution, Morphology, and Possible Sources, Environ. Sci. Technol. 56, 23, 16676–16685 (2022), https://doi.org/10.1021/acs.est.2c05885

Picó I., Manzoor I., Soursou V., Barceló D., Microplastics in water, from treatment process to drinking water: analytical methods and potential health effects, Water. Emerg. Contam. Nanoplastics 1, 13 (2022), 10.20517/wecn.2022.04

Pittroff M., Mü Y.K., Witzig C.S., Scheurer M., Storck F.R., Zumbülte N., Microplastic analysis in drinking water based on fractionated filtration sampling and Raman microspectroscopy, Environ. Sci. Pollut. Res. 28, 59439–59451 (2021), https://doi.org/10.1007/s11356-021-12467-y

a. Pivokonsky M., Cermakova L., Novotna K., Peer P., Cajthaml T., Janda V., Occurrence of microplastics in raw and treated drinking water, Sci. of the Total Environ. 643, 1644–1651 (2018), ISSN 0048-9697, https://doi.org/10.1016/j.scitotenv.2018.08.102

b. Pivokonsky M., Pivokonská L., Novotna K., Čermáková L., Klimtová M., Occurrence and fate of microplastics at two different drinking water treatment plants within a river catchment, Sci. of the Total Environ. 741, 140236 (2020), ISSN 0048-9697, https://doi.org/10.1016/j.scitotenv.2020.140236

Praveena S.M., Laohaprapanon S., Quality assessment for methodological aspects of microplastics analysis in bottled water – A critical review, Food Control 130, 108285 (2021), ISSN 0956-7135, https://doi.org/10.1016/j.foodcont.2021.108285

a. Primpke S., Lorenz C., Rascher-Friesenhausen R., Gerdts G., An automated approach for microplastics analysis using focal plane array (FPA) FTIR microscopy and image analysis, Anal. Methods 9, 1499-1511 (2017), DOI: 10.1039/C6AY02476A

b. Primpke S., Cross R.K., Mintenig S.M., Simon M. , Vianello A., Gerdts G., Vollertsen J., Toward the Systematic Identification of Microplastics in the Environment: Evaluation of a New Independent Software Tool (siMPle)

for Spectroscopic Analysis, Appl. Spectrosc., 74, 9, 1127–1138 (2020), DOI: 10.1177/0003702820917760

Ren Z., Gui X., Wei Y., Chen X., Xu X., Zhao L., Qiu H., Cao X., Chemical and photo-initiated aging enhances transport risk of microplastics in saturated soils: Key factors, mechanisms, and modeling, W. Res. 202, 117407 (2021), ISSN 0043-1354, https://doi.org/10.1016/j.watres.2021.117407

Roblin B., Ryan M., Vreugdenhil A., Aherne J., Ambient Atmospheric Deposition of Anthropogenic Microfibers and Microplastics on the Western Periphery of Europe (Ireland), Environ. Sci. Technol. 54, 18, 11100–11108 (2020), https://doi.org/10.1021/acs.est.0c04000

Ryan P., Moloney C. Marine litter keeps increasing, Nature 361, 23, (1993), https://doi.org/10.1038/361023a0

Sánchez A., Rodríguez-Viso P., Domene A., Orozco H., Vélez D., Devesa V., Dietary microplastics: Occurrence, exposure and health implications, Environ. Res. 212, A, 113150 (2022), ISSN 0013-9351, https://doi.org/10.1016/j.envres.2022.113150

Schirinzi G.F., Pérez-Pomeda I., Sanchís J., Rossini C., Farré M., Barceló D., Cytotoxic effects of commonly used nanomaterials and microplastics on cerebral and epithelial human cells, Environ. Res. 159, 579-587 (2017), ISSN 0013-9351, https://doi.org/10.1016/j.envres.2017.08.043

a. Schymanski D., Oßmann B.E., Benismail N., Boukerma K., Dallmann G., von der Esch E., Fischer D., Fischer F., Gilliland D., Glas K., Hofmann T., Käppler A., Lacorte S., Marco J., Rakwe EL M., Weisser J., Witzig C., Zumbülte N., Ivleva N.P., Analysis of microplastics in drinking water and other clean water samples with micro-Raman and micro-infrared spectroscopy: minimum requirements and best practice guidelines, Anal. Bioanal. Chem. 413, 5969–5994 (2021), https://doi.org/10.1007/s00216-021-03498-y

b. Schymanski D., Goldbeck C., Humpf H., Fürst P., Analysis of microplastics in water by micro-Raman spectroscopy: Release of plastic particles from different packaging into mineral water, W. Res. 129, 154-162 (2018), ISSN 0043-1354, https://doi.org/10.1016/j.watres.2017.11.011

Shao L., Li Y., Jones T., Santosh M., Liu P., Zhang M., Xu L., Li W., Lu J., Yang C., Zhang D., Feng X., BéruBé K., Airborne microplastics: A review of current perspectives and environmental implications, J. of Clean. Prod. 347, 131048 (2022), ISSN 0959-6526, https://doi.org/10.1016/j.jclepro.2022.131048

Shen M., Song B., Zhu Y., Zeng G., Zhang Y., Yang Y., Wen X., Chen M., Yi H., Removal of microplastics via drinking water treatment: Current knowledge and future directions, Chemosphere 251, 126612 (2020), ISSN 0045-6535, https://doi.org/10.1016/j.chemosphere.2020.126612

Simon M., Vianello A., Shashoua Y., Vollertsen J., Accelerated weathering

affects the chemical and physical properties of marine antifouling paint microplastics and their identification by ATR-FTIR spectroscopy, Chemosphere 274, 129749 (2021), ISSN 0045-6535, https://doi.org/10.1016/j.chemosphere.2021.129749

Simonescu C.M., Application of FTIR Spectroscopy in Environmental Studies, Advanced Aspects of Spectroscopy, Ch. 2 (2012), http://dx.doi.org./10.5772/48331

Smith E., Dent G., Modern Raman Spectroscopy: A Modern Approach, ISBN 9781119440581 (2019)

Sobhani Z., Zhang X., Gibson C., Naidu R., Megharaj M., Fang C., Identification and visualisation of microplastics/nanoplastics by Raman imaging (i): Down to 100 nm, W. Res. 174, 115658 (2020), ISSN 0043-1354, https://doi.org/10.1016/j.watres.2020.115658

Soltani N.S., Taylor M.P., Wilson S.P., Quantification and exposure assessment of microplastics in Australian indoor house dust, Environ. Pollut., 283, 117064 (2021), ISSN 0269-7491, https://doi.org/10.1016/j.envpol.2021.117064

Sridharan S., Kumar M., Singh L., Bolan N.S., Saha M., Microplastics as an emerging source of particulate air pollution: A critical review, J. of Hazard. Mater. 418, 126245 (2021), ISSN 0304-3894, https://doi.org/10.1016/j.jhazmat.2021.126245

Stock F., Kochleus C., Bänsch-Baltruschat B., Brennholt N., Reifferscheid G., Sampling techniques and preparation methods for microplastic analyses in the aquatic environment – A review, TrAC Trends in Anal. Chem. 113, 84-92 (2019), ISSN 0165-9936, https://doi.org/10.1016/j.trac.2019.01.014

Surette M.C., Mitrano D.M., Roger K.R., Extraction and concentration of nanoplastic particles from aqueous suspensions using functionalized magnetic nanoparticles and a magnetic flow cell, Micropl. & Nanopl. 3, 2 (2023), https://doi.org/10.1186/s43591-022-00051-1

Swan S.H., Environmental phthalate exposure in relation to reproductive outcomes and other health endpoints in humans, Environ. Res., 108, 2, 177-184 (2008), ISSN 0013-9351, https://doi.org/10.1016/j.envres.2008.08.007

Tcharkhtchi A., Abbasnezhad N., Zarbini Seydani M., Farzaneh Z.S., Shirinbayan M., An overview of filtration efficiency through the masks: Mechanisms of the aerosols penetration, Bioact. Mater., 6, 1, 106-122 (2021), ISSN 2452-199X, https://doi.org/10.1016/j.bioactmat.2020.08.002

a. Thompson R.C., Olsen Y., Mitchell R.P., Davis A., Rowland S.J., John A.W.G, McGonigle D., Russell A.E., Lost at Sea: Where Is All the Plastic?, Science, 304, 5672, 838 (2004), 10.1126/science.1094559

b. Thompson R.C., Swan S.H., Moore C.J., vom Saal F.S. Our plastic age, Phil.

Trans. R. Soc., B3641973-1976 (2009), http://doi.org/10.1098/rstb.2009.0054

Tirkey A., Upadhyay L.S.B., Microplastics: An overview on separation, identification and characterization of microplastics, Mar. Pollut. Bull. 170, 112604 (2021), ISSN 0025-326X, https://doi.org/10.1016/j.marpolbul.2021.112604

Veerasingam S., Ranjani M., Venkatachalapathy R., Bagaev A., Mukhanov V., Litvinyuk D., Mugilarasan M., Gurumoorthi K., Guganathan L., Aboobacker V.M., Vethamony P., Contributions of Fourier transform infrared spectroscopy in microplastic pollution research: A review, Crit. Rev. in Environ. Sci. and Technol. 51, 22, 2681-2743 (2021), DOI: 10.1080/10643389.2020.1807450

Vianello A., Jensen R.L., Liu L., Vollertsen J., Simulating human exposure to indoor airborne microplastics using a Breathing thermal Manikin, Scientific Reports 9, 8679 (2019), https://doi.org/10.1038/s41598-019-45054-wwww.nature.com/scientificreports

Wang Z., Dong H., Wang Y., Ren R., Qin X., Wang S., Effects of microplastics and their adsorption of cadmium as vectors on the cladoceran Moina mongolica Daday: Implications for plastic-ingesting organisms, J. of Hazard. Mat. 400, 123239 (2020), ISSN 0304-3894, https://doi.org/10.1016/j.jhazmat.2020.123239

Wang Z., Lin T., Chen W., Occurrence and removal of microplastics in an advanced drinking water treatment plant (ADWTP), Sci. of the Total Environ., 700, 134520 (2020), ISSN 0048-9697, https://doi.org/10.1016/j.scitotenv.2019.134520

Weber F., Kerpen J., Wolff S., Langer R., Eschweiler V., Investigation of microplastics contamination in drinking water of a German city, Sci. of The Total Environ., 755, 2, 143421 (2021), ISSN 0048-9697, https://doi.org/10.1016/j.scitotenv.2020.143421

WHO, Microplastics in drinking water, ISBN 978-92-4-151619-8 (2019)

Wieland S., Balmes A., Bender J., Kitzinger J., Meyer F., Ramsperger A.F.R.M., Roeder F., Tengelmann C., Wimmer B.H., Laforsch C., Kress H., From properties to toxicity: Comparing microplastics to other airborne microparticles, J. of Hazard. Mater., 428, 128151 (2022), ISSN 0304-3894, https://doi.org/10.1016/j.jhazmat.2021.128151

Winkler A., Santo N., Ortenzi M.A., Bolzoni E., Bacchetta R., Tremolada P., Does mechanical stress cause microplastic release from plastic water bottles?, W. Res. 166, 115082 (2019), ISSN 0043-1354, https://doi.org/10.1016/j.watres.2019.115082

a. Wright S.L., Kelly F.J., Plastic and Human Health: A Micro Issue?, Environ. Sci. Technol., 51, 12, 6634–6647 (2017), https://doi.org/10.1021/acs.est.7b00423

b. Wright S.L., Levermore J.M., Kelly F.J., Raman Spectral Imaging for the De-

tection of Inhalable Microplastics in Ambient Particulate Matter Samples, Environ. Sci. Technol. 53, 15, 8947–8956 (2019), https://doi.org/10.1021/acs.est.8b06663

Xue J., Samaei S.HA., Chen J., Doucet A., Tsun Wan Ng K., What have we known so far about microplastics in drinking water treatment? A timely review, Front. Environ. Sci. Eng. 16, 58 (2022). https://doi.org/10.1007/s11783-021-1492-5

Yadav H., Khan M.R.H., Quadir M., Rusch K.A., Mondal P.P., Orr M., Xu E.G., Iskander S.M., Cutting Boards: An Overlooked Source of Microplastics in Human Food?, Environ. Sci. Technol., 57, 22, 8225–8235 (2023), https://doi.org/10.1021/acs.est.3c00924

Zamani A., Maini B., Flow of dispersed particles through porous media — Deep bed filtration, J. of Pet. Sci. and Eng. 69, 1–2, 71-88 (2009), ISSN 0920-4105, https://doi.org/10.1016/j.petrol.2009.06.016

Zha F., Shang M., Ouyang Z., Guo X., The aging behaviors and release of microplastics: A review, Gondwana Res., 108, 60-71 (2022), ISSN 1342-937X, https://doi.org/10.1016/j.gr.2021.10.025

Zhang J., Peng M., Lian E., Xia L., Asimakopoulos A.G., Luo S., Wang L., Identification of Poly(ethylene terephthalate) Nanoplastics in Commercially Bottled Drinking Water Using Surface-Enhanced Raman Spectroscopy, Environ. Sci. Technol., 57, 22, 8365–8372 (2023), https://doi.org/10.1021/acs.est.3c00842

Zhang Q., He Y., Cheng R., Li Q., Qian Z., Lin X., Recent advances in toxicological research and potential health impact of microplastics and nanoplastics in vivo, Environ. Sci. Pollut. Res. 29, 40415–40448 (2022), https://doi.org/10.1007/s11356-022-19745-3

Zhang W., Ma X., Zhang Z., Wang Y., Wang J., Wang J., Ma D., Persistent organic pollutants carried on plastic resin pellets from two beaches in China, Mar. Pollut. Bull., 99, 1–2, 28-34 (2015), ISSN 0025-326X, https://doi.org/10.1016/j.marpolbul.2015.08.002

Zhou G., Wu Q., Tang P., Chen C., Cheng X., Wei X., Ma J., Liu B., How many microplastics do we ingest when using disposable drink cups?, J. of Hazard. Mater., 441, 129982 (2023), ISSN 0304-3894, https://doi.org/10.1016/j.jhazmat.2022.129982

Zhu J., Effective hydraulic conductivity of discrete fracture network with aperture-length correlation, Geosci. J. 24, 329–338 (2020), https://doi.org/10.1007/s12303-019-0025-8

Zhu J., Zhang X., Liao K., Wu P., Jin H., Microplastics in dust from different indoor environments, Sci. of The Total Environ. 833, 155256 (2022), ISSN 0048-9697, https://doi.org/10.1016/j.scitotenv.2022.155256

Part II

Scientific papers

Paper I

Do drinking water plants retain microplastics? An exploratory study using Raman micro-spectroscopy

L. Maurizi, L. Iordachescu, I.V. Kirstein, A.H. Nielsen, J. Vollertsen

The paper has been published in
Heliyon Vol. 9(6), pp.e17113, 2023.

Heliyon 9 (2023) e17113

Contents lists available at ScienceDirect

Heliyon

journal homepage: www.cell.com/heliyon

Do drinking water plants retain microplastics? An exploratory study using Raman micro-spectroscopy☆

Luca Maurizi [a,*], Lucian Iordachescu [a], Inga V. Kirstein [b], Asbjørn H. Nielsen [a], Jes Vollertsen [a]

[a] Department of the Built Environment, Aalborg University, Thomas Manns Vej 23, 9220, Aalborg, Denmark
[b] Alfred-Wegener-Institute Helmholtz Centre for Polar and Marine Research, Biologische Anstalt Helgoland, Helgoland, Germany

ARTICLE INFO

Keywords:
Microplastics
Nanoplastics
Raman micro-spectroscopy
Drinking water
Water quality
Plastic pollution

ABSTRACT

The retainment of microplastics (MPs) down to 1 μm by a Danish drinking water plant fed with groundwater was quantified using Raman micro-spectroscopy (μRaman). The inlet and outlet were sampled in parallel triplicates over five consecutive days of normal activity. For each triplicate, approximately 1 m^3 of drinking water was filtered with a custom-made device employing 1 μm steel filters. The MP abundance was expressed as MP counts per liter (N/L) and MP mass per liter (pg/L), the latter being estimated from the morphological parameters provided by the μRaman analysis. Hence the treated water held on average 1.4 MP counts/L, corresponding to 4 pg/L. The raw water entering the sand filters held a higher MP abundance, and the overall efficiency of the treatment was 43.2% in terms of MP counts and 75.1% in terms of MP mass. The reason for the difference between count-based and mass-based efficiencies was that 1–5 μm MP were retained to a significantly lower degree than larger ones. Above 10 μm, 79.6% of all MPs were retained by the filters, while the efficiency was only 41.1% below 5 μm. The MP retainment was highly variable between measurements, showing an overall decreasing tendency over the investigated period. Therefore, the plastic elements of the plant (valves, sealing components, etc.) likely released small-sized MPs due to the mechanical stress experienced during the treatment. The sub-micron fraction (0.45–1 μm) of the samples was also qualitatively explored, showing that nanoplastics (NPs) were present and that at least part hereof could be detected by μRaman.

1. Introduction

Humans are exposed to microplastics (MPs) and nanoplastics (NPs) with consequences still unclear [1]. Contact with MPs and NPs may happen *via* pathways such as air [2], water [3], and food [4]. Consequently, the human organism is continuously subjected to plastic fragments below the millimetric size [5], which, for example, has been confirmed by analyzing human stool and placentas ([6, 7]).

By implicit yet unofficial convention, plastic particles smaller than 1 μm have been termed *nanoplastics* [8], while *microplastics* span between 1 μm and 5 mm in size. This categorization was also followed in the present paper. The MP category may be further divided into "large microplastics" (above 1 mm) and "small microplastics" (below 1 mm) [9], as well as "primary microplastics" (purposely

☆ Luca Maurizi reports financial support was provided by European Commission.
* Corresponding author.
E-mail address: lucam@build.aau.dk (L. Maurizi).

https://doi.org/10.1016/j.heliyon.2023.e17113
Received 25 May 2023; Received in revised form 6 June 2023; Accepted 7 June 2023
Available online 9 June 2023

added to cosmetics and personal-care products) and "secondary microplastics" (produced by plastic objects breaking down in the environment) [10].

A report published by the World Health Organization (WHO) in 2019 claimed that there is no evidence that MPs in drinking water could be harmful to humans [11]. However, the same report stressed the lack of a comprehensive overview of MP and NP occurrence in drinking water plants and urban water networks. At the same time, a growing number of studies have pointed out that MPs and NPs can have a wide range of biological effects [12] on plants [13] and animals [14] in their habitats. Although most of the studies published so far address marine species as models for MP and NP toxicity, a cautionary approach would suggest also studying the exposure of humans [15]. In general, MPs and NPs are believed to increase their toxicity as they get smaller ([16,17]), probably due to translocation across biological membranes such as intestines and accumulation in tissue [18]. Different exposure routes for humans are possible, drinking water being one of them [19]. As a response to this, the European Union has recently put microplastics on their watch list for the quality of water intended for human consumption [20].

Drinking water can be distinguished according to its source, namely groundwater and surface water [21]. The MP analysis may be conducted either on the raw water ([22–24]), after the water treatment, or at the inlet and outlet of a waterworks ([25–27]). The latter also enables estimating the plant's removal efficiency for MPs within a certain size range. Generally implementing more treatment steps improves the MP removal [28], hence drinking water plants equipped only with coagulation-flocculation-sedimentation (CFS) and sand filtration tend to show rather low MP retainment efficiency (~40%) [28]. In contrast, more advanced waterworks with CFS-sand filtration-ozonation-granular active carbon (GAC) filtration can reach ~80% of MP removal [28]. The performance of each treatment step seems influenced by the size, shape, polymer type, surface electric charge of the MPs in the raw water, and, additionally, by the chemicals employed in the treatment. For CFS, the choice of polyaluminium chloride (PACl) as coagulant has led to higher MP removal than ferric chloride ($FeCl_3 \cdot 6H_2O$) in laboratory-scale tests [29], probably thanks to stronger electrostatic interactions between the MPs and coagulant flocs. While fibres are reportedly better retained than fragments in CFS [30], the role of MP size is still under debate, as the literature provides contrasting findings. After CFS, media filtration is normally performed, however, the MP retainment reached in this step depends on the media employed. [31] saw that 5–10 μm MP can elude sand filters, therefore additional treatments should be implemented after sand filtration. GAC seems a valid complement to sand filtration and has been shown to remove up to 61% of the residual MPs in the water, despite losing efficiency for fibrous shapes [32]. Transport, attachment, and detachment are the main mechanisms involved in media filtration of particles [33], and, according to granular media filtration theories, particles close to 1 μm exhibit the minimum net transport efficiency [34]. However, dedicated studies on the effect of different porous media filtration conditions on MP removal lack, hence only indirect insights can be drawn from past works. Besides CFS and porous media filtration, the impact of ozonation on MP removal was also investigated [32]. After the ozonation step, the MP concentration slightly increased, possibly because of the breakdown of larger MPs into smaller particles.

The most widely employed spectroscopic methods for environmental MP analysis are Fourier-Transform Infrared micro-spectroscopy (μFTIR) and Raman micro-spectroscopy (μRaman). Schymanski et al. [35] underlined the urgent need for improving harmonization and reproducibility among the protocols based on these techniques. A plea similar to that of [35] was expressed by Kirstein et al. [36], regarding MP toxicology assessment and MP quantification in drinking water.

The aim of this work is to assess whether and to what extent a drinking water plant fed by groundwater can retain MPs down to 1 μm, preventing them to reach the distribution network. Despite being a more protected environment than surface waters, groundwater sources can indeed also be affected by MP pollution [37]. The study assesses the MP retainment by comparing two MP parameters: counts and mass, the latter being estimated from the morphological data provided by the μRaman analysis. Currently, mass estimation of MPs and NPs is mostly performed with Pyr-GC/MS [38], which provides quantitatively accurate results. However, it does not provide information about particle size distribution and morphology. In addition, its quantification limit is roughly in the order of 1 μg per sample and polymer type, of course depending on the polymer to be quantified and the instrumentation used. The mass of small (<10 μm) MPs and NPs in a drinking water sample may however be orders of magnitude below such a detection limit. There is therefore a need for an analytical method capable of providing more information on small MPs and NPs, their chemical identity, size, abundance as well as mass in a reasonable time and within one analytical run.

2. Materials and methods

2.1. Drinking water sampling

The investigated plant produces approximately 500,000 m^3/year of drinking water and it is located in North Jutland. The raw water is extracted from a limestone aquifer (4 wells with screens 72–92 m below ground) using submersible pumps and treated through aeration and rapid sand filtration (see also Supplementary Information, Fig. S1). The closed environment of the aquifer is not affected by seasonal variations, having an age of many years. From the wells, the water is conveyed approximately 800 m in high-density polyethylene (HDPE) pipes to the waterworks, whereafter it is transported in steel pipes between the individual process steps of the facility. Before being sent to the water distribution network, the treated water is stored in two stainless steel tanks of 110 m^3 each (daytime retention time 2–3 h).

Two custom made devices were employed on Series 1 of the facility, which operates symmetrically. Each device had 4 parallel flow lines holding 1 μm sintered steel filters (Mesh Masters, The Netherlands) of 46 mm diameter. One device was placed at the inlet before the sand filters and one at the outlet after the storage tanks. The sampling devices were connected at the sampling points by flexible

steel pipes and the plant was sampled daily between the 27th of September and the 1st of October 2021 (9 a.m.–2 p.m.). Approx. 1 m^3 of drinking water was filtered on each of the parallel operated filters along the first three flow lines of the two devices [39]. Inlet and outlet were sampled in parallel, resulting in a total of 5 inlet and 5 outlet samples collected in triplicate (n = 30). A flowmeter mounted at the outlet of each flow line measured the filtered volume for each filter. At the beginning of each sampling, the flow per line was adjusted to approximately 3 L/min.

Field blanks were collected in parallel with the drinking water samples by equipping the fourth flow line of each device with two filter holders coupled in series. The first held a muffled 0.7 μm glass fibre membrane (Th. Geyer GmbH, Germany), and the second a 1 μm sintered steel filter. The glass-fibre membrane served as a pre-filter to sample the drinking water matrix while excluding the MPs above 0.7 μm [39]. For each field blank, the filtered volume was recorded by a flowmeter at the outlet of the flowline, and the average flow was adjusted to 3 L/min. Contamination occurs during the preparation stage of the filters and during the analysis, but not during the sampling itself, where the filter is isolated from the surroundings. Consequently, the degree of contamination of a field blank is independent of the sampled volume, and it was chosen to filter approx. 20 L for each field blank (n = 10). After the sampling, the steel filters of the drinking water samples and the field blanks were stored in Petri dishes prior to the sample preparation. Further details on the sampling device are given in Supplementary Information.

2.2. Preparation of recovery samples

Standard plastic fragments (poly-ethylene 45–100 μm, poly-styrene 10–40 μm, and poly-ethylene terephthalate 10–40 μm, GoodFellow Corp., USA) were chosen to provide a recovery assessment comparable with data commonly reported in the literature. The particles were added to three clean beakers with 5 mL Milli-Q water (Type 1 ultrapure water, 18.2 MΩ cm) (Purelab Ultra Elga, UK) and counted with a FlowCam (Yokogawa Fluid Imaging Technologies, Inc., USA). The three suspensions with a known amount of each MP standard were filtered through a 1 μm sintered steel filter each with a vacuum filtration system. The so-enriched filters were placed in one of the sampling devices used at the waterworks. Similar to what was done with the field blanks, a filter holder with a muffled 0.7 μm glass fibre membrane was placed before each enriched steel filter and 1 m^3 of tap water was filtered through each flow line. The purpose of this procedure was to reproduce the sampling conditions without adding further MP above 0.7 μm to the recovery samples. The flow was adjusted to approximately 3 L/min per flow line. Finally, the enriched steel filters were stored in Petri dishes prior to sample preparation.

2.3. Contamination prevention

The steel filters were sonicated in Milli-Q water (18.2 MΩ cm), dried at 50 °C in an oven, and stored in muffled Petri dishes in a laminar flow bench before use. All chemicals were filtered through muffled 0.7 μm glass fibre membranes. All glassware was muffled at 500 °C for 4 h, and metallic labware was thoroughly rinsed with Milli-Q water. All sample preparation took place in a laminar flow bench, which was regularly cleaned with 50% EtOH. Pure cotton lab coats were worn during the entire sample preparation.

2.4. Sample preparation and analysis

All samples (drinking water samples, field blanks, and recovery samples) were processed following a protocol similar to that employed by Ref. [39]. In brief: each filter was incubated for 24 h in 5% SDS at 50 °C, upon which the particles were transferred to the SDS solution by ultrasonication. The particle-enriched mixture was then filtered through the same filter on which the sample originally was collected. Hereafter the particles were sonicated from the filter into 50% EtOH, and the filtration procedure repeated with the ethanolic particle-enriched solution. Finally, the filter was immersed in 99.5% EtOH, ultrasonicated, and scratched with a metallic spatula to collect all particles. The ethanolic mixture was poured into a 10 mL vial and evaporated under nitrogen flow until exhaustion.

Sample reconstitution, deposition, and analysis took place at Renishaw plc UK (Wotton-under-Edge, UK). Samples were reconstituted with 1.0 mL of >99.5% EtOH in a flow bench. Upon reconstitution, neither sedimentation nor flotation of particles could be observed, and the mixtures were quite clear. Immediately before the deposition, the ethanolic mixture was homogenized with a vortex mixer (VWR, Denmark) for 30 s. Then, 25.0 μL from each vial were deposed on a 10 × 10 mm single-crystal silicon (Si) substrate (SmartMembranes GmbH, Germany), using a manual micropipette mounting a 25.0 μL glass tip (Brand GmbH, Germany). The deposition was restricted to a circular area of 2 mm diameter by a custom-made device, obtaining an active area of approximately $3.14 \cdot 10^6$ μm^2 for each sample. Finally, the samples were dried at 55 °C overnight on a heating plate (W10 VWR, Denmark). Depositing the 2.5% of each sample allowed for obtaining active areas with no particles covering each other and with an average number of MPs analyzable without employing any sort of sub-mapping, i.e., the full area was analyzed by the Raman microscope in one session.

The employed Raman microscope was a Renishaw InVia equipped with a 1024 × 256 pixel CCD detector cooled at −70 °C and a 532 nm Nd: YAG solid-state laser source (Renishaw plc UK, UK). The software module "Particle Analysis" (Renishaw plc UK, UK) was used to perform the analysis of the visible image, the μRaman analysis, and the spectral processing and recognition. For the μRaman analysis, a grating density of 1800 ll/mm and two LD (long distance) objectives (Leica, Germany) 50 × (NA 0.75) and 100 × (NA 0.90) were chosen, and the spectral range was set to 300–2000 cm^{-1}. The system was previously calibrated by zero-order correction on the first-order Raman emission of single-crystal Silicon at 519.5 ± 0.5 cm^{-1}. Fig. 1 shows the analysis process followed for the samples.

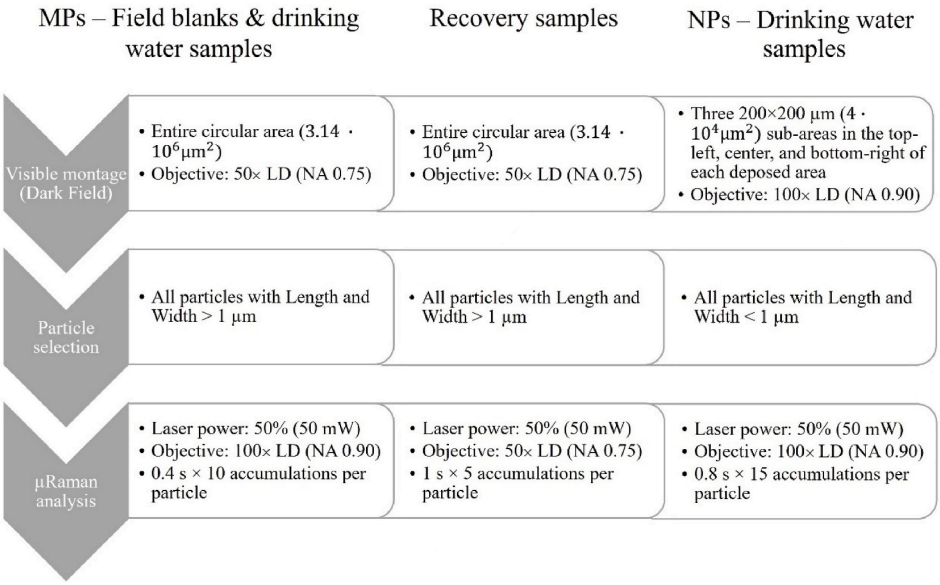

Fig. 1. Scheme of the analysis protocol followed for the field blanks, drinking water samples, and recovery samples.

Briefly: after the acquisition of the visible image (montage), the software calculated the morphological parameters of the particles in the montage and saved their XY coordinates. The particles were virtually selected according to their size, and the laser was automatically driven onto each particle to obtain its Raman spectrum.

The environmental particles in the analyzed active areas looked transparent, and no fluorescence was encountered during the spectral acquisition. The µRaman spectra were baseline-corrected and compared with the Renishaw Polymer Library, and only spectra with hit quality (HQ, quality of the fit result between the experimental spectrum and the model composed by a linear combination of reference spectra from the library) of at least 80% were considered for the MP quantification [35]. Accordingly, the particles not fulfilling this criterium were considered non-plastic. For the recovery samples, the HQ threshold could be reached at a lower magnification objective during the spectral acquisition, given the larger mean size of the fragments employed for the recovery test in comparison with the mean size of the MPs found in the field blanks and drinking water samples. For the qualitative analysis of the NPs, a HQ above 50% was considered sufficient. Figs. 2 and 3 are examples of experimental spectra from an MP and NP, respectively.

Further details, pictures, and examples of spectra are given in Supplementary Information.

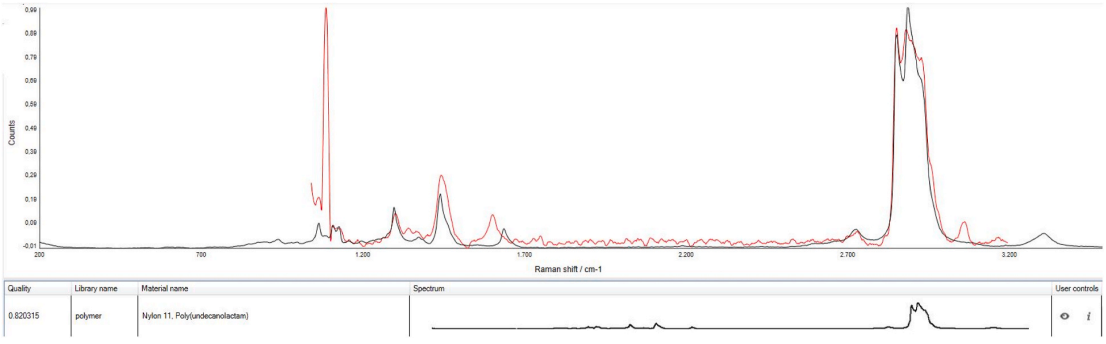

Fig. 2. Raman spectrum of Nylon 11 MP (category PA), also showing a peak belonging to bicarbonate (~1000 cm-1) (HQ 0.82).

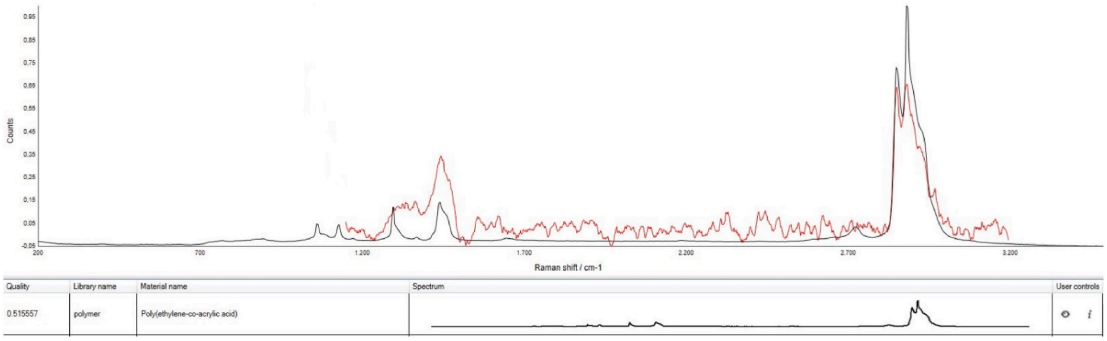

Fig. 3. Raman spectrum of PE nanoparticle (HQ 0.51).

2.5. Post-processing of the μRaman data

The MP mass from the drinking water samples and field blanks was estimated from the morphological parameters of the particles in the active areas. The analysis of the visible montage yielded the area of the 2D projection and the length (L) of each particle. Then, the width of the equivalent ellipse (W_{eq}) was calculated from the area and the length, and it was assumed that the third diameter (perpendicular to the remaining two) was 60% of the W_{eq} [40]. Hence the volume (V) of each particle was calculated according to equation (1):

$$V = (4/3) \cdot \pi \cdot (L/2) \cdot (W_{eq}/2) \cdot (0.6 \cdot W_{eq}/2) \quad (1)$$

Next, each plastic particle was assigned a pure polymer density according to its spectral identification from the μRaman analysis, which allowed for the particle mass in picograms (pg, 10^{-12} g) to be estimated.

The plant's removal efficiency R was calculated by comparing the cumulated MP counts or estimated mass of the inlet with that of the outlet (equation (2)):

$$R = -(([MPs_{outlet}] - [MPs_{inlet}]) / [MPs_{inlet}]) \cdot 100\% \quad (2)$$

Where [MPsinlet] and [MPsoutlet] respectively indicate the cumulated MP abundance in either counts (N/L) or mass (pg/L) at the plant's inlet and outlet. The cumulated MP abundance was calculated by adding the MP abundance of each investigated day at the plant's inlet or outlet.

LOD (Limit of Detection) and LOQ (Limit of Quantification) were calculated from the field blanks. They were calculated for total MP abundance and each identified polymer in the blanks, both for the MP counts and mass estimation. Equations (3) and (4) were applied [35]:

$$LOD = mean_{blanks} + 3 \cdot s_{mean} \quad (3)$$

$$LOQ = mean_{blanks} + 10 \cdot s_{mean} \quad (4)$$

Where meanblanks is the mean count or mass of each polymer found in the 10 field blanks and smean the corresponding standard deviation. The mean blank value of each polymer was subtracted from the corresponding value determined in the sample, which was considered only if above the LOQ after the correction.

The recovery rate Q for each positive control was calculated as follows (equation (5)):

$$Q = (N_{recovered} / N_{initial})\ 100\% \quad (5)$$

Where Nrecovered is the count of standard fragments recovered and normalized to the fraction of volume deposited, and Ninitial is the count of standard fragments initially added.

Uncertainty was calculated by selecting a coverage factor $k = 2$ ($P = 95\%$) and considering only the A-type (statistical) contribution. Statistical tests were performed with Rstudio v. 2022.02.1. ANOVA test was conducted for significance assessment ($\alpha = 0.05$) and Tukey-test for pair-wise factor comparison. Normality was assessed with the Shapiro-Wilk test. The samples were labeled as Dxy, where D means "Day", x is the sampling day (1–5), and y is either i for inlet or o for outlet.

3. Results and discussion

3.1. Field blanks, LOD, LOQ, and recovery

Although great care was exercised to avoid contamination from the environment, MPs were present in the blanks. The polymers identified in the blanks were common and widely used in laboratory items [25]. To relate the LOD and LOQ to a sampled volume, the

LOD and LOQ per sample were divided by the volume filtered (approx. 1 m^3). Hence LOD = 0.255 N/L and LOQ = 2.559 N/L for the abundance measured as counts, and LOD = 0.645 pg/L and LOQ = 1.957 pg/L for the abundance measured as mass.

The mean recovery rate for the MP counts was 91.7 ± 12.3% for the length range 10–120 μm, which is comparable with the value obtained by Weber et al. [41] (53 ± 14% for the 22–27 μm range and 89 ± 28% for the 45–53 μm range). Further details on LOD, LOQ, and MP recovery are given in section 4 of the Supplementary Information.

3.2. Removal at the plant

Fig. 4 shows the overall MP abundance at the inlet and outlet as counts per liter and pg per liter. The average inlet abundance was 2.5 N/L, corresponding to 16.0 pg/L, while the average outlet abundance was 1.4 N/L (4.0 pg/L). In terms of MP counts, the outlet on D1 (0.1 ± 0.1 N/L) was substantially below that of the inlet (6.3 ± 11.7 N/L), while it on D2 was approx. three times above that of the inlet (1.0 ± 0.6 N/L *versus* 3.9 ± 5.6 N/L). In terms of mass, MPs were retained on D2 (inlet 14.9 ± 29.5 pg/L, outlet 2.2 ± 1.7 pg/L), albeit to a lower degree than on D1 (inlet 31.8 ± 56.3 pg/L, outlet 0.6 ± 0.6 pg/L). Hence the counts showed a production of total MP over the treatment works, while the mass showed a retainment. Similarly, on D5 there was no net retainment in terms of counts (inlet 0.8 ± 0.4 N/L, outlet 0.8 ± 0.5 N/L), but there was a net retainment in terms of mass (inlet 6.5 ± 7.9 N/L, outlet 2.6 ± 1.5 N/L). Therefore, on those two days, the MPs in the outlet tended to hold less mass altogether than in the inlet, meaning that they were generally small-sized. In particular, the pre-aeration step before the sand filtration may have led to a first breakdown of the MPs in the raw groundwater, which may have been followed by a secondary degradation in the sand filters due to the friction between MPs, non-plastic particles, and the granular medium. In addition, the generally low retainment efficiency for MPs <10 μm characterizing sand filters, may have further enhanced the enrichment in small-sized MPs of the treated water. This hypothesis is also backed by the general overview of the effect of the different treatment steps on MP retainment provided in section 1. On D3 and D4 the MP abundance at the outlet proved to be quite stable for both MP counts (D3: 1.2 ± 1.1 N/L, D4: 1.1 ± 0.6 N/L) and mass (D3: 6.7 ± 2.6 pg/L, D4: 7.8 ± 4.5 pg/L), but also comparable with that of D5 in terms of MP counts. Hence the release of MPs that occurred on D2 likely also involved the three following investigated days, whose MP counts abundance at the outlet was "sustained" with additional MPs. Since the MP mass abundance at the outlet on D3 and D4 was the highest recorded over the investigated period, some of the MPs were likely characterized by a larger size than on D2 (see also section 3.4).

Because of the persisting presence of MPs after the treatment, no significative difference ($p > 0.05$) could be seen for the MP counts and mass abundances between the inlet and outlet or among the investigated days. Note that Fig. 4 takes into account the overall MP abundances without distinguishing among the different polymeric types, hence the variation between MP counts and estimated mass should be considered indicative only.

The water retention time in the treatment works, including its storage tanks, was overall short, hence each sampling day was considered independently. Consequently, the retention time in the sand filters, despite being unknown, was assumed shorter than 24 h, provided that the plant operated continually.

A daily mean MP removal efficiency could hence be calculated from equation (2). The production of MPs on some days suggested that a release of a significant number of MPs may have occurred between the inlet and outlet. Overall, the accumulated efficiency at the

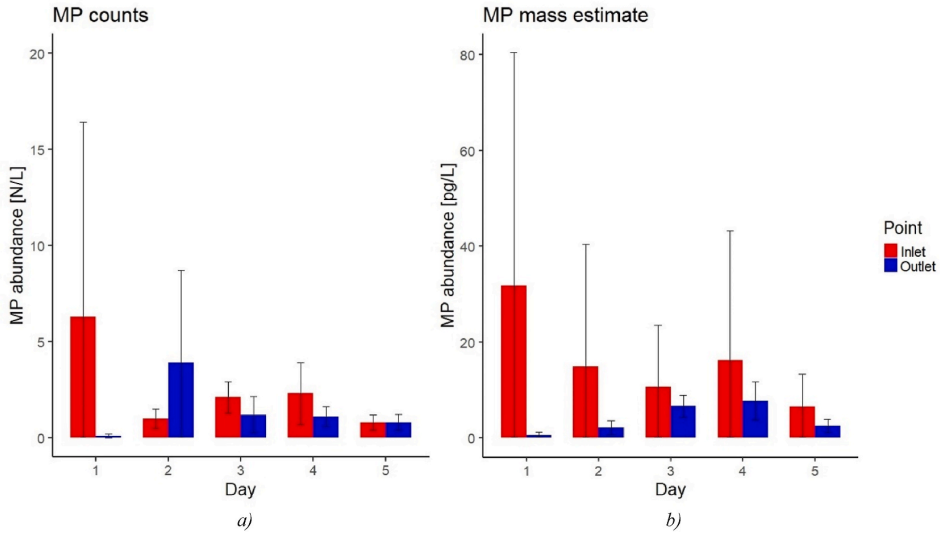

Fig. 4. Overall MP abundance in a) counts per liter and b) estimated mass per liter at the plant's inlet and outlet for each investigated day. The error bars indicate the standard deviation for each day.

treatment plant was 43.2 ± 45.9% in terms of counts, and 75.1 ± 28.2% in terms of mass, indicating that while retainment fluctuated from day to day, with some days even seeing a release of MPs, the drinking water treatment plant on average retained MPs. The difference between the two MP retainment efficiencies might be related to the breaking process involving the larger MPs from the inlet at the sand filtration step, which will cause the MP counts retainment to decrease, as opposed to the MP mass retainment. The treatment efficiency was furthermore comparable to those reported by previous studies [3].

The variabilities around means depicted in Fig. 4 were found from the three replicates which are behind each mean value. However, although the three replicates were taken in parallel from the same water, the MP distribution in the water flow may not have been homogeneous, hence a different number of particles may have reached the filter surfaces.

Further, a contributing factor to the variability can be the subsampling for the Raman analysis, where 25 out of 1000 μL were subsampled per replicate. When subsampling, it was assumed that MPs were homogeneously distributed in the liquid matrix of the treated samples and the MP abundance was calculated by way of proportions. However, MPs might not have been homogeneously distributed even though the sample was thoroughly mixed before collecting a subsample for deposition. For the MP mass estimation, further uncertainty may come from the assumption of an ellipsoid shape and the way the volume of a particle was calculated, as this approach generally ignores shape variations (despite the scarce presence of elongated morphotypes in the analyzed samples, see section 3.4). The standard deviation seemed generally related to the MP abundance value, hence D1 showed the highest MP counts and estimated mass as well as the largest error. Finally, it should be considered that Fig. 4 includes the identified MPs altogether, hence part of the standard deviation derived from the error associated with the abundance of the different polymer types over the investigated period.

Non-plastics were quantified for comparison: many of these would have been natural organic and inorganic particles, however, their materials were not identified (hence mass could not be calculated as non-plastics were not assigned a chemical ID). The removal efficiency of the non-plastic particles was 32.8 ± 0.9% based on particle counts. Since the removal efficiency of MPs was above that of non-plastics, one could expect the MP to non-plastic ratio at the plant's outlet to be lower than that of the inlet. However, this was not the case, suggesting again that MPs were created in the treatment works at least during some days. How this happened was not investigated but could be due to mechanical stress on plastic elements within the facility (e.g. valves, o-rings, sealing components, compressors, etc.) or the breakdown of larger MPs in the sand filter (further details are given in Supplementary Information).

Albeit there are many studies on MPs in drinking water in general, only one study on MPs in Danish drinking water has so far been published [42]. The authors sampled tap water in households and workplaces, analyzed particles down to 10 μm with μFTIR, and found an average abundance of 0.2 N/L for the 10–100 μm size range. The lower abundances found by Ref. [42] may have been due to the MP size limit of their study, which did not address the contribution of the 1–10 μm particles. Indeed, the spectral resolution limit of μFTIR does not make it suitable to analyze items much below 10 μm, as opposed to μRaman, which can go into the sub-micron size range. If the abundance at the outlet of a waterworks remains unchanged until the water reaches the tap, the abundance found in the present study was, apart from D1, higher than those found by Ref. [42].

Pitroff et al. [43] investigated the MP occurrence in drinking water produced from groundwater by two plants in Germany down to 5 μm using μRaman, finding 66 ± 76 N/m^3 at the outlet. The authors employed a cascade filtration apparatus to sample particles down to 5 μm and calculated the LOQ of the method from field blanks with equation (4). However, they found no significant difference between their drinking water samples and their blanks. Bäuerlein et al. [44] studied two drinking water plants fed from underground aquifers in the Netherlands and two household taps connected to the same network. LDIR (Laser Direct InfraRed) was employed to identify particles down to 20 μm, and in one of the plants the MP abundance at the inlet was 2223 N/m^3. At one of the investigated taps, high levels of PA were detected, which the authors could not explain. Mintenig et al. [25] investigated 5 drinking water plants and related households in a German region served by treated groundwater. After sampling at different points in each facility (300–1000 L per sample) and at the taps (1200–2500 L per sample), μFTIR was employed for the MP analysis down to 20 μm. The overall average MP counts were 0.7 N/m^3, and the authors speculated that abrasion of plastic equipment during the water treatment could be a source of MP. These examples of other studies show that direct comparison among studies can be challenging. Nevertheless, they also indicate that MPs occur in drinking water at roughly comparable concentrations as in the present studies, especially when allowing for lower size detection limits.

3.3. Polymer composition

The polymer composition of the MPs might give further hints at how additional MPs were formed in the plant (Figs. 5 and 6). In terms of counts, poly (amide) (PA) MPs dominated in 3 out of 5 inlet samples (mean 39%) and all outlet samples (mean 78%) ($p < 0.05$). The category "Other", a mix of many different polymer types occurring in small numbers, dominated in the inlet on D1 (78%), while poly-acrylics dominated on D3 (96%). With respect to the mass estimate (Fig. 6), PA was the most abundant polymer in the inlet on D1 (77%), while it was only present at low concentrations on the other days. Instead, PS prevailed on D2 (67%) and D5 (93%), while poly-acrylics dominated on D3 and D4 (D3: 97%, D4: 96%). The outlet, on the other hand, showed a quite stable polymer composition, with poly-acrylics mass accounting for 55–72% (mean 65%) on all days, followed by PA with 27–42% (mean 34%). The origin of the MPs measured in inlet and outlet cannot be traced back, but there may well be plastic parts upstream of the sampling points consisting of PA and poly-acrylics, for example sealings in valves and fittings (notice the pure oxygen compressors before the inlet sampling point in Fig. S1). Here it should be kept in mind that the overall abundance in terms of MP mass was quite low, namely around 16 pg/L on average in the inlet to the sand filters (corresponding to 8 mg/year of plastic), hence a quite small amount of what totally could be present as part of the plant's construction. Further details are given in Supplementary Materials.

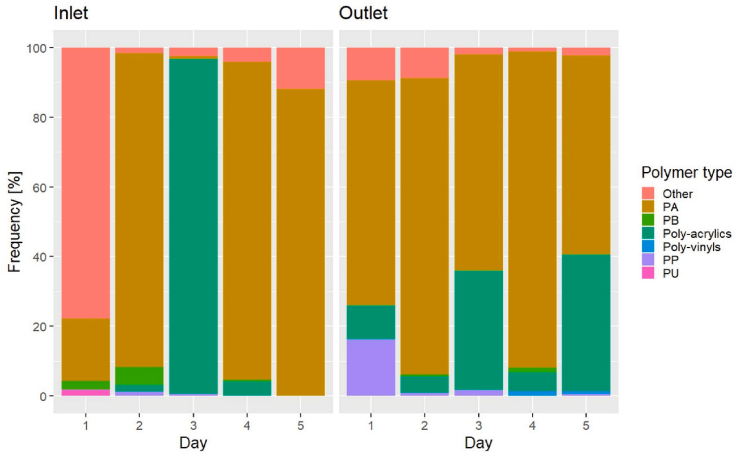

Fig. 5. MP counts abundance as polymer frequency over time at the plant's inlet and outlet.

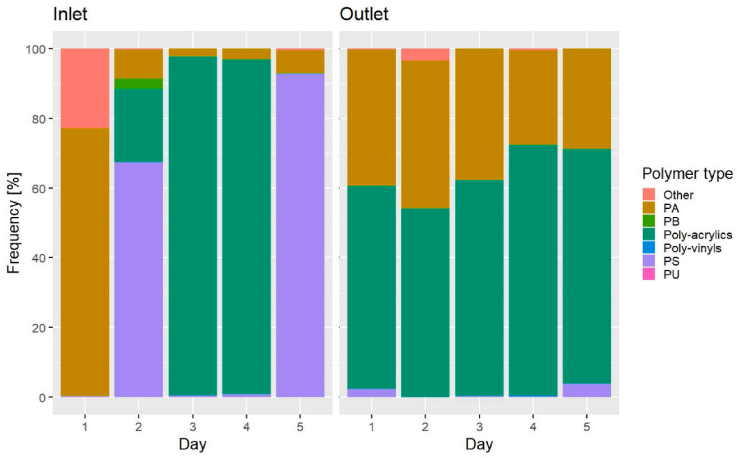

Fig. 6. MP mass abundance as polymer frequency over time at the plant's inlet and outlet.

PA and poly-acrylics dominated the outlet, but were of different relative sizes, with MPs of PA being smaller than MPs of poly-acrylic. There was furthermore an overall retainment of all MPs, probably in the sand filters of the plant (Fig. S1). It seems reasonable to assume that the sand filters smoothed out the MP load, retaining preferentially the larger ones, but also releasing the smaller ones.

3.4. Microplastic morphological analysis

The data behind the morphological analysis were not blank corrected. The largest MP particle found in the samples was 204.6 μm long and the MP median length was 2.4 μm. Fig. 7 shows MPs divided into five size classes: 1–5 μm, 5–10 μm, 10–20 μm, 20–50 μm, and 50+ μm in length. In all samples, the most populated size class was 1–5 μm (mean inlet 83.3%, mean outlet 92.7%, $p < 0.05$), followed by the 5–10 μm class (mean inlet 11.9%, mean outlet 5.7%). The frequencies of the larger size classes were far lower than the 1–5 μm and 5–10 μm ones. The 10–20 μm class held 3.6% and 1.0% of the mean inlet and outlet, respectively, while the 20–50 μm class held even less (mean inlet 0.9%, mean outlet 0.6%), and the 50+ μm class held the least number of MPs (mean inlet 0.3%, mean outlet <0.1%). Interestingly, on D3 and D4 the 10–20 μm frequency at the outlet was higher than on D2 and D5 (0.94 and 1.09% respectively), which could explain the related higher MP mass abundance in Fig. 4. Similarly, the 20–50 μm frequency showed a slight increase on D3 and D4 at the outlet if compared with D2, and it was comparable with that of D5. The abundance of the 1–5 μm particles in the inlet was 28.56 N/L while the outlet held 16.83 N/L, i.e., only 41.1% of this size class was on average retained. For 5–10 μm MP,

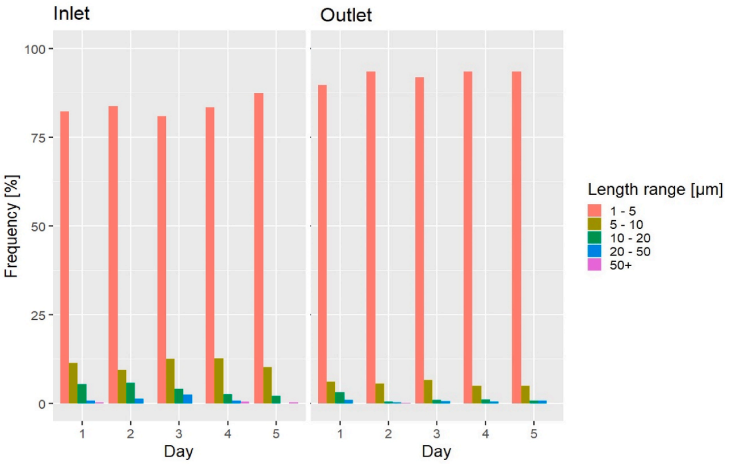

Fig. 7. MP length ranges frequency over Days 1–5 at the plant's inlet and outlet.

the abundance was 4.06 N/L and 1.03 N/L, respectively, i.e., 74.6% were on average retained. For MPs >10 μm, numbers were significantly lower, but retainment was significantly higher, namely 0.55 N/L in the inlet, 0.099 N/L in the outlet, and hence 81.3% retainment. Therefore, the sand filters seemed to preferentially retain the MPs above roughly 5–10 μm [45], possibly breaking the larger MPs into smaller particles Also, larger MPs may have been retained by sedimentation in the storage tanks before the treated water was sampled, which is a process mostly depending on particle size, roughness, and density [46]. Consequently, the frequency of the 1–5 μm MP at the outlet overall increased.

The findings confirmed the common observation that there tend to be more small MPs than large ones, for example [47,48], who also employed μRaman in their studies. Ref. [39] however found that only 32% of MPs were smaller than 20 μm compared to 98.8% (inlet) and 99.4% (outlet) found in the present study. This might well be due to differences in analytical techniques, as they used μFTIR in transmission mode, where the absorption signal decreases with the particle thickness. This problem does not occur for μRaman, which is a surface analysis technique. Classifying MPs with a ratio between length (Feret maximum diameter) and width (Feret minimum diameter) ≥3 as fibres and the rest as fragments [2] showed that fibre counts in the inlet were higher than in the outlet on D1, D4, and D5, while it was the other way around on D2 and D3. Hence there was no systematic trend to fibres being more or less retained compared to fragments when measured as MP counts. Overall, fragments were the most common shape, accounting for more than 98% of the MPs. This stands in contrast to what Kanganike and Babel [49] found in their study on MPs in drinking water during the rainy and dry seasons in Thailand. Their study focused on a drinking water plant fed by a river and applying clarification, dual filtration with sand and anthracite coal, and chlorination. The authors speculated that the prevalence of fibres in the samples (30–40%) was due to the relatively high MP abundance in the river used to feed the investigated waterworks, and to the inherent ability of the fibres to escape filter pores.

3.5. Nanoplastic qualitative exploration

While analyzing the drinking water samples, several sub-micron particles were observed in the visible images taken in dark field, i.e., particles of smaller size than the nominal pore size of the filter employed in the sampling and sample preparation. A subset of these was analyzed after filtering out particles above 1 μm in length and width (Fig. 1). Three sub-areas of 200 × 200 μm were selected from each deposition area and analyzed, yielding a total of 621 sub-micron particles with plastic-like Raman spectra. As previously stated, a poorer HQ (50%) was accepted for the NP evaluation compared to the MP analysis (80%), yielding lower confidence in the NP versus MP material assignment. Only NPs having both dimensions above 0.45 μm could be considered, as the HQ for smaller particles was below 50% when compared to the library references (area delimited by the blue dotted line in Fig. 8). Furthermore, analyzing single items below 0.45 μm would be technically demanding due to the Airy diffraction limit, which is ~0.36 μm with a 532 nm laser and a 100 × objective.

No quantitative results could be drawn from the NP evaluation since the filters used for sampling and sample preparation had a nominal pore size of 1 μm and the field blanks were not analyzed for the NPs. However, this evaluation illustrates the potential and limitations of μRaman for NP analysis of environmental samples and shows that the development of reliable analytical protocols for these analytes deserves further research. In comparison with other known categories of nanopollutants, NP quantification and interaction with living organisms are still considered an open challenge [50], and μRaman seems able to push the analysis for plastic particles into the nanoscale. The work of Sobhani et al. [51] showed that characteristic Raman signals of environmental particles down to 100 nm can be experimentally obtained, even though with decreasing spectral quality as smaller particles were considered.

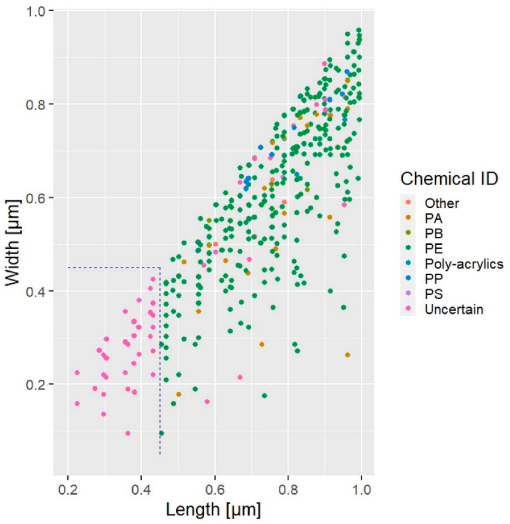

Fig. 8. Length vs width (Feret maximum vs Feret minimum diameters) for all analyzed NPs. The blue dotted line indicates the size limit above which the NP spectra presented a HQ above 50%. (For interpretation of the references to colour in this figure legend, the reader is referred to the Web version of this article.)

Moreover, Frehland et al. [52] demonstrated that the removal rates of the NPs (66.5%) and MP fibres were correlated to that of the total suspended solids in a pilot wastewater treatment plant. As suggested by the outcomes of the present study regarding MPs in a drinking water plant, contributions from plastic parts within such a plant may occur, and the sand filters typically applied probably will be only partly effective to retain NPs.

3.6. Human microplastic intake

The WHO Guidelines for Drinking – water quality (WHO 2009) [53] recommended an average adult drinking water consumption of 3 L/(day·capita). Applying this intake and the average MP abundance in the outlet of the treatment plant (1.4 N/L of MPs >1 µm), an annual adult MP intake *via* tap water can be estimated as 1533 N (4.4 ng/(year·capita)). The MP count abundance is several orders of magnitudes above the estimation by Ref. [39], and the main reason for the difference is that the present study achieved a lower size quantification limit. To make a comparison with other major exposure pathways, the review of Bai et al. [4] reported a total dietary intake of 1.42–1.54 $\cdot 10^5$ N/(year·capita), while [2] calculated an average inhaled intake of 272 N/h for a male individual ($2.38 \cdot 10^6$ N/(year·capita)). Hence drinking water produced from a protected groundwater source would account for only a small part of the potential total MP intake by humans. However, human MP intake estimations should generally be taken with care, as much uncertainty is still associated with MP exposure routes, absorption, and excretion rates, and finally, toxicity [54].

4. Conclusions

The studied drinking water plant was able to retain MPs (i.e., plastic particles >1 µm), although to a different extent depending on the MP size. The water in its outlet held 1.4 N/L, corresponding to an estimated MP mass of 4 pg/L. It achieved an average removal over 5 days of 43.2% in terms of MP counts. The efficiency was best for the larger MPs, deteriorating as particles became smaller than approx. 5–10 µm. Below 5 µm the efficiency was as low as 41.1%, while it increased to 74.6% for the 5–10 µm range, and to 81.3% for MPs >10 µm. The efficiency for MP mass retainment was higher, accounting for 75.1%. Extrapolating measured MP masses to a full year of operation showed that approx. 8 mg/year of plastic entered the sand filters, which is sufficiently low to allow the assumption that the MPs could have originated from the aging of plastic parts upstream of the filters.

The retainment efficiency of the facility was highly variable over the investigated period. This dynamic behavior means that substantial uncertainty is related to single measurements and assessing the operation of such a plant hence requires intensive monitoring. The preferential retainment of larger MPs compared to the smaller ones furthermore show that a measured retainment efficiency will depend heavily on the lower size quantification limit, and hence the analytical approach. This also impacts the interpretation of human exposure from the intake of MPs from drinking water. Finally, the study showed that NPs were present in the analyzed drinking water samples, and that µRaman was able to characterize at least the larger ones.

Supplementary Information

Supplementary Information: μRaman spectra for the identified polymer, additional experimental details and methods, including photographs of experimental setup.

Author contribution statement

Luca Maurizi 1) conceived and designed the experiments; 2) performed the experiments; 3) analyzed and interpreted the data; 4) contributed reagents, materials, analysis tools or data; 5) wrote the paper.

Lucian Iordachescu 2) performed the experiments; 4) contributed reagents, materials, analysis tools or data; 5) wrote the paper.

Inga V. Kirstein 3) analyzed and interpreted the data; 5) wrote the paper.

Asbjørn H. Nielsen 3) analyzed and interpreted the data; 5) wrote the paper.

Jes Vollertsen 3) analyzed and interpreted the data; 5) wrote the paper.

Data availability statement

Data will be made available on request.

Additional information

Supplementary content related to this article has been published online at [URL].

Declaration of competing interest

The authors declare that they have no known competing financial interests or personal relationships that could have appeared to influence the work reported in this paper.

Acknowledgments

The authors would like to thank Renishaw plc UK and the staff of the drinking waterworks for all their support. This work has received funding from the European Union's Framework Programme for Research and Innovation Horizon 2020 under the Marie Skłodowska-Curie Grant Agreement MONPLAS No. 860775. The authors declare that they have no conflict of interest.

Appendix A. Supplementary data

Supplementary data to this article can be found online at https://doi.org/10.1016/j.heliyon.2023.e17113.

References

[1] C. Wang, J. Zhao, B. Xing, Environmental source, fate, and toxicity of microplastics, J. Hazard Mater. 407 (2021), 124357, https://doi.org/10.1016/j.jhazmat.2020.124357. ISSN 0304-3894.

[2] A. Vianello, R.L. Jensen, L. Liu, J. Vollertsen, Simulating human exposure to indoor airborne microplastics using a Breathing Thermal Manikin, Sci. Rep. 9 (2019) 8670, https://doi.org/10.1038/s41598-019-45054-w.

[3] M. Enfrin, F.L. Dumée, J. Lee, Nano/microplastics in water and wastewater treatment processes – origin, impact and potential solutions, Water Res. 161 (2019) 621–638, https://doi.org/10.1016/j.watres.2019.06.049.

[4] C. Bai, L. Liu, Y. Hu, E.Y. Zeng, Y. Guo, Microplastics: a review of analytical methods, occurrence and characteristics in food, and potential toxicities to biota, Sci. Total Environ. 806 (1) (2022), 150263, https://doi.org/10.1016/j.scitotenv.2021.150263. ISSN 0048-9697.

[5] Q. Zhang, E.G. Xu, J. Li, Q. Chen, L. Ma, E.Y. Zeng, H. Shi, A review of microplastics in table salt, drinking water, and air: direct human exposure, Environ. Sci. Technol. 54 (2020) 3740–3751, https://doi.org/10.1021/acs.est.9b04535.

[6] P. Schwabl, S. Koeppel, P. Koenigshofer, T. Bucsics, M. Trauner, T. Reiberger, B. Liebmann, Detection of various microplastics in human stool: a prospective case series, Ann. Intern. Med. 171 (2019) 453–457, https://doi.org/10.7326/M19-0618.

[7] A. Ragusa, A. Svelato, C. Santacroce, P. Catalano, V. Notarstefano, O. Carnevali, F. Papa, M.C.A. Rongioletti, F. Baiocco, S. Draghi, E. D'Amore, D. Rinaldo, M. Matta, E. Giorgini, Plasticenta: first evidence of microplastics in human placenta, Environ. Int. 146 (2021), 106274, https://doi.org/10.1016/j.envint.2020.106274. ISSN 0160-4120.

[8] J.P. da Costa, P.S.M. Santos, A.C. Duarte, T. Rocha-Santos, Nano)plastics in the environment – sources, fates and effects, Sci. Total Environ. 566–567 (2016) 15–26, https://doi.org/10.1016/j.scitotenv.2016.05.041.

[9] M. Eriksen, L.C.M. Lebreton, H.S. Carson, M. Thiel, C.J. Moore, J.C. Borerro, F. Galgani, P.G. Ryan, J. Reisser, Plastic pollution in the 'world's oceans: more than 5 trillion plastic pieces weighing over 250,000 tons afloat at sea, PLoS One 9 (12) (2014), e111913, https://doi.org/10.1371/journal.pone.0111913.

[10] Sources, fate and effects of microplastics in the marine environment: Part Two of a global assessment, 93, rep. Stud. GESAMP, in: P.J. Kershaw, C.M. Rochman (Eds.), Joint Group of Experts on the Scientific Aspects of Marine Environmental Protection, 2016, p. 220. https://digitallibrary.un.org/record/247441?ln=en.

[11] Microplastics in Drinking-Water, World Health Organization, Geneva, 2019. Licence: CC BY-NC-SA 3.0.

[12] J. Bhagat, N. Nishimura, Y. Shimada, Toxicological interactions of microplastics/nanoplastics and environmental contaminants: current knowledge and future perspectives, J. Hazard Mater. 405 (2021), 123913, https://doi.org/10.1016/j.jhazmat.2020.123913. ISSN 0304-3894.

[13] T. Roy, T.K. Dey, M. Jamal, Microplastic/nanoplastic toxicity in plants: an imminent concern, Environ. Monit. Assess. 195 (2023) 27, https://doi.org/10.1007/s10661-022-10654-z.
[14] D. Huang, J. Tao, M. Cheng, R. Deng, S. Chen, L. Yin, R. Li, Microplastics and nanoplastics in the environment: macroscopic transport and effects on creatures, J. Hazard Mater. 407 (2021), 124399, https://doi.org/10.1016/j.jhazmat.2020.124399. ISSN 0304-3894.
[15] K. Yin, Y. Wang, H. Zhao, D. Wang, M. Guo, M. Mu, Y. Liu, X. Nie, B. Li, J. Li, M. Xing, A comparative review of microplastics and nanoplastics: toxicity hazards on digestive, reproductive and nervous system, Sci. Total Environ. 774 (2021), 145758, https://doi.org/10.1016/j.scitotenv.2021.145758. ISSN 0048-9697.
[16] Q. Chen, A. Allgeier, D. Yin, H. Hollert, Leaching of endocrine disrupting chemicals from marine microplastics and mesoplastics under common life stress conditions, Environ. Int. 130 (2019), 104938, https://doi.org/10.1016/j.envint.2019.104938. ISSN 0160-4120.
[17] V.K. Sharma, X. Ma, E. Robert D. Lichtfouse, Nanoplastics are potentially more dangerous than microplastics, Environ. Chem. Lett. (2022), https://doi.org/10.1007/s10311-022-01539-1.
[18] N.J. Clark, F.R. Khan, D.M. Mitrano, D. Boyle, R.C. Thompson, Demonstrating the translocation of nanoplastics across the fish intestine using palladium-doped polystyrene in a salmon gut-sac, Environ. Int. 159 (2022), 106994, https://doi.org/10.1016/j.envint.2021.106994.
[19] P.A. Stapleton, Microplastic and nanoplastic transfer, accumulation, and toxicity in humans, Curr. Opin. Toxicol. 28 (2021) 62–69, https://doi.org/10.1016/j.cotox.2021.10.001. ISSN 2468-2020.
[20] Directive (EU), 2184 of the European Parliament and of the Council of 16 December 2020 on the quality of water intended for human consumption, 2020. https://eur-lex.europa.eu/eli/dir/2020/2184/oj.
[21] Y. Li, W. Li, P. Jarvis, W. Zhou, J. Zhang, J. Chen, Q. Tan, Y. Tian, Occurrence, removal and potential threats associated with microplastics in drinking water sources, J. Environ. Chem. Eng. 8 (2020), 104527, https://doi.org/10.1016/j.jece.2020.104527.
[22] S.V. Panno, W.R. Kelly, J. Scott, W. Zheng, R.E. McNeish, N. Holm, T.J. Hoellein, E.L. Baranski, Microplastic contamination in karst groundwater systems, Groundw 57 (2019) 189–196, https://doi.org/10.1111/gwat.12862.
[23] L. Zhang, J. Liu, Y. Xie, S. Zhong, B. Yang, D. Lu, Q. Zhong, Distribution of microplastics in surface water and sediments of qin river in beibu gulf, China, Sci. Total Environ. 708 (2019), 135176, https://doi.org/10.1016/j.scitotenv.2019.135176.
[24] E. Uurasjarvi, S. Hartikainen, O. Setala, M. Lehtiniemi, A. Koistinen, Microplastic concentrations, size distribution, and polymer types in the surface waters of a northern European lake, Water Environ. Res. 92 (2019) 149–156, https://doi.org/10.1002/wer.1229.
[25] S.M. Mintenig, M.G.J. Loeder, S. Primpke, G. Gerdts, Low numbers of microplastics detected in drinking water from ground water sources, Sci. Total Environ. 648 (2019) 631–635, https://doi.org/10.1016/j.scitotenv.2018.08.178.
[26] M. Pivokonský, L. Cermakova, K. Novotna, P. Peer, T. Cajthaml, V. Janda, Occurrence of microplastics in raw and treated drinking water, Sci. Total Environ. 643 (2018) 1644–1651, https://doi.org/10.1016/j.scitotenv.2018.08.102.
[27] UKWIR, Sink to River - River to Tap, A Review of Potential Risks from Nanoplastics and Microplastics, UK water industry research limited (UKWIR), London, 2019. https://ukwir.org/view/$NvDnwfm.
[28] J. Xue, S.H.A. Samaei, J. Chen, A. Doucet, K.T.W. Ng, What have we known so far about microplastics in drinking water treatment? A timely review, Front. Environ. Sci. Eng. 16 (2022) 58, https://doi.org/10.1007/s11783-021-1492-5.
[29] G. Zhou, Q. Wang, J. Li, Q. Li, H. Xu, Q. Ye, Y. Wang, S. Shu, J. Zhang, Removal of polystyrene and polyethylene microplastics using PAC and FeCl3 coagulation: performance and mechanism, Sci. Total Environ. 752 (2021), 141837, https://doi.org/10.1016/j.scitotenv.2020.141837. ISSN 0048-9697.
[30] N.K. Shahi, M. Maeng, D. Kim, S. Dockko, Removal behavior of microplastics using alum coagulant and its enhancement using polyamine-coated sand, Process Saf. Environ. Protect. 141 (2020) 9–17, https://doi.org/10.1016/j.psep.2020.05.020. ISSN 0957-5820.
[31] M. Pivokonský, L. Pivokonská, K. Novotná, L. Čermáková, M. Klimtová, Occurrence and fate of microplastics at two different drinking water treatment plants within a river catchment, Sci. Total Environ. 741 (2020), 140236, https://doi.org/10.1016/j.scitotenv.2020.140236. ISSN 0048-9697.
[32] Z. Wang, T. Lin, W. Chen, Occurrence and removal of microplastics in an advanced drinking water treatment plant (ADWTP), Sci. Total Environ. 700 (2020), 134520, https://doi.org/10.1016/j.scitotenv.2019.134520. ISSN 0048-9697.
[33] M.B. Emelko, P.M. Huck, B.M. Coffey, A review of Cryptosporidium removal by granular media filtration, Am. W. Works Assoc. 97 (12) (2005) 101–115, https://doi.org/10.1002/j.1551-8833.2005.tb07544.x.
[34] A. Amirtharajah, Some theoretical and conceptual views of filtration, Am. W. Works Assoc. 80 (12) (1988) 36–46, https://doi.org/10.1002/j.1551-8833.1988.tb03147.x.
[35] D. Schymanski, B.E. Oßmann, N. Benismail, K. Boukerma, G. Dallmann, E. von der Esch, D. Fischer, F. Fischer, D. Gilliland, K. Glas, T. Hofmann, A. Käppler, S. Lacorte, J. Marco, E.L.M. Rakwe, J. Weisser, C. Witzig, N. Zumbülte, N.P. Ivleva, Analysis of microplastics in drinking water and other clean water samples with micro-Raman and micro-infrared spectroscopy: minimum requirements and best practice guidelines, Anal. Bioanal. Chem. 413 (2021) 5969–5994, https://doi.org/10.1007/s00216-021-03498-y.
[36] a Kirstein I V, A. Gomiero, J. Vollertsen, Microplastic pollution in drinking water, Curr. Opin. Toxicol. 28 (2021) 70–75, https://doi.org/10.1016/j.cotox.2021.09.003. ISSN 2468-2020.
[37] SAPEA, Science Advice for Policy by European Academies - A Scientific Perspective on Microplastics in Nature and Society, SAPEA, Berlin, 2019.
[38] A. Gomiero, K.B. Øysæd, L. Palmas, G. Skogerbø, Application of GCMS-pyrolysis to estimate the levels of microplastics in a drinking water supply system, J. Hazard Mater. 416 (2021), 125708, https://doi.org/10.1016/j.jhazmat.2021.125708. ISSN 0304-3894.
[39] b. Kirstein I V, F. Hensel, A. Gomiero, L. Iordachescu, A. Vianello, H.B. Wittgren, J. Vollertsen, Drinking plastics? – Quantification and qualification of microplastics in drinking water distribution systems by μFTIR and Py-GCMS, Water Res. 188 (2021), 116519, https://doi.org/10.1016/j.watres.2020.116519. ISSN 0043-1354.
[40] M. Simon, N. van Alst, J. Vollertsen, Quantification of microplastic mass and removal rates at wastewater treatment plants applying Focal Plane Array (FPA)-based Fourier Transform Infrared (FT-IR) imaging, Water Res. 142 (2018) 1–9, https://doi.org/10.1016/j.watres.2018.05.019.
[41] F. Weber, J. Kerpen, S. Wolff, R. Langer, V. Eschweiler, Investigation of microplastics contamination in drinking water of a German city, Sci. Total Environ. 755 (2) (2021), 143421, https://doi.org/10.1016/j.scitotenv.2020.143421. ISSN 0048-9697.
[42] L. Feld, V.H.d. Silva, F. Murphy, N.B. Hartmann, J. Strand, A study of microplastic particles in Danish tap water, Water 13 (2021) 2097, https://doi.org/10.3390/w13152097.
[43] M. Pittroff, Y.K. Müller, C.S. Witzig, M. Scheurer, F.R. Storck, N. Zumbülte, Microplastic analysis in drinking water based on fractionated filtration sampling and Raman microspectroscopy, Environ. Sci. Pollut. Res. 28 (2021) 59439–59451, https://doi.org/10.1007/s11356-021-12467-y.
[44] P.S. Bäuerlein, R.C.H.M. Hofman-Caris, E.N. Pieke, T.L. ter Laak, Fate of microplastics in the drinking water production, World Resour. 221 (2022), 118790, https://doi.org/10.1016/j.watres.2022.118790. ISSN 0043-1354.
[45] A. Zamani, B. Maini, Flow of dispersed particles through porous media — deep bed filtration, J. Pet. Sci. Eng. 69 (1–2) (2009) 71–88, https://doi.org/10.1016/j.petrol.2009.06.016. ISSN 0920-4105.
[46] R. Liu, Z. Tan, X. Wu, Y. Liu, Y. Chen, J. Fu, H. Ou, Modifications of microplastics in urban environmental management systems: a review, Water Res. 222 (2022), 118843, https://doi.org/10.1016/j.watres.2022.118843. ISSN 0043-1354.
[47] D. Adib, R. Mafigholami, H. Tabeshkia, Identification of microplastics in conventional drinking water treatment plants in Tehran, Iran, J. Environ. Health. Sci. Engineer 19 (2021) 1817–1826, https://doi.org/10.1007/s40201-021-00737-3.
[48] M. Shen, Z. Zeng, X. Wen, X. Ren, G. Zeng, Y. Zhang, R. Xiao, Presence of microplastics in drinking water from freshwater sources: the investigation in Changsha, China, Environ. Sci. Pollut. Res. 28 (2021) 42313–42324, https://doi.org/10.1007/s11356-021-13769-x.
[49] D. Kankanige, S. Babel, Contamination by ≥6.5 μm-sized microplastics and their removability in a conventional water treatment plant (WTP) in Thailand, J. Water Process Eng. 40 (2021), 101765, https://doi.org/10.1016/j.jwpe.2020.101765. ISSN 2214-7144.
[50] D.M. Mitrano, P. Wick, B. Nowack, Placing nanoplastics in the context of global plastic pollution, Nat. Nanotechnol. 16 (2021) 491–500, https://doi.org/10.1038/s41565-021-00888-2.

[51] Z. Sobhani, X. Zhang, C. Gibson, R. Naidu, M. Megharaj, C. Fang, Identification and visualisation of microplastics/nanoplastics by Raman imaging (i): down to 100 nm, Water Res. 174 (2020), 115658, https://doi.org/10.1016/j.watres.2020.115658. ISSN 0043-1354.
[52] S. Frehland, R. Kaegi, R. Hufenus, D.M. Mitrano, Long-term assessment of nanoplastic particle and microplastic fiber flux through a pilot wastewater treatment plant using metal-doped plastics, Water Res. 182 (2020), 115860, https://doi.org/10.1016/j.watres.2020.115860. ISSN 0043-1354.
[53] WHO Guidelines for Drinking – Water Quality, World Health Organization, Geneva, 2009. https://www.who.int/publications/i/item/WHO-HSE-WSH-09.05.
[54] P. Wu, S. Lin, G. Cao, J. Wu, H. Jin, C. Wang, M.H. Wong, Z. Yang, Z. Cai, Absorption, distribution, metabolism, excretion and toxicity of microplastics in the human body and health implications, J. Hazard Mater. 437 (2022), 129361, https://doi.org/10.1016/j.jhazmat.2022.129361. ISSN 0304-3894.

Paper II

It matters how we measure – Quantification of microplastics in drinking water by µFTIR and µRaman

L. Maurizi, L. Iordachescu, I.V. Kirstein, A.H. Nielsen, J. Vollertsen

The paper is currently under review

It matters how we measure - Quantification of microplastics in drinking water by µFTIR and µRaman

L. Maurizi[a,], L. Iordachescu[a], I. V. Kirstein[b], A. H. Nielsen[a], J. Vollertsen[a]*

[a] *Department of The Built Environment, Aalborg University, 9220 Aalborg, Denmark*

[b] *Alfred-Wegener-Institute Helmholtz Centre for Polar and Marine Research, Biologische Anstalt Helgoland, Helgoland, Germany*

[*]*Correspondence: lucam@build.aau.dk (L.M.)*

Abstract: The water treatment for microplastics (MP) at a Danish groundwater-based waterworks was assessed by Fourier-Transform micro-spectroscopy (µFTIR) (nominal size limit 6.6 µm) and compared to results from Raman micro-spectroscopy (µRaman) (nominal size limit 1.0 µm) on the same sample set. The MP abundance at the waterworks' inlet and outlet was quantified as MP counts per cubic metre (N/m^3) and estimated MP mass per cubic metre (µg/m^3). The waterworks' MP removal efficiency was found to be higher when analysing by µFTIR (counts: 78.14 ± 49.70%, mass: 98.73 ± 11.10%) and less fluctuating than when using µRaman (counts: 43.2%, mass: 75.1%). However, both techniques pointed to a value of ~80% for the counts' removal efficiency of MPs > 6.6 µm. Contrarily to what was shown by µRaman, no systematic leaking of MPs from the plastic elements of the facility could be identified for the µFTIR dataset, either from the counts (inlet 31.86 ± 17.17 N/m^3, outlet 4.98 ± 2.09 N/m^3) or mass estimate (inlet 76.30 ± 106.30 µg/m^3, outlet 2.81 ± 2.78 µg/m^3). The estimation of human MP intake from drinking water calculated from the µFTIR data (5 N/(year·capita)) proved to be approximately 332 times lower than that calculated from the µRaman dataset, although in line with previous studies employing µFTIR. By merging the MP length datasets from the two techniques, it could be shown that false negatives became prevalent in the µFTIR

dataset already below 50 µm. Further, by fitting the overall frequency of the MP length ranges with a power function, it could be shown that µFTIR missed approximately 95.7% of the extrapolated MP population (1 – 1865.9 µm). Consequently, relying on only µFTIR may have led to underestimating the MP content of the investigated drinking water, as most of the 1 – 50 µm MPs would have been missed.

Keywords: microplastics; Raman micro-spectroscopy; FTIR micro-spectroscopy; drinking water

1. Introduction

Since the beginning of the century, when it was first demonstrated that microscopic plastic fragments and fibres accumulate in the marine environment [1], the study of microplastic pollution has evolved into a mature research field. Following the findings of Ref. [1], a debate arose around the origin of these small plastic fragments and how they could be classified. Regarding the latter, a standard definition of the term "microplastic" (and its close relative "nanoplastic") is still lacking, but plastic debris smaller than 1 µm is generally called *nanoplastics* (NPs), while *microplastics* commonly are associated with particles between 5 mm and 1 µm [2]. Furthermore, plastic particles with a size between 1 and 5 mm are sometimes called "large microplastics" [3]. In the present paper, these conventions were also followed.

Regarding the origin of the plastics, intentionally produced microplastics, such as microbeads added to cosmetic and personal care products are one source of MPs [4], commonly called "primary microplastics". A more common type is "secondary microplastics", that is, MPs created by fragmentation of everyday plastic objects [5]. The main parameter by which MPs are classified is the "size", which commonly is defined as the major dimension of its 2D projection [6]. Size is important, as the toxic impact of MPs among others depends on particle size, where small MPs and NPs are believed to exert higher toxicity than larger ones [7]. For example, 1 – 10 µm poly-styrene (PS) MPs have been shown to cause necroptosis and inflammation in mice [8], and enhanced cellular uptake was observed in three human cell lines exposed to ~1 µm PS and 400 nm poly-methylmethacrylate (PMMA) NPs [9]. Therefore, the accurate quantification of small sized MPs

and NPs is an important topic due to the potential effects on human health as a consequence of daily exposure [10].

Human intake of MPs can occur *via* three major pathways, inhalation, dermal contact, and through the ingestion of food and beverages [11]. Also drinking water represents a source of MP intake by humans [12], with bottled water generally showing higher abundance than tap water [13]. Nonetheless, tap water can be an important contributor to human MP exposure. Tap water is produced by purifying a raw water source, and understanding MP occurrence before and after the treatment in the waterworks can provide useful insights into the efficiency of the facility in removing the MPs [14]. Typically, advanced drinking water plants employing a series of treatment steps show higher MP removal efficiency than simpler facilities [15].

For measuring MPs in drinking water, spectroscopic techniques have often been the method of choice [16], although no standardized protocols are yet agreed on for the analysis of drinking water [17]. Among the spectroscopic methods, Fourier-Transform InfraRed micro-spectroscopy (µFTIR) is by far the most widely used technique. It allows for analysing particles and fibres on an active area either on filters [18] or windows [19]. Today, many of these instruments are equipped with a Focal Plane Array (FPA) detector enabling them to take extensive chemical images in a relatively short time, even if complex analytes such as fibres are present [20].

Raman micro-spectroscopy (µRaman) is considered an alternative or complementary analytical technique to µFTIR. It is characterized by a finer spatial resolution in the XY plane than µFTIR [21]. Therefore, it is generally utilized for the smallest particle fraction down to around 0.4 µm, depending on the chosen analytical parameters. For particles above 10 µm, µFTIR is generally the preferred technique [21]. µRaman analysis is typically performed directly on the filters where the samples were previously deposited. Generally, a so-called "point and shoot" approach is followed: the instrument's laser is automatically driven to each particle, identified from the visible image's background by contrast [22]. Consequently, the analysis time of a µRaman investigation depends on the number of items to be analysed, the spectral acquisition time, and the number of spectral accumulations selected. Thus, µRaman is generally a more time-consuming method than µFTIR [23].

Up to now, there have been limited attempts to compare the outcome of these two techniques concerning the analysis of MPs in environmental samples. Marine water from the North Sea was analysed [24], and the results from µFTIR and µRaman were compared. The authors showed that the MP abundance in the same size ranges from µRaman data was higher than that estimated from µFTIR. The difference was due to the inherently better ability of µRaman to detect MPs below 10 µm, which were found to be the most abundant size fraction in the samples. More recently, atmosphere pollution from MPs has been studied. Ref. [25] published a study where MPs from indoor and outdoor air were analysed with µFTIR and µRaman. In this case, the two techniques found different polymers in the samples for the size range 20 – 8961 µm: µFTIR data showed a prevalence of poly-styrene (PS), while µRaman indicated poly-vinyl chloride (PVC) as the most common plastic type. This discrepancy may be due to the different spectral identification methods used by the authors for the two techniques.

In the present work, we applied µFTIR to quantify the MP content of drinking water samples from a Danish waterworks and compared the result with that of µRaman, which we described in Ref. [26]. Although these two spectroscopic techniques have so far been the most widely employed for MP analysis in drinking water [27], a systematic experimental comparison between the two methods is still lacking for this environmental compartment. Hence, we believe that such a study is imperative to put the current state-of-the-art into perspective, in light of the upcoming requirement of the European regulation on MP monitoring in drinking water [28].

2. Materials and methods

2.1. Sampling of drinking water and field blanks

The waterwork structure and sampling process were described in Ref. [26]. In short, the investigated waterworks produces around 500000 m^3/year of drinking water from groundwater, utilizing a simple treatment process consisting only of oxidation and rapid sand filtration. The groundwater is extracted from a limestone aquifer at a depth of 72 – 92 m. A network of pumps and pipes transfers the raw water from the wells to the waterworks. After the treatment, the water is retained in two tanks with a storage capacity of 110

m^3 each, corresponding to a retention time of approximately 2 – 3 hours during daytime. From here, the water is pumped into the distribution network.

The sampling campaign took place between the 28th of September and the 1st of October 2021. Both the waterworks' inlet and outlet were sampled for five consecutive days, from 9 a.m. to 2 p.m. with two custom-made sampling devices. Each sampling device consisted of four flow lines hosting one or two filter holders and terminating with a flowmeter to quantify the sampled volume. The inlet of the devices was connected to the sampling points by a flexible steel tube. Approximately 1 m^3 of drinking water was filtered on each of the filters (1 µm sintered steel filters (Mesh Masters, The Netherlands)) along the first three flow lines of the two sampling devices (3 L/min). Inlet and outlet were sampled in parallel, resulting therefore in a total of 5 inlet and 5 outlet samples collected in triplicates (n = 30).

For the field blanks, the fourth flow line of the two sampling devices was equipped with two filter holders in series. The first one hosted a muffled 0.7 µm glass fibre membrane (Th. Geyer GmbH, Germany), whilst the second one held a 1 µm sintered steel filter. Approximately 20 L of drinking water were pre-filtered through the glass fibre membrane onto the sintered steel filter for each field blank. Two field blanks were sampled in parallel on each day, thus obtaining 10 replicates in total. The volume sampled for the field blanks was lower than that of the drinking water samples since blank contamination mainly occurs during sample preparation at the laboratory and is not related to the amount of sampled water. The 1 µm sintered steel filters were stored in Petri dishes before sample preparation. Further information on the waterworks and the sampling is available in the Supplementary Information.

2.2. Contamination prevention

All chemicals were filtered through muffled glass fibre membranes to remove any particles and fibres above 0.7 µm. The glassware was muffled at 500°C for 4 hours, and metallic labware was thoroughly rinsed with particle-free water before use. Moreover, the filters were stored in muffled Petri dishes inside a laminar flow bench until treatment. Pure cotton lab coats were worn during the entire sample preparation, and the usage of plastic gloves was avoided during sample preparation. All sample preparation was done in a laminar flow bench, which was regularly cleaned with 50% EtOH.

2.3. Sample preparation and deposition

The sample preparation protocol for the µRaman analysis was presented in Ref. [26] (see also Supplementary Information, section 2 and Figure S3). In short: after the sampling, the 1 µm sintered steel filters were incubated in 5% SDS (Sodium Dodecylsulphate, Th. Geyer GmbH, Germany) at 50°C for 24 h, and, after 5 minutes of ultrasonication, the particle-enriched SDS mixture was filtered through the same filter with a vacuum filtering system. After a further round of ultrasonication in 50% EtOH (EtOH for HPLC, Th. Geyer GmbH, Germany) and vacuum filtration, the particles on each filter were recovered in 50% EtOH and the ethanolic mixture was poured into a 10 mL vial. Finally, the mixture was dried at 55°C under gentle nitrogen flux in a water bath (TurboVap Biotage, Sweden) and reconstituted with 1000 µL of ~99.5% EtOH. The µRaman analysis was performed on the active area of each sample obtained by deposition.

For the µFTIR analysis, the same samples were dried under gentle nitrogen flow in a water bath at 55°C and reconstituted with 2000 µL of 50% EtOH. The deposition was performed by means of compression cells onto 13 mm diameter Zinc Selenide (ZnSe, Crystran Ltd., UK) windows of 2 mm thickness with a manual pipette equipped with 200 µL glass tips (Brand GmbH, Germany). 1000 µL were deposed for the drinking water samples, and 600 µL for the field blanks. The samples were dried at 55°C on a heating plate (W10 VWR, Denmark) overnight, which produced an active area of approx. 10 mm in diameter. Sample reconstitution, deposition, and analysis took place in March – September 2022.

2.4. µFTIR analysis and spectral recognition

Analysis was conducted with a Focal Plane Array (FPA) – µFTIR. A Cary 620 FTIR microscope coupled with a Cary 670 IR spectroscope (Agilent Technologies, USA) was used to scan the active area of the enriched ZnSe transmission windows. The microscope was equipped with a 25× Cassegrain objective, producing 3.3 µm pixel resolution on a 128×128 mercury cadmium telluride (MCT) FPA detector. The detector was cooled down to the operative temperature of 80K with liquid nitrogen continuously pumped into the FPA dewar from a holding tank (Norhof, The Netherlands). All scans were carried out in transmission mode with a spectral range of 3750 – 850 cm^{-1} at 8 cm^{-1} resolution applying 30 co-added scans in transmission mode. A background tile was collected before each sample's scan, using the same

parameters, but co-adding 120 scans instead of 30. A chemical image of the sample's active area was obtained, where each pixel contained an IR background-corrected spectrum.

The µFTIR chemical images were analysed with the software siMPle [29] v. 1.3.1β. It can automatically detect the particles in a µFTIR spectral image, determine their morphological parameters, and estimate their volume and mass. Specifically, the volume of a particle was estimated from its 2-dimensional projection by first calculating its equivalent ellipse where the major diameter equals its longest Feret diameter, then calculating an equivalent ellipsoid where the third diameter equals 0.6 times the second diameter of the equivalent ellipse. The mass was then found by multiplying the volume of the ellipsoid by the density of the identified polymer ([6], [30]).

Each pixel containing an IR spectrum was compared with the built-in software's library, which led to an estimation of the Pearson correlation coefficient. Both the original spectrum and the first derivative were compared with the library's references (Supplementary Information, section 5 for examples of experimental µFTIR spectra) after an automatic removal of the CO_2 peaks. Moreover, spectral matches from the software were manually checked to further assess their reliability.

Considering the filters' pore size (1 µm), the nominal pixel size of the µFTIR at 25× magnification (3.3 µm), and the observation that objects represented by only one pixel on the FPA image sometimes were false positives, it was decided to include only objects occupying at least 3 pixels, corresponding to a triangular shape, i.e. particles of a minimum length of 6.6 µm (Kirstein *et al.* 2021) [30]. Cellulose and protein particles could also be successfully identified in the samples as done with the MPs, and they represented the non-plastic fraction in the MPs/non-plastic ratio quantification.

The µRaman analysis of the blanks and drinking water samples was conducted as reported in Ref. [26]. Briefly: a visible montage of the sample's active area was taken at 50×, and the spectral acquisition was automatically performed at 100× with a 532 nm laser (power 50 mW, grating 1200 ll/mm) onto each particle above 1 µm in the visible picture. The spectral recognition was conducted with the commercial library associated with the software of the µRaman system, and the particle mass was estimated as done for the µFTIR data.

2.5. Post-processing of the μFTIR data

For each drinking water sample replicate, the MP counts and estimated mass was calculated as the sum of the counts or estimated mass of each identified polymer. The values of MP abundance were corrected by subtracting the corresponding blank mean. Then, the values for the three replicates were averaged and normalized to 1 m^3, thus leading to the MP counts in N/m^3 and estimated MP mass in $\mu g/m^3$.

The waterworks' removal efficiency *R* was calculated as the cumulated efficiency over the five investigated days. Hence the sum of the MP counts or mass abundance at the inlet ([MPs_{inlet}]) was compared with that of the outlet ([MPs_{outlet}]) according to equation (1):

$$R = -(([MPs_{outlet}] - [MPs_{inlet}])/[MPs_{inlet}]) \cdot 100\% \quad (1)$$

Uncertainty was calculated by selecting a coverage factor $k = 2$ ($P = 95\%$) and considering only the A-type (statistical) contribution. The statistical tests and non-linear regression of the MP length frequency were performed with RStudio v. 2022.02.1+461. Normality was assessed with the Shapiro-Wilk test. ANOVA was conducted for significance assessment ($\alpha = 0.05$) and Tukey-test for pair-wise factor comparison. The samples were labeled as Dxy, where D means "Day", x is the sampling day (1 – 5), and y is either i or o (i = inlet, o = outlet).

The MP quantification from the μRaman analysis was described in Ref. [26]. Briefly: for each polymer in the replicates, the MP counts and estimated mass were corrected by subtracting the blank mean, and the value obtained was considered only if above the corresponding LOQ. The MP counts and estimated mass for each replicate were obtained as the sum of the polymers above the LOQ, and then the three replicates were averaged. Equation (1) was finally applied to calculate the MP removal efficiency over the investigated period and also according to the MP size ranges 1 – 10 μm, 10 – 20 μm, 20 – 50 μm, and 50+ μm.

3. Results and discussion

3.1. Microplastic morphological analysis

The morphological data from the μFTIR analysis were not blank-corrected. The MPs were grouped into five length ranges (6.6 – 50 μm, 50 – 100 μm, 100 – 200 μm, 200 – 500 μm, and 500+ μm), and their frequency was calculated for each investigated day for both inlet and outlet (Figure 1).

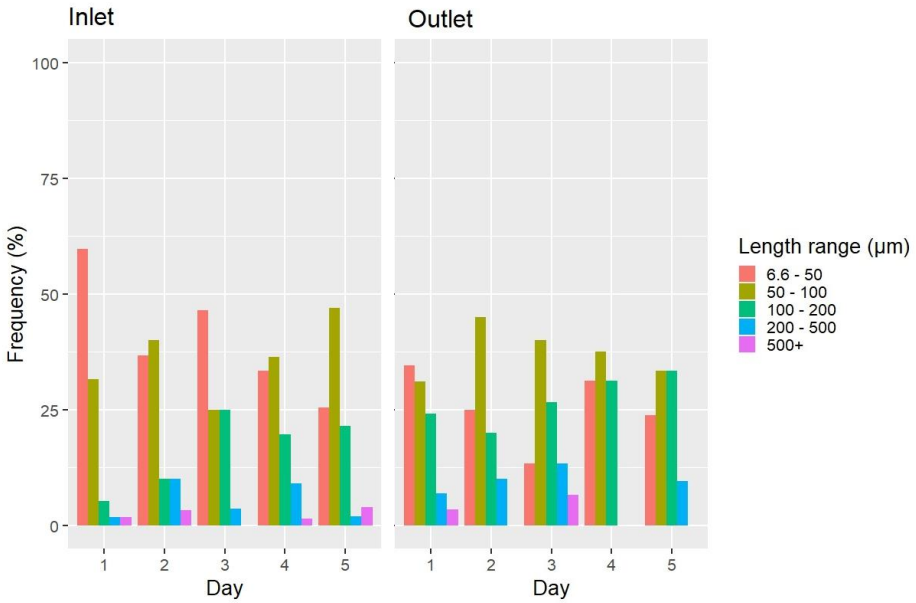

Figure 1. Barplots of the MP length ranges frequency over Days 1 – 5 at the waterworks' inlet and outlet. Values not corrected for blank contamination (µFTIR analysis).

In the inlet samples, the majority of MPs belonged to the 6.6 – 50 µm length range (mean 40.1%), followed by those sized between 50 and 100 µm (mean 36.6%). The remaining three length ranges accounted for approximately 23% of the entire inlet MP population. In the outlet samples, the 50 – 100 µm length range was the most populated (mean 36.6%), whilst the 6.6 – 50 µm and the 100 – 200 µm length ranges were equally represented (mean 26.7%). The MPs above 200 µm accounted for approximately 10% ($p < 0.05$). According to [24] and [31], the MP size frequency increases with decreasing MP size according to a power law. However, Figure 1 suggests that this was not the case for the MP size data from the µFTIR analysis reported in this work, where the 6.6 – 50 µm MP frequency was generally comparable with that of 50 – 100 µm MPs. Hence µFTIR may have missed some of the MPs below 50 µm during the analysis, thus leading to an MP size frequency differing from what was expected (see also section 3.3). Ref.s [32] and [33], who investigated the MP occurrence down to 20 µm in drinking water plants in respectively Korea and Spain with µFTIR, also reported that the frequency of >200 µm MPs decreased after the water treatment.

The largest analysed MP was 1865.9 µm long and the median length was highest in the outlet samples (65.3 *versus* 60.5 µm at the inlet). The smallest detected MP was 13.3 µm long, approximately twice the theoretical size limit considered acceptable with the employed FPA detector (see section 2.4). This may likely be due to the recognition thresholds chosen in the siMPle software upon the spectral matching, which may have caused the dismissal of potential MPs due to a low hit quality. The spectral quality of an IR transmission analysis is strongly affected by the thickness of the sample [34], and it rapidly deteriorates if thin samples, like MPs < 20 µm, are analysed. Therefore, setting the quality thresholds was subject to a compromise between reducing the false positives and recovering as many MPs as possible from the IR maps of the samples.

The MP shape was investigated by defining those with a length/width ratio greater or equal to 3 as fibres, otherwise as fragments [35]. For both morphotypes, the inlet samples presented higher counts of items than the outlet samples except for D1, where six fibres were found in the inlet samples and 8 in those of the outlet. Overall, the fragments accounted for 79.3% of the analysed MPs, the rest being fibres.

These findings were strongly different from what was found in the µRaman investigation [26], where the MPs longer than 50 µm represented the least populated fraction, and the largest item was 204.6 µm long (median length inlet and outlet 2.4 µm). In addition, the fibres represented less than 2% of the total MP population in the µRaman dataset, which suggested the fibre-like morphotype to be increasingly rare as smaller size ranges are considered. This observation is supported by Ref. [36] who employed µFTIR to analyse MPs in Danish drinking water above 100 µm and found that the majority had a fibre shape.

3.2. Microplastic quantification with µFTIR

3.2.1. Microplastics in the field blanks

Despite great care being exercised when preparing the samples, MPs were found in the field blanks. The mean counts estimate was 13.4 ± 12.0 N/m^3, with the following polymeric frequency: PVC 31.9%, poly-ester (PET) 25.5%, poly-propylene (PP) 25.5%, poly-vinyl dichloride (PVDC) 12.8%, and alkyd 4.2%. The mean mass estimate was 2.0 ± 2.3 µg/m^3, with the following polymeric composition: PET 60.9%, PVC 21.2%, PP 13.5%, alkyd 3.2%, and PVDC 1.2%. All inlet samples presented a mean MP abundance above the blank

mean, whilst the MP abundance of the outlet samples was lower (with the exception of D1 and D3 for the estimated mass). Since in the drinking water samples there were also different polymers from those in the blanks, the mean MP counts of the blanks have to be considered indicative.

3.2.2. Microplastic abundance in the drinking water samples

Combining the data from µFTIR and Raman, Figure 2 shows the MP abundance according to the counts and mass estimates for both sampling locations on each investigated day. The source of the error for the µFTIR data might come from a true variability between the triplicates, or it might be an artefact of the deposition procedure, as only half of the sample extract was deposited and analysed. That is, the MPs might have been inhomogeneously distributed inside the vials while the deposition took place. For the MP mass estimate, the usage of the ellipsoid model is an additional source of uncertainty, as it cannot fully cover the variety of MP morphotypes. Furthermore, the data in Figure 2 show the sum of all polymers, hence the error also depends on the variation associated with the single polymers.

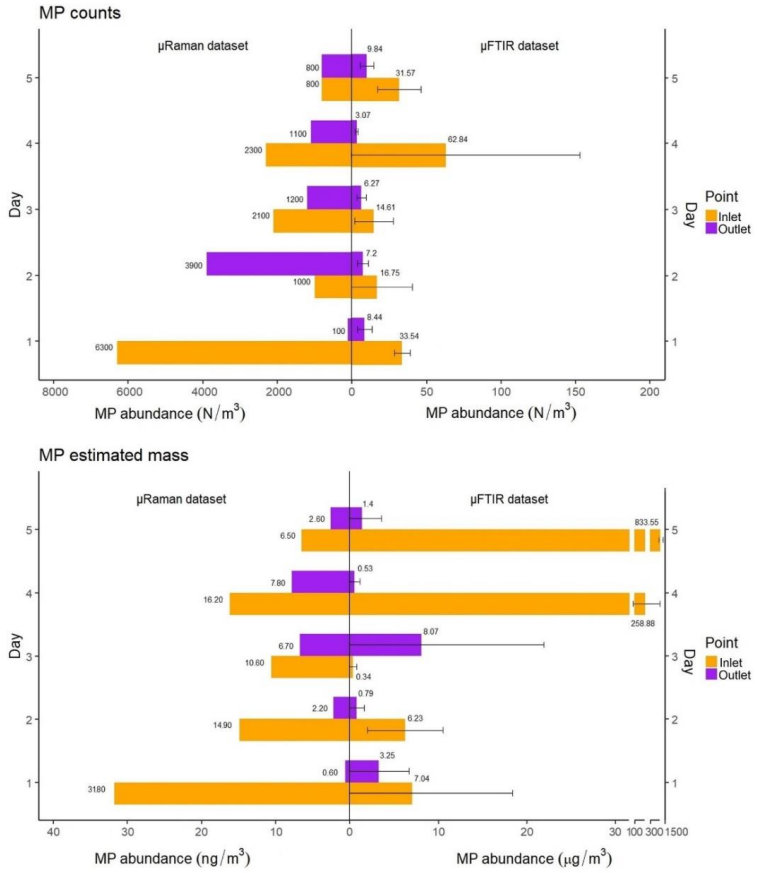

Figure 2. MP counts and estimated mass over the investigated period according to the µFTIR and µRaman analysis.

The outcome of the µFTIR analysis was not in line with that of the µRaman study. According to the µFTIR data, none of the five days had MP counts at the inlet higher than that at the outlet. Consequently, the ANOVA and Tukey test showed a significant difference ($p < 0.05$) between "inlet" and "outlet", which meant the waterworks removed MPs. The µRaman investigation on the other hand showed that the MP counts at the outlet on D2 were higher (3900 N/m^3) than that at the inlet (1000 N/m^3). The MP mass estimate provided by µFTIR was approximately 23 times higher at the outlet (8.07 ± 16.05 µg/m^3) than at the inlet (0.34 ± 0.49 µg/m^3) on D3, whilst on the remaining four days it was always lower at the outlet. The single event that occurred on D3 did not influence the outlet values on D4 and D5, which showed a strong retainment by the waterworks. Scrutinizing the data, it became clear that a few but large-sized MPs were

released on D3, which accounted for the mass at the outlet being larger than at the inlet. On average, the µFTIR analysis yielded 31.86 ± 17.17 N/m^3 at the inlet and 6.96 ± 2.27 N/m^3 at the outlet, whilst the mean MP mass estimate was 221.21 ± 320.04 µg/m^3 at the inlet and 2.81 ± 2.78 µg/m^3 at the outlet (Figure 2). The mean MP counts provided by the µRaman analysis [26] were markedly higher (inlet: 2500 ± 2000 N/m^3, outlet: 1400 ± 1300 N/m^3), whilst the mean MP mass was approximately 10^{-3} times lower (inlet: 16.0 ± 8.5 ng/m^3, outlet: 4.0 ± 2.7 ng/m^3). Ref. [24] also found that µRaman led to far higher MP counts than µFTIR (39 – 2621 N/m^3 and 22 – 228 N/m^3, respectively) when applied to the MP analysis of marine water. The authors addressed the higher degree of automatization of µRaman as the main reason why this method proved to be more efficient in recognizing the 10 – 500 µm MPs. In the case of this work, the µFTIR system performed automatized FPA mapping, so the bias was minimal, and no manual selection of particles was necessary. Hence the discrepancy between µFTIR and µRaman regarding the MP abundance in the analysed drinking water samples should mainly be associated with the different spatial resolution of the two methods, which for µFTIR seems larger than expected (sections 3.1 and 3.3). Comparing the outcomes of the two methods, it is evident that the usage of only µFTIR would have led to a ~150 times underestimation of the MP counts abundance in the analysed drinking water. Ref. [25] also reported that µFTIR underestimated the MP counts abundance of air samples if compared with µRaman by approx. 10 times and by manually selecting the particles to be analysed.

3.2.3. Removal efficiency of the waterworks

The MP counts removal efficiency calculated from the µFTIR analysis was higher (78.1 ± 49.7%) than that calculated from the µRaman dataset (43.2 ± 45.9%). Moreover, the counts removal efficiency as per the µFTIR exhibited an increasing tendency over the investigated five days, contrary to the decreasing tendency shown by µRaman. Nonetheless, the MP counts removal efficiency provided by µFTIR was in line not only with previous studies from the literature ([37], [38]) but also with the value obtained for the 6.6+ µm MPs from the µRaman dataset (81.3%). However, the µRaman analysis also showed that the removal efficiency of the 1 – 6.6 µm MPs was approx. 40%, a finding not provided by µFTIR (due to differences in nominal size limits) and which could explain the overall lower value of MP counts retainment as per µRaman.

A similar picture emerged from the MP mass removal efficiency. In this case, the µFTIR analysis provided a mean value of 98.7 ± 11.1% *versus* 75.1 ± 28.2% from µRaman. Although the MPs sized 1 – 6.6 µm approx. represented the majority in terms of MP counts in the µRaman dataset, they did not account for a large mass altogether, which was in the order of ng/m^3. On the contrary, the MPs identified by µFTIR, being larger, held a mass in the order of µg/m^3. Hence the influence of the smaller MPs on the mass balance was not decisive and close values of MP mass removal efficiency could be obtained with the two techniques. Overall, these findings indicated that larger MPs could be more efficiently retained than smaller ones, which is in accordance with previous studies on deep bed filtration in granular media ([39], [40], [41], [42]).
µFTIR also allowed for the identification of non-plastic particles, namely cellulose and proteic polymers [25], whilst during the µRaman analysis the non-plastic particles could not be identified [26]. Overall, the MPs/non-plastic ratio provided by µFTIR was generally higher (inlet 30.0 – 468.7%, outlet 7.6 – 79.5%) than that of µRaman (inlet 0.9 – 29.0%, outlet 0.3 – 21.5%). Therefore, µRaman may have been less efficient in detecting the MPs (i.e. false negatives showing a not recognizable Raman spectrum due to fluorescence and low scattering), which led to a smaller fraction of the MPs in the active area being identified. In this regard, the MPs/non-plastic ratio may also be considered an efficiency parameter of the analytical device employed. However, it should be considered that the quality thresholds set in the software siMPle also played a role in determining the MP counts calculated in the drinking water samples as per the µFTIR analysis, as well as the spectral hit quality criteria chosen in the µRaman study.

3.2.4. MP composition of the drinking water samples

The polymer frequency (as determined by µFTIR) in the outlet samples was characterized by an increase in PET in both the MP counts and estimated mass, as shown in Figures 3 and 4. According to the counts estimate (Figure 3), the most abundant polymeric category at the inlet was PV(D)C (7.0% – 54.0%), followed by acrylic (0 – 60.4%) and PE (0 – 42.5%). At the outlet, PV(D)C was again the most abundant plastic (0 – 84.7%), but PET immediately followed (0.0 – 70.8%). No enrichment in PA at the outlet could be seen in this case, contrary to what was shown by µRaman (mean inlet 39%, mean outlet 78%). This was

not surprising, considering that the majority of the PA particles were sized 1 – 5 µm, so they could not be analysed by µFTIR.

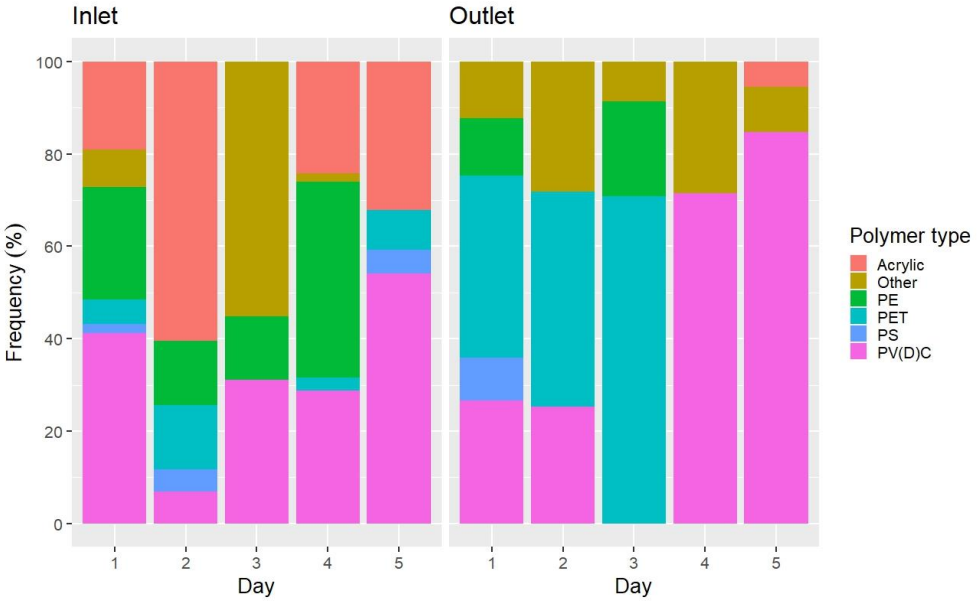

Figure 3. MP frequency at the inlet and outlet over the investigated period according to the µFTIR analysis (counts).

The mass estimate showed a different picture (Figure 4). At the inlet, PET was indeed the most common polymer (mean 97.9%), followed by PV(D)C (mean 1.45%). At the outlet, PET accounted for 88.7% on average (0 – 99.2%), resulting in the most abundant polymer of the mass estimate. Therefore, the higher MP mass abundance at the outlet on D3 as per the µFTIR analysis may have been caused by a temporary leaking of PET particles sized above 6.6 µm. On the other hand, PA (mean inlet 37%, mean outlet 34%) and poly-acrylics (mean inlet 19%, mean outlet 65%) were the most frequent polymers in the mass estimate provided by µRaman. Overall, the significance test could not associate any of the polymer groups identified by µFTIR with a contribution in terms of a *persistent* release of MPs during the treatment. On the contrary, a significative and systematic presence of PA particles at the outlet was identified by µRaman.

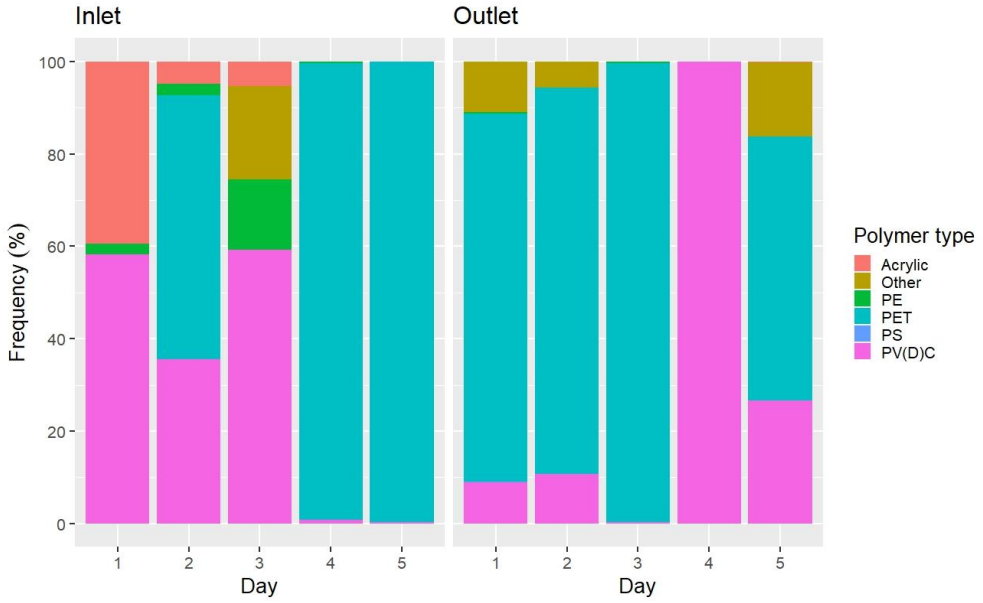

Figure 4. MP frequency at the inlet and outlet over the investigated period according to the µFTIR analysis (estimated mass).

3.3. Overall comparison between µFTIR and µRaman

Figure 5 graphically emphasizes the two distinct "MP size domains" of µFTIR and µRaman, by plotting the width *vs* length of all the analysed MPs in Ref. [26] and the current study in a $\log_{10}$ graph. As can be seen, between 1 and 2 of the log(Length) (10 – 100 µm), µFTIR started missing the smaller MPs, and data from µRaman became prevalent. Hence the experimental size quantification limit for µFTIR (at the applied analysis conditions) proved to be approx. in the centre of this range (50 µm), well above the nominal one (6.6 µm at 25×). Accordingly, in section 3.1 it was observed that the frequency of 6.6 – 50 µm MPs was lower than expected from the literature. This does not mean that µFTIR cannot analyze MPs below 50 µm (the smallest MP identified in the present study by µFTIR was indeed 13.3 µm long), but rather, that the false negatives risk overcoming the true positives. Therefore, the µFTIR data associated with the 6.6 – 50 µm range should be considered indicative not only in the present study, but also in the previous works based on

µFTIR reported in the literature. Consequently, µRaman should be employed to efficiently target MPs below 50 µm.

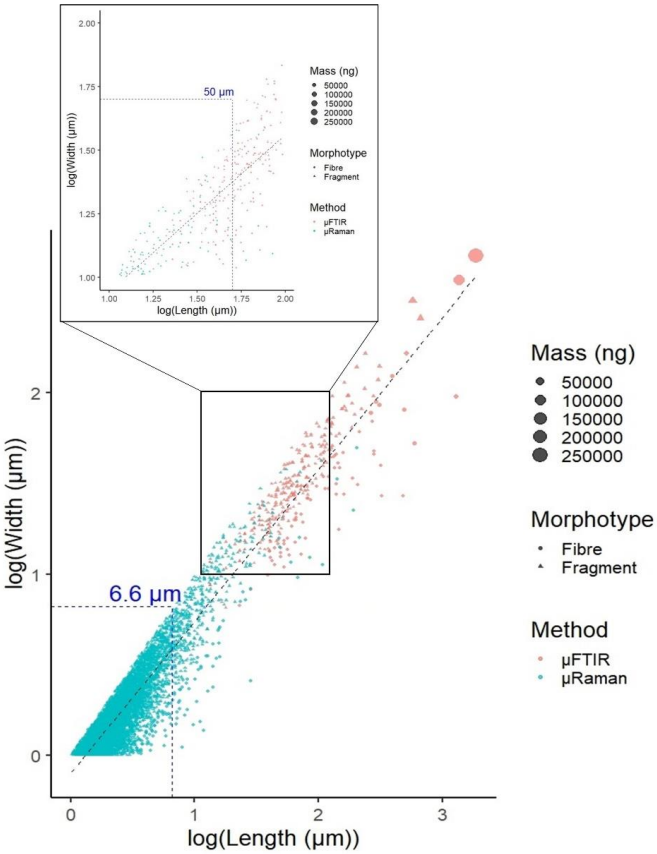

Figure 5. Width vs length graph for all the analysed MPs in the two datasets (the axes scale is in log_{10}). On the left: detail of the small-sized MP distribution. Values not corrected for blank contamination.

The MP length datasets from the inlet and outlet provided by the two techniques were merged to extrapolate the MP population from 1 (size limit of µRaman [26]) to 1865.9 µm (largest MP identified by µFTIR in the present study) and quantify the percentage of MPs missed by µFTIR. For the 1 – 50 µm interval (1 – 5, 5 – 10, 10 – 20, and 20 – 50 µm), the µRaman dataset was employed, while the µFTIR data was used for the 50+ µm interval (50 – 100, 100 – 200, 200 – 500, and 500+ µm). The outcome of this investigation is illustrated in Figure 6.

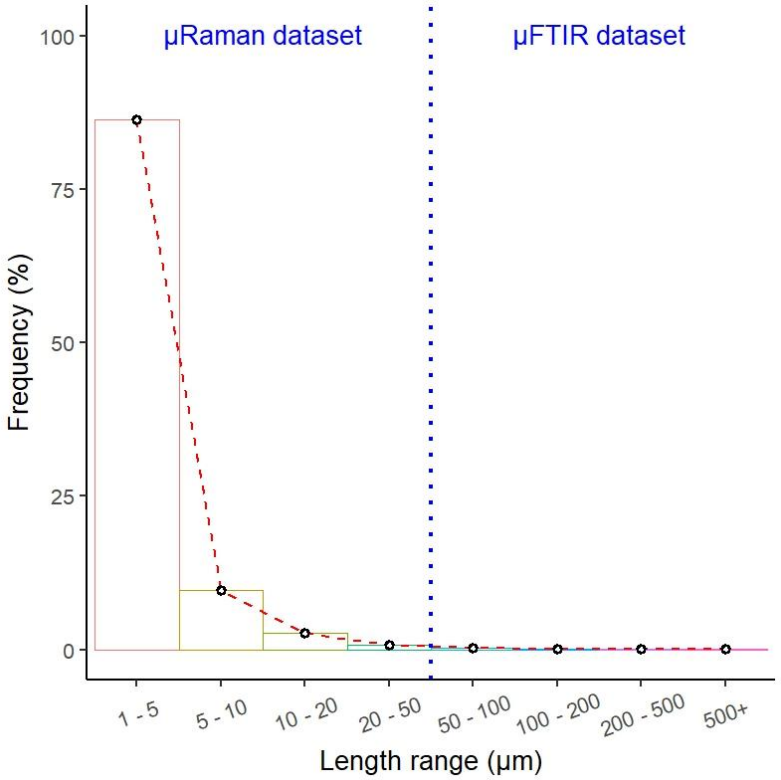

Figure 6. Frequency distribution of 1 – 1865.9 μm MPs in the analysed drinking water samples. Values not corrected for blank contamination. The blue dashed line divides the length ranges according to the relevant spectroscopic dataset.

86.0% of the identified MPs had a length between 1 and 5 μm. The other length categories accounted increasingly less with increasing MP size (5 – 10 μm 9.7%, 10 – 20 μm 2.7%, 20 – 500+ μm 1.3%). Therefore, the MP length distribution was skewed towards the left (i.e. the smallest values of MP length), and μFTIR missed approx. 95.7% of the extrapolated MP population. Specifically, the frequency values could be fitted against the overall MP length range of 1 – 1865.9 μm according to a power function (Eq. 2):

$$\text{Frequency (\%)} = 133.88 \cdot \text{Length}^{-3.933} \quad (R^2 = 0.99) \qquad (2)$$

Eq. 2 was obtained by a non-linear regression using the package nlraa of R and presented in the same form as the theorical power function developed by [31] for the MP size distribution from various environmental matrices.

µFTIR and µRaman clearly performed differently during the analysis of the drinking water samples, omitting the fact that µFTIR could not analyse the MPs between 1 and 6.6 µm. The first reason for this outcome is associated with the finer spatial resolution of the µRaman, which is usually addressed as the main advantage of the technique over µFTIR [43]. Therefore, the µRaman dataset was mostly populated by the smaller particles since they were the most abundant in the samples. The second reason may be due to the different sample deposition methods employed: for the µRaman, 25 µL over 1000 µL were deposed (2.5% of the total volume), while for µFTIR 1000 µL over 2000 µL (50% of the total volume). This meant the probability to deposit larger particles was higher in the µFTIR protocol, given their scarce frequency in comparison with the smaller size fractions. Since the stage is moved according to the coordinates of each particle to be excited with a laser of choice, the analysis time with µRaman can sometimes be prohibitive and semi-quantitative strategies may have to be adopted (e.g. choice of sub-areas and quantification of the total counts of particles afterwards). FPA-µFTIR, on the other hand, was used by taking advantage of its ability to map quite extended surfaces relatively quickly, despite its lower spatial resolution. The third reason, as already mentioned, may be represented by the settings employed in the software siMPle for the µFTIR data post-processing, and, in particular, the decision to ignore MPs smaller than 3 pixels on the chemical map. In general, relying only on µFTIR could have led to a severe underestimation of the MP abundance, or alternatively to an acceptance of a higher ratio of false positives, as discussed in section 3.2 and by Ref. [24]. The "frequency of appearance" of the identified polymer groups in the µFTIR and µRaman datasets also proved to be different (Figure 7). Since blank correction was performed separately for the MP counts and mass estimation, some plastic groups present in the counts investigation could not lead to values higher than the blanks' mean, so they were excluded. µRaman could identify more plastic groups than µFTIR (the "Other" category represents 9 distinct minor polymers in the µRaman dataset and 8 in that of µFTIR). In the plastic groups recognized by both methods, the frequencies did not prove to be comparable for PA, acrylic, and PP. In the case of PA, most of the particles were sized 1 – 5 µm, so they could exclusively be analysed with the µRaman. The opposite applied to acrylic, which was less abundant in the µRaman dataset because of its lower counts when compared to the smaller MPs. Most of the plastic mass in the µFTIR dataset was represented by PET which could not be quantified by the µRaman analysis.

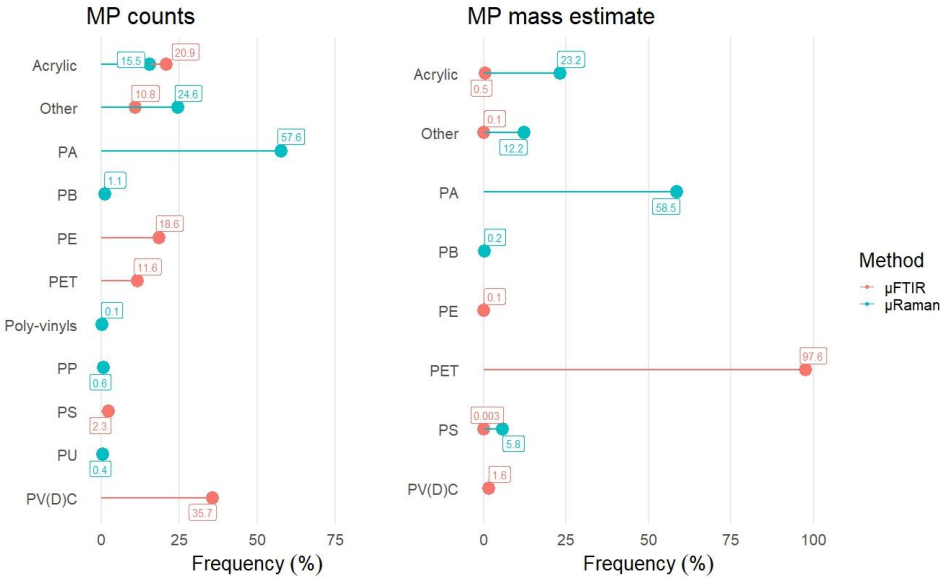

Figure 7. "Frequency of appearance" of the polymers identified by µFTIR and µRaman according to the MP counts and estimated mass.

3.4. Estimations of human MP intake from drinking water: a method-related issue

By adopting the same approach outlined in the µRaman study, it was possible to estimate the MP intake for an average drinking water consumer also from the µFTIR data. Specifically, the 6.6 – 150 µm MPs, which are more likely to translocate to the gut epitelium according to [44], represented 90.9% of the analysed MPs in the outlet samples. Therefore, assuming a mean water consumption of 2 L/(day·capita) [45] with an MP counts equal to the waterworks' outlet mean (6.96 N/m^3), the final result was (4):

$$\text{Intake} = 6.96\ \text{N/m}^3 \times 2\ \text{L/(day·capita)} \times 90.9\% \times 365\ \text{day/year} \approx 5\ \text{N/(year·capita)} \quad (4)$$

Corresponding to 1.86 µg/(year·capita) if the mean outlet MP mass (2.81 µg/m^3) is used in equation (4). The outcome was consistent with the findings of Ref. [30] and Ref. [46] (27 N/(year·capita)), who employed µFTIR down to respectively 6.6 and 20 µm. However, it was also decidedly lower (~332 times) than the estimation provided by the µRaman analysis (1533 N/(year·capita)). The strongly different estimations for the human MP intake from drinking water obtained with µFTIR and µRaman clearly represent a method-

related issue, as also discussed in sections 3.2 and 3.3 for the MP quantification and morphology. This is a point to be considered especially by those regulatory bodies involved in the monitoring of MPs in drinking water, such as [28], [47], and [48]. Hence future regulations on MPs should be based on a comprehensive background taking into account the pros and cons of the analytical methods usually employed for the MP analysis, thus clarifying the perimeter of applicability of the legal requirements.

4. Conclusion

Mainly because of their spatial resolution limit, µFTIR and µRaman provided different outcomes for the MP amount in the investigated drinking water samples, and, consequently, on the MP occurrence between the waterworks' inlet and outlet. By merging the two datasets, it was possible to demonstrate that the experimental size quantification limit for µFTIR was approx. 50 µm, in contrast to the nominal one of 6.6 µm at 25×. Below 50 µm, the rate of false positives associated with µFTIR makes µRaman the method of choice for MP analysis in drinking water. Further, the MP frequency in the range 1 – 1865.9 µm could be fitted *vs.* the MP length with a power function, showing that the 1 – 10 µm MPs represented the majority of the MP population in the drinking water samples. These outcomes seem to suggest that previous investigations relying only on µFTIR could have underestimated the MP abundance in drinking water. Overall, µFTIR provided lower (~150 times) values of MP counts in the investigated drinking water samples than µRaman. The estimated MP mass, on the other hand, was approximately 10^3 times higher in the µFTIR dataset due to the larger size characterizing the identified MPs. Remarkably, the counts removal efficiency for the MPs above 6.6 µm calculated with µFTIR data proved to be close to that of µRaman (~80%). Hence the investigated waterworks poorly retained the MPs sized approx. 1 – 10 µm and proved to be highly efficient for the larger ones. The estimation of the human MP intake provided by µFTIR as MP counts was also decidedly lower (~332 times) than that obtained from the µRaman analysis. This study is an important step forward in understanding the cons and the pros characterising µFTIR and µRaman as premiere techniques for the MP analysis of drinking water, as well as their complementarity and pivotal role in the MP science field.

Funding

This work has received funding from the European Union's Framework Programme for Research and Innovation Horizon 2020 under the Marie Skłodowska-Curie Grant Agreement MONPLAS No. 860775. The authors declare that they have no conflict of interest.

References

[1] Thompson R. C., Olsen Y., Mitchell R. P., Davis A., Rowland S. J., John A. W. G., McGonigle D., Russel A. D., Lost at Sea: Where Is All the Plastic?, Science 304 (5672), 838 (2004), DOI: 10.1126/science.1094559

[2] Ali I., Cheng Q., Ding T., Yiguang Q., Yuechao Z., Sun H., Peng C., Naz I., Li J., Liu J., Micro- and nanoplastics in the environment: Occurrence, detection, characterization and toxicity – A critical review, J. of Clean. Prod. 313, 127863 (2021), https://doi.org/10.1016/j.jclepro.2021.127863

[3] Ivleva N. P., Chemical Analysis of Microplastics and Nanoplastics: Challenges, Advanced Methods, and Perspectives, Chem. Rev. 121 (19), 11886–11936 (2021), https://doi.org/10.1021/acs.chemrev.1c00178

[4] Anagnosti L., Varvaresou A., Pavlou P., Protopapa E., Carayanni V., Worldwide actions against plastic pollution from microbeads and microplastics in cosmetics focusing on European policies. Has the issue been handled effectively?, Mar. Pollut. Bull. 162, 111883 (2021), ISSN 0025-326X, https://doi.org/10.1016/j.marpolbul.2020.111883

[5] Andrady A. L., The plastic in microplastics: A review, Mar. Pollut. Bull. 119 (1), 12 – 22 (2017), https://doi.org/10.1016/j.marpolbul.2017.01.082

[6] Simon M., van Alst N., Vollertsen J., Quantification of microplastic mass and removal rates at wastewater treatment plants applying Focal Plane Array (FPA)-based Fourier Transform Infrared (FT-IR) imaging, Water Res. 142, 1 – 9 (2018), https://doi.org/10.1016/j.watres.2018.05.019

[7] Prata J.C., da Costa J.P., Lopes I., Duarte A.C., Rocha-Santos T., Environmental exposure to microplastics: An overview on possible human health effects, Sci. of The Total Environ. 702, 134455 (2020), ISSN 0048-9697, https://doi.org/10.1016/j.scitotenv.2019.134455

[8] Wang Y., Wang S., Xu T., Cui W., Shi X., Xu S., A new discovery of polystyrene microplastics toxicity: The injury difference on bladder epithelium of mice is correlated with the size of exposed particles, Sci. of The Total Environ., 821, 153413 (2022), ISSN 0048-9697, https://doi.org/10.1016/j.scitotenv.2022.153413

[9] da Silva Brito W.A., Singer D., Miebach L., Saadati F., Wende K., Schmidt A., Bekeschus S., Comprehensive in vitro polymer type, concentration, and size correlation analysis to microplastic toxicity and inflammation, Sci. of The Total Environ., 854, 158731 (2023), ISSN 0048-9697, https://doi.org/10.1016/j.scitotenv.2022.158731

[10] Sangkham S., Faikhaw O., Munkong N., Sakunkoo P., Arunlertaree C., Chavali M., Mousazadeh M., Tiwari A., A review on microplastics and nanoplastics in the environment: Their occurrence, exposure routes, toxic studies, and potential effects on human health, Mar. Pollut. Bull., 181, 113832 (2022), ISSN 0025-326X, https://doi.org/10.1016/j.marpolbul.2022.113832

[11] Casillas G., Hubbard B.C., Telfer J., Zarate-Bermudez M., Muianga C., Zarus G.M., Carroll Y., Ellis A., Hunter C.M, Microplastics Scoping Review of Environmental and Human Exposure Data, Microplastics, 2, 78-92 (2023), https://doi.org/10.3390/microplastics2010006

[12] Ageel H. K., Harrad S., Abdallah M.A.E., Occurrence, human exposure, and risk of microplastics in the indoor environment, Environ. Sci.: Processes Impacts, 24, 1, 17-31 (2022), DOI: 10.1039/D1EM00301A

[13] Koelmans A.A., Nor N.H.M., Hermsen E., Kooi M., M. Mintenig S.M., De France J., Microplastics in freshwaters and drinking water: Critical review and assessment of data quality, W. Res., 155, 410-422 (2019), ISSN 0043-1354, https://doi.org/10.1016/j.watres.2019.02.054

[14] Liu R., Tan Z., Wu X., Liu Y., Chen Y., Fu J., Ou H., Modifications of microplastics in urban environmental management systems: A review, W. Res., 222, 118843 (2022), ISSN 0043-1354, https://doi.org/10.1016/j.watres.2022.118843

[15] Xue J., Samaei S. H. A., Chen J., Doucet A., Ng, K. T. W., What have we known so far about microplastics in drinking water treatment? A timely review, Front. Environ. Sci. Eng. 16, 58 (2022), https://doi.org/10.1007/s11783-021-1492-5

[16] Guo X., Lin H., Xu S., He L., Recent advances in spectroscopic techniques for the analysis of microplastics in food, J. Agric. Food Chem, 70, 5, 1410-1422 (2022), https://doi.org/10.1021/acs.jafc.1c06085

[17] Nirmala K., Rangasamy G., Ramya M., Uma Shankar V., Rajesh G., A critical review on recent research progress on microplastic pollutants in drinking water, Environ. Res., 222, 115312 (2023), ISSN 0013-9351, https://doi.org/10.1016/j.envres.2023.115312

[18] Harrison J. P., Ojeda J. J., Romero-González M. E., The applicability of reflectance micro-Fourier-transform infrared spectroscopy for the detection of synthetic microplastics in marine sediments, Sci. of The Total Environ. 416, 455-463 (2012), https://doi.org/10.1016/j.scitotenv.2011.11.078

[19] Löder M., Günter J., Kuczera M., Mintenig S., Lorenz C., Gerdts G., Focal plane array detector-based micro-Fourier-transform infrared imaging for the analysis of microplastics in environmental samples, Environ. Chem. 12, 563-581 (2015), https://doi.org/10.1071/EN14205

[20] Primpke S., Dias P.A., Gerdts G., Automated identification and quantification of microfibres and microplastics, Anal. Methods 11, 2138-2147 (2019), DOI: 10.1039/C9AY00126C

[21] Müller, Y.K., Wernicke, T., Pittroff, M., Witzig C.S., Storck F.R., Klinger J., Zumbülte N., Microplastic analysis—are we measuring the same? Results on the first global comparative study for microplastic analysis in a water sample, Anal. Bioanal. Chem., 412, 555 – 560 (2020), https://doi.org/10.1007/s00216-019-02311-1

[22] Araujo C. F., Nolasco M. M., Ribeiro A. M. P., Ribeiro-Claro P. J. A, Identification of microplastics using Raman spectroscopy: Latest developments and future prospects, Water Res. 142, 426 – 440 (2018), https://doi.org/10.1016/j.watres.2018.05.060

[23] Sridhar A., Kannan D., Kapoor A., Prabhakar S., Extraction and detection methods of microplastics in food and marine systems: A critical review, Chemosphere, 286, 1, 131653 (2022), ISSN 0045-6535, https://doi.org/10.1016/j.chemosphere.2021.131653

[24] Cabernard L., Roscher L., Lorenz C., Gerdts G., Primpke S., Comparison of Raman and Fourier Transform Infrared Spectroscopy for the Quantification of Microplastics in the Aquatic Environment, Environ. Sci. Technol. 52 (22), 13279 – 13288 (2018), https://doi.org/10.1021/acs.est.8b03438

[25] Gaston E., Woo M., Steele C., Sukumaran S., Anderson S., Microplastics Differ Between Indoor and Outdoor Air Masses: Insights from Multiple Microscopy Methodologies, Appl. Spectrosc. 74 (9), 1079 – 1098 (2020), doi:10.1177/0003702820920652

[26] Maurizi L., Iordachescu L., Kirstein I.V., Nielsen A.H., Vollertsen J., Do drinking water plants retain microplastics? An exploratory study using Raman micro-spectroscopy, Heliyon, 9, 6, e17113 (2023), ISSN 2405-8440, https://doi.org/10.1016/j.heliyon.2023.e17113

[27] Oßmann B.E., Microplastics in drinking water? Present state of knowledge and open questions, Curr. Opin. in Food Sci. 41, 44-51 (2021), ISSN 2214-7993, https://doi.org/10.1016/j.cofs.2021.02.011

[28] EU, Directive 2020/2184, 2020, http://data.europa.eu/eli/dir/2020/2184/oj

[29] Primpke S., Cross R. K., Mintenig S. M., Simon M., Vianello A., Gerdts G., Vollertsen J. EXPRESS: toward the systematic identification of microplastics in the environment: evaluation of a new independent software tool (siMPle) for spectroscopic analysis, Appl. Spectrosc., Article 0003702820917760 (2020)

[30] Kirstein I. V., Hensel F., Gomiero A., Iordachescu L., Vianello A., Wittgren H. B., Vollertsen J.,

Drinking plastics? – Quantification and qualification of microplastics in drinking water distribution systems by µFTIR and Py-GCMS, Water Res. 188, 116519 (2021), https://doi.org/10.1016/j.watres.2020.116519

[31] Kooi M., Koelmans A.A., Simplifying Microplastic via Continuous Probability Distributions for Size, Shape, and Density, Environ. Sci. & Technol. Lett. 6 (9), 551-557 (2019), doi: 10.1021/acs.estlett.9b00379

[32] Jung J., Kim S., Kim Y., Jeong S., Lee J., Tracing microplastics from raw water to drinking water treatment plants in Busan, South Korea, Sci. of The Total Environ. 825, 154015 (2022), ISSN 0048-9697, https://doi.org/10.1016/j.scitotenv.2022.154015

[33] Dalmau-Soler J., Ballesteros-Cano R., Boleda M.R., Paraira M., Ferrer N., Lacorte S., Microplastics from headwaters to tap water: occurrence and removal in a drinking water treatment plant in Barcelona Metropolitan area (Catalonia, NE Spain), Environ. Sci. Pollut. Res. 28, 59462–59472 (2021), https://doi.org/10.1007/s11356-021-13220-1

[34] Käppler A., Fischer D., Oberbeckmann S., Schernewski G., Labrenz M., Eichorn K., Voit B., Analysis of environmental microplastics by vibrational microspectroscopy: FTIR, Raman or both?, Anal. Bioanal. Chem. 408, 8377–8391 (2016), https://doi.org/10.1007/s00216-016-9956-3

[35] Vianello A., Jensen, R.L., Liu L., Vollertsen J., Simulating human exposure to indoor airborne microplastics using a Breathing Thermal Manikin. Sci. Rep. 9, 8670 (2019). https://doi.org/10.1038/s41598-019-45054-w

[36] Feld L., Silva V.H.d., Murphy F., Hartmann N.B., Strand J, A Study of Microplastic Particles in Danish Tap Water, Water 13, 2097 (2021), https://doi.org/10.3390/w13152097

[37] Novotna K., Cermakova L., Pivokonska L., Cajthaml T., Pivokonsky M., Microplastics in drinking water treatment – Current knowledge and research needs, Sci. of The Total Environ., 667, 730-740 (2019), ISSN 0048-9697, https://doi.org/10.1016/j.scitotenv.2019.02.431

[38] Li Y., Li W., Jarvis P., Zhou W., Zhang J., Chen J., Tan Q., Tian Y., Occurrence, removal and potential threats associated with microplastics in drinking water sources, J. of Environ. Chem. Eng. 8, 6, 104527 (2020), ISSN 2213-3437, https://doi.org/10.1016/j.jece.2020.104527

[39] Le Goff P., Delachambre Y., Study of a model of clogging of a filter medium: Flow of a suspension of microspheres through a mass of macrospheres, Rev. Fr. Corps Gras., 12, 3 (1965)

[40] Yao K., Influence of suspended particle size on the transport aspect of water filtration, The University of North Carolina at Chapel Hill (1968)

[41] McDowell-Boyer L.M., Hunt J.R., Sitar N., Correction to "Particle Transport Through Porous Media", Water Resour. Res., 27, 4, 665 (1991)

[42] Elimelech M., Gregory J., Jia X., Particle deposition and aggregation: measurement, modelling and simulation, Butterworth-Heinemann, 2013

[43] Xu J., Thomas K.V., Luo Z., Gowen A.A., FTIR and Raman imaging for microplastics analysis: State of the art, challenges and prospects, TrAC Trends in Anal. Chem. 119, 115629 (2019), ISSN 0165-9936, https://doi.org/10.1016/j.trac.2019.115629

[44] EFSA 2016, EFSA, Statement on the presence of microplastics and nanoplastics in food, with particular focus on seafood, EFSA J. (2016), p. 30, (EFSA Panel on Contaminants in the Food Chain)

[45] WHO, Guidelines for drinking-water quality: fourth edition incorporating the first and second addenda. Geneva: World Health Organization; 2022. Licence: CC BY-NC-SA 3.0 IGO.

[46] Dronjak L., Exposito N., Rovira J., Florencio K., Emiliano P., Corzo B., Schuhmacher M., Valero F., Sierra J., Screening of microplastics in water and sludge lines of a drinking water treatment plant in Catalonia, Spain, Water Res. 225, 119185 (2022), ISSN 0043-1354, https://doi.org/10.1016/j.watres.2022.119185

[47] The division of drinking water, State water resources control board, State of California, Resolution no. 2022-0032: Adopting a policy handbook establishing a standard method of testing and reporting of

microplastics in drinking water (2022),

https://www.waterboards.ca.gov/board_decisions/adopted_orders/resolutions/2022/rs2022-0032.pdf

[48] UN, A/RES/75/212: United Nations Conference on the Midterm Comprehensive Review of the Implementation of the Objectives of the International Decade for Action, "Water for Sustainable Development", 2018–2028 (2020),

https://undocs.org/Home/Mobile?FinalSymbol=A%2FRES%2F75%2F212&Language=E&DeviceType=Desktop&LangRequested=False

Paper III

Every breath you take: high concentration of breathable microplastics in indoor environments

L. Maurizi, L. Simon-Sánchez, A. Vianello, A.H. Nielsen, J. Vollertsen

The paper is currently under review

Every breath you take: high concentration of breathable microplastics in indoor environments

L. Maurizi[a,*], *L. Simon-Sánchez*[a], *A. Vianello*[a], *A. H. Nielsen*[a], *J. Vollertsen*[a]

[a]*Department of The Built Environment, Aalborg University, 9220 Aalborg, Denmark*

[*]*Correspondence: lucam@build.aau.dk (LM)*

Abstract: Raman micro-spectroscopy (µRaman) was employed to assess the concentration of indoor airborne MPs > 1 µm in four indoor locations (a meeting room, a workshop, and two apartments of different ages) on workdays and weekends. Further, the filtration performance of a commercial surgical facemask was assessed in the same environments with duplicates taken *via* a pumping sampling system (24 hours each). The indoor airborne MP concentration spanned between 58 and 684 MP counts per cubic meter (N/m^3) (median 212 ± 233 N/m^3, MPs/non-plastic ratio 0 – 1.6%), depending not only on the type and level of human activity but also on the extension and air circulation of the investigated locations. Overall, the surgical facemasks could retain 85.4 ± 3.9% of the MPs; however, only 57.6% of the 1 – 5 µm MPs could be filtered out. Hence the frequency of the breathable MPs increased in the samples taken with the surgical facemask. We estimated a human MP intake by indoor air of 3415 ± 2881 N/day (mostly poly-amide MPs), which could be decreased to 283 ± 317 N/day using the surgical facemask.

Keywords: microplastics; Raman micro-spectroscopy; air pollution; human exposure

1. Introduction

Since the 1950s, everyday life has been dominated by plastic materials (Andrady and Neal 2009), which are praised for their durability and adaptability to different purposes. However, many years of waste mismanagement have led to the accumulation of plastic waste in the natural environment, as already reported in the late 1980s by Ryan and Moloney (1990). The authors coined the term microplastic (MP) to indicate the small plastic debris found on South African beaches. In the following years, size-based definitions of MP were proposed (Arthur *et al.* 2009), and that of Gigault *et al.* (2018) (1 – 5000 µm) has been frequently adopted by unofficial convention in the literature.

MP pollution has been reported ubiquitously in natural and anthropogenic environments (Karbalaei *et al.* 2018), including the atmosphere (Fan *et al.* 2022). In this regard, the understanding of atmospheric circulation's role in MP dispersion is emerging. Recent studies reported the recirculation and re-suspension of MPs induced by precipitation and dry deposition, hereby corroborating that these pollutants can be transported over long distances (Brahney *et al.* 2020), ultimately reaching remote areas (Allen *et al*. 2019). Even the climate may potentially be affected by the presence of airborne MPs in the lower atmosphere due to the scattering capacity of plastic particles towards solar radiation (Revell *et al.* 2021). The presence of airborne MPs was also reported in indoor environments such as households (Vianello *et al.* 2019, Xumiao *et al.* 2021), offices and educational institutes (Yao *et al.* 2022), and surgical environments (Field *et al.* 2022). Sources of indoor airborne MPs can be synthetic clothes and textiles (Dris *et al.* 2015a), tearing and weathering of building materials, abrasions from plastic products, landfilling, and waste incineration (Rahman A. *et al.* 2021). Despite only a few studies focusing on indoor airborne plastic pollution, the MP abundance and composition in indoor environments are likely influenced by the type of human activity performed in the chosen location and its surroundings (Kacprzak and Tijing 2022).

Investigating the sources and fate of indoor airborne MPs is of pivotal importance since we spend up to 90% of our lifetime in indoor locations (Sarigiannis *et al.* 2019), meaning an almost constant exposure to airborne MPs *via* inhalation. Indeed, inhalation may represent humans' primary source of MP intake (Zhang *et al.* 2020a), overcoming ingestion and dermal contact (Wu *et al.* 2022). The penetration of airborne particles in

the airways is driven by the Aerodynamic Equivalent Diameter (AED). The so-called Particulate Matter (PM) classification is based on the AED of the particles (Wieland *et al*. 2022) and, specifically, the PM_{10} (AED < 10 µm) and $PM_{2.5}$ (AED < 2.5 µm) have been intensely studied due to their ability to overcome the mucociliary clearance in the upper airways (Vianello *et al.* 2019, Warheit *et al.* 2001). Indeed, PM_{10} can penetrate the low respiratory tract (Wieland *et al.* 2022), and $PM_{2.5}$ can reach the alveoli (Prata 2018a). In this context, larger particles (>5 µm) subject to mucociliary clearance are also called inhalable particulates. Oppositely, the breathable (or respirable) particulates are represented by smaller particles (<5 µm; EN 1993). Finer particulate is potentially more prone to cellular uptake, leading to stronger responses at exposure sites due to the large surface-to-volume ratio (Schmid and Stoeger 2016). In this regard, Wieland *et al.* (2022) tentatively compared the toxicity properties of known airborne particle types with that of MPs, concluding that the potential biotoxicity of airborne MPs could be driven not only by the size but also by the shape and surface charge (Silva *et al*. 2014). Accordingly, Shao *et al.* (2022) elaborated that airborne MP fibres might lead to the "fibre paradigm" (i.e. increased bioreactivity due to the fibre shape). Further, airborne MPs exhibit an increased cellular internalisation due to a biopolymeric layer generated by environmental exposure (Ramsperger *et al.* 2020). Airborne MPs can also be vectors for other micropollutants (Wang J. *et al.* 2016) and pathogens (Kirstein *et al*. 2016) by surface absorption. Finally, depending on the polymer type composing the MP, additives, dyes, and pigments may also be present and cause adverse health effects (Gasperi *et al.* 2018). Proportionately to their complex bioreactivity, airborne MPs may potentially lead to several adverse health effects in humans, e.g. pneumoconiosis (Studnicka *et al.* 1995), chronic bronchitis (Miller *et al.* 1975), and interstitial lung disease (Eschenbacher *et al.* 1999).

Still, little is known about airborne MP occurrence, distribution, composition, and potential effects, also because the techniques used for collecting, isolating, and analyzing these particles are biased by technological and methodological limitations, leading to hardly comparable and reliable data. Vethaak and Legler (2021) consequently claimed the need for improved analytical methods targeting the 1 – 10 µm MPs, previously overlooked due to the limitations of the sampling protocols and analytical methods employed. Nonetheless, analysing the breathable fraction of indoor airborne MPs remains challenging. To our

knowledge, only two works focused on breathable MPs in indoor air by employing μRaman (Rahman L. *et al.* 2021, Xie *et al.* 2022). Hence there is a pressing need for advancing the state-of-the-art and gaining a deeper understanding of the sources, occurrence, and fate of indoor breathable MPs, to provide reliable insights on the current human exposure and potential health effects.

The present study focuses on the potential human exposure to airborne MPs in indoor environments, emphasising the breathable size fraction. In particular, the objectives were 1) to develop an analytical protocol to quantify MPs down to 1 μm in air samples; 2) to compare the potential human exposure in different indoor environments and during distinct periods. Furthermore, we examined how MP exposure may be prevented by using surgical facemasks under the same conditions. Four indoor locations with diverse potential MP sources were selected, and samples were collected under two distinct levels of human activity. The active sampling filtration described in this study permits avoiding sample preparation, thus minimising particle loss and contamination. The state-of-the-art analytical method based on μRaman following a semi-random approach for choosing a particle subset allows particle detection and characterisation in an unbiased and reproducible mode.

2. Materials and methods

2.1. Indoor locations and sampling technique

The indoor air sampling was conducted in four indoor locations in Aalborg (Denmark) during October and November 2022 (see also Supplementary Information, Figure S1). The activities and characteristics were different across locations; however, they were selected to represent the daily exposure to MPs within common environments. Briefly, the locations:

1. The workshop (hereafter "Workshop") of the Department of the Built Environment, Aalborg University. Various materials (e.g. wood, concrete, metal, plastic, and electronic components) are stored, handled, and crafted by ten technicians as part of their daily job. During the weekend, no activities are carried on. The workshop covers 256.8 m^2.
2. A meeting room (hereafter "Meeting Room") in the same Department with an extension of 8.1 m^2. The room is furnished with three chairs, a table, a conference system connected to a TV, and a

whiteboard. The room is actively ventilated by the building's ventilation system (G4 filter for particulates larger than 10 µm, BS EN779). Besides, during workdays, the room's door is open, whilst it is kept closed during weekends.

3. An apartment located on the 1st floor of a building built in the late XIX century (hereafter "Old flat"). It has an area of 92 m^2 and consists of a studio, a kitchen, a living room, a bath, and a bedroom. The floor is parquet and the apartment is naturally ventilated, equipped with a wall heater per room. The only occupier leaves the flat every workday to go to the workplace whilst spending most of the weekend inside.
4. An apartment on the 8th floor of a building from 2019 (hereafter "New flat"). It has an area of around 65 m^2 and consists of a bathroom, an open-plan kitchen/living room, a bedroom, and a studio. The apartment is equipped with a manually controlled air ventilation system (G4 filter for particulates larger than 10 µm, BS EN779) and floor heating (installed beneath a wooden floor). The two occupiers leave the flat every workday to go to the workplace whilst spending most of the weekend inside.

In the present study, a weekday is one day between Monday morning at 8:00 am to Friday afternoon at 4:00 pm included, while the weekend consists of either Saturday or Sunday. The people occupying the investigated indoor environments were asked to act normally while the sampling was performed. For each sample, the sampling was conducted in active mode for 24 hours (EN 12341:2014) using a stainless steel funnel/filtration device (EMD Millipore Corporation, USA) placed at the average adult breathing height of 1.60 m by means of a laboratory stand (see also Supplementary Information, Figure S3) and connected to a laboratory pump (Lab Logistics Group GmbH, Germany) with a flexible plastic hose. The airflow was adjusted to 2 L/min using the pump's flowmeter (RS Components A/S, Denmark) and was directed inwards from the indoor atmosphere to the centre of the funnel, where a 13 mm × 200 µm Silicon (Si) filter (Smart Membranes GmbH, Germany) of 1 µm pore size was hosted. A poly-tetrafluoroethylene (PTFE) o-ring (approx. 10 mm inner diameter) was placed on the filter's surface to avoid breaking it while sealing the upper part of the funnel. Consequently, the active area of each filter (~314 mm^2) was defined by the diameter of the

PTFE o-ring. Two air samples were taken in each location on workdays and weekends: without the facemask (n = 8) and with a surgical facemask (n = 8, type IIR). The surgical facemask was mounted onto the inlet of the sampling funnel by means of elastic rubber bands, which kept the mask tight over the funnel's inlet. After the sampling, the Si filters were carefully removed from the holder and stored in pre-cleaned Petri dishes until they were analysed.

2.2 Contamination prevention

The funnel's components, Si filters, metallic labware, and facemasks were flushed in a flow bench with pre-filtered nitrogen gas (1.5 Bar) before use to remove potential contamination from the external environment. All the laboratory glassware employed was previously muffled at 500°C for 4 hours. After the sampling, the filters were carefully removed from the metallic funnel in a flow bench, and 100% cotton lab coats were worn during the entire operation. In addition, to account for potential contamination, three clean 1 µm Silicon filters were flushed with pre-filtered nitrogen gas (1.5 Bar) and directly analysed as procedural blanks. During data processing, particles identified as PTFE MPs were not considered when calculating the MP concentration due to the potential contamination from the sampling set-up.

2.3 µRaman analysis and spectral identification

The enriched filters were directly analyzed with a Nano Xplora Plus confocal Raman microscope equipped with a Peltier-cooled 2048 × 70 pixel CCD Syncerity detector, three solid-state laser sources (Horiba SAS, France), and a 50× objective of numerical aperture (NA) 0.75 (Olympus, Japan). The system was previously calibrated on the Si first-order Raman emission (520.7 cm^{-1}) by zero-order correction with a single-crystal Si wafer. For the spectral acquisition, slit 100 µm, hole 300 µm, 638 nm laser, and grating 600 ll/mm (spectral range 0 – 3500 cm^{-1}) were chosen. The software LabSpec6 (Horiba SAS, France) was employed to set the analysis parameters, whilst the visible image analysis was performed by the module Particle Finder (Horiba SAS, France). Figure 1 shows the workflow followed for the µRaman analysis of the indoor air samples.

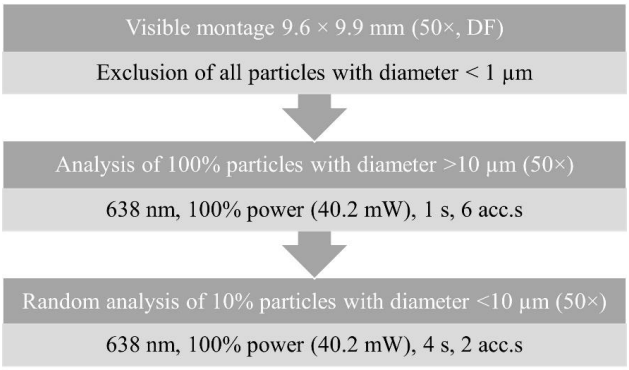

Figure 1. Workflow for the µRaman analysis of the indoor air samples.

10% of the particles with a Feret diameter of 1 – 10 µm were randomly selected on the entire active area of the filter by choosing the "Random" analysis mode of Particle Finder. This function allows the analysis of a chosen number of particles in the area represented in the visible montage, the total number of particles being already known from the morphological analysis of the visible picture (first step in Figure 1). The spectra were automatically baseline-corrected upon acquisition by selecting the FLAT option of LabSpec6. The choice of considering 10% of the 1 – 10 µm particles represented a compromise between the analytical representability of the sub-sample and analytical time. For the procedural blanks, 100% of the particles in both size fractions (Figure 1) were analysed with the same analysis parameters as for the air samples, given the relatively low number of particles on the blank filters. See also Supplementary Information for further details on the µRaman analysis process.

The spectral identification of the µRaman spectra was conducted with the software siMPle (Primpke *et al.* 2020) v. 1.3.1β. Upon spectral matching, the signals from the Si filter (~519 and ~990 cm^{-1}) were automatically removed, and the corrected spectra were compared with the references of a custom-built library (Munno *et al.* 2020) comprising 406 Raman spectra of synthetic polymers, pigments, and non-synthetic materials. In brief, siMPle performs spectral matching considering the Raman spectrum and the first-order derivative of the experimental spectrum and library references. The spectral quality match with the references is calculated as a Pearson correlation coefficient (Supplementary Information, section 5 for some examples of experimental Raman spectra from the air samples). The spectra presenting a matching quality above 0.50 were considered for further expert manual validation to assess the reliability of the

identification. Particles displaying a lower spectral quality match were classified as unidentified. For simplicity, in the discussion, the identified polymers were grouped into the following clusters: Other (cellulose acetate, EvOH, poly-carbonate, poly-methyl-methacrylate, poly-formaldehyde, poly-urethane, silicone, and styrene – isoprene (SIS) rubber), PA (poly-amide), PE (poly-ethylene, poly-ethylene chloride, poly-ethylene-co-propylene), PEST (poly-butylene-terephthalate, poly-ethylene-terephthalate), PP (poly-propylene), PS (acrylonitrile-butadiene-styrene, poly-styrene), and PV (poly-vinyl acetate, poly-vinyl butyral, poly-vinyl chloride, poly-vinyl alcohol, poly-vinyl pyrrolidone). The group "Other" gathers the synthetic polymers occurring with low frequency, whilst the other clusters are based on the chemical group characterizing the monomer.

2.4 FTIR – ATR analysis of the surgical facemask

The surgical facemasks used for the air sampling were analysed by Attenuated Total Reflection Fourier Transform Infrared Spectroscopy (ATR – FTIR, Cary 630 FTIR, Agilent, USA) equipped with a single bounce diamond crystal and a DTGS detector. Sixty – four scans were collected for the background and the sample at 4 cm^{-1} resolution in the spectral range 600 – 4000 cm^{-1}. The raw spectra of the facemasks were automatically corrected (apodization) by the instrument's software (MicroLab PC, Agilent, USA) and compared with the Agilent Polymer Handheld ATR library, being identified as PP (Supplementary Information, section 5).

2.5 Data analysis

The data of MP concentration were not blank-corrected and were expressed as counts of MPs per cubic meter (N/m^3). The human exposure to airborne MPs per day (HE_{day}) was calculated with equation (1):

$$HE_{day} = [MPs] \times I \times T \quad (1)$$

Where [MPs] is the MP concentration in N/m^3, I the inhalation rate equal to 16 m^3/day for an adult male (Stifelman 2007), and T the exposure time in hours/day (8/24=0.3 for the two workplaces during workdays and 24/24=1 for the two flats in the weekend).

The filtration efficiency (F) of the surgical facemask was calculated according to equation (2):

$$F\ (\%) = (-([Particles]_{mask} - [Particles]_{nomask})/[Particles]_{nomask}) \times 100\% \quad (2)$$

Where $[Particles]_{mask}$ is the total particle concentration in N/m^3 obtained from the samples taken with the surgical facemask, and $[Particles]_{nomask}$ is the corresponding total particle concentration from the samples taken without the facemask.

The statistical software R v. 4.2.1 was used to analyse the experimental datasets and perform the statistical tests. The Shapiro-Wilk test was employed to assess the normality of the data. Kruskal-Wallis test was performed to assess the significance of MP concentration, MP size, and the estimated human exposure, and Dunn test was employed for pair-wise comparison ($\alpha = 0.05$). For the MP diameter frequency and polymeric composition, a generalized linear model (GLM) was used to assess the significance of the data and for the pair-wise comparison among the crossed factors "Location" (Meeting room, New flat, Old flat, and Workshop), "Activity" (High, Low), and "Facemask" (Without Facemask, Surgical Facemask). The p-value of the GLM test was calculated from the corresponding Wald z value and was considered significant if < 0.05. A Principal Component Analysis (PCA) was conducted on the MP Feret diameter distribution frequency data to explore how the use of the facemask influences the size distribution of MPs. The results in section 3 were expressed as median or mean ± one standard deviation (SD) as specified in the discussion.

3. Results and discussion

3.1 Blank contamination

Despite all the procedures employed to minimise MP contamination throughout the analytical workflow, an average of 22 ± 14 N was found in the procedural blanks, corresponding to 8.1 ± 5.5% of the average MP counts in the samples (414 ± 344 N). The median Feret diameter of the MPs found in the blanks was 1.5 µm (min. – max. 1.0 – 17.0 µm). The main polymeric composition of these particles was PUR 73.8%, PA 10.8%, PP 7.7%, PS 4.6%, and PE 3.1%. Even if all materials, including the Si membranes, were thoroughly flushed with pre-filtered nitrogen before use, the predominance of PUR was probably caused by remaining traces from the packaging material of the Si filters, made of a PUR foam layer. The rest of the polymers were more common and could have been introduced onto the Si filters during sample handling.

3.2 Microplastics versus non-plastic materials

The MPs/non-plastic ratio spanned between 0 – 1.6%, with the surgical facemask samples registering a higher mean value than the samples taken without the facemask (0.6 ± 0.6% and 0.2 ± 0.1%, respectively). Among the non-plastic particles, most of them were cotton (52.2%) and cellulose (47.8%), but small amounts of calcium sulfate ($CaSO_4$, <0.1%) were also present. These MPs/non-plastic ratio values were lower than those reported by Vianello *et al*. (2019, 4%), whose dataset included only organic particles, and Torres-Agullo *et al.* (2022, 16%) with µFTIR. Nonetheless, they are in accordance with the general consensus that MPs represent a small fraction of the total airborne particulates, yet still more abundant than that of other matrices like soil (Wright *et al.* 2019, Wang X. *et al*. 2022). The MP/non-plastic ratio reported in our study may depend on the randomised strategy chosen to analyse the filters, which may have underestimated the 1 – 10 µm MP fraction, despite avoiding the bias associated with the manual selection of particles. Also, the spectral library employed (which also contains cellulose- and protein – based materials) and the quality threshold set in the siMPle to identify the experimental spectra may have led to false negatives, thus further decreasing the MPs/non-plastic ratio.

3.3 Microplastics in indoor environments

The presence of MPs in indoor environments has been documented in field studies worldwide (Yao *et al.* 2022, Uddin *et al.* 2022, Zhai *et al*. 2023), and it is suspected to be a significant pathway for human exposure to this emerging pollutant (Zhao *et al.* 2023). Our results showed an almost ubiquitous presence of MPs in the air of the investigated sites. Seven out of eight samples contained MPs, with concentrations ranging from 58 N/m^3 to 684 N/m^3, depending on the location and the level of human activity (Figure 2). Overall, the median MP concentration increased on average from 85 ± 317 at low activity levels to 335 ± 149 N/m^3 under high activity conditions.

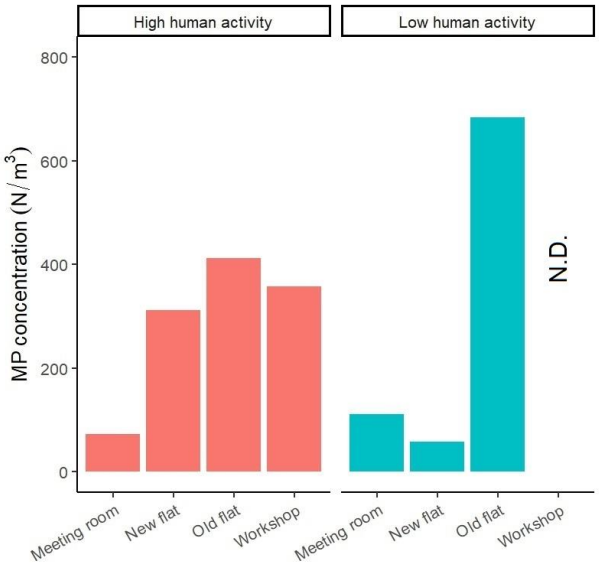

Figure 2. Indoor MP concentration (N/m^3) in the four locations according to the level of human activity.

The highest MP concentrations were recorded in the two private apartments. The "old-flat" household had an average (mean of high and low activity levels) concentration of 548 ± 192 N/m^3, while the "new-flat" showed 185 ± 180 N/m^3. The university workshop had a comparable average concentration of 179 N/m^3, whereas the lowest concentration of 92 N/m^3 was recorded in the meeting room. Significant variability was found between the replicates collected under different activity levels (Kruskal – Wallis p = 0.03), but not with respect to the location (Kruskal – Wallis p = 1). Interestingly, the workshop showed high MP concentration (358 N/m^3) during high activity levels, while no MPs were found in the sample collected under low activity conditions. The activity in the workshop stops during weekends, with consequent low to no emission of airborne particulate (Mølgaard *et al.* 2015). This, along with the large area of the workshop (256.8 m^2, section 2.1) and the height of the ceiling (3.5 m), implies a potential dilution effect of the residual airborne MPs (Memarzadeh and Jiang 2004). Additionally, due to the sampling device's restricted active filtration area (314 mm^2, section 2.1), the sampling volume might not have been sufficiently representative to collect such a diluted particulate concentration in this location.

Generally, variations in indoor ventilation patterns must also be considered when investigating particulate occurrence in indoor air (Liu S. *et al.* 2022). Specifically, opening doors and windows can lead to higher air change rates, thus depleting the concentration of indoor particulates (Hussein 2017), whilst more confined indoor environments with scarce ventilation usually show higher particulate concentrations (Liu S. *et al.* 2022). Hence the outcomes from the meeting room and the "old flat" can be explained in terms of particulate exchange with the outdoor environment. As for the meeting room, the door was kept slightly open during the workdays to simulate human activities (thus generating more air change) and closed on the weekend, which may have concentrated the indoor particulate inside the room. Similarly, the tenant of the "old flat" regularly keeps the windows open while doing housework during the weekend, enhancing the air change with the outdoor environment and, therefore, momentarily diluting the indoor airborne particle concentration. Further, the MP concentration measured in the old flat during low activity (684 N/m^3) was approximately ten times that found in the new flat (58 N/m^3), which is equipped with an active mechanical ventilation system. Stabile *et al.* (2019) reported that mechanical systems are more efficient than natural ventilation in providing air exchange and avoiding the accumulation of different pollutants, including submicron particulate. Hence the absence of such a ventilation system in the old flat and the consequent poor degree of air exchange may well have been a sink for airborne MPs (Chen Y. *et al.* 2022). On the contrary, human activity was the major source of indoor airborne MPs in the "new flat". Similar findings were reported for mechanically ventilated apartments in Sweden (Isaxon *et al.* 2015).

The indoor MP concentrations in the current study (58 – 684 N/m^3) are higher than those previously reported for residential environments in Denmark (2 – 16 N/m^3; Vianello *et al.* 2019), Portugal (0.7 – 1.6 N/m^3; Xumiao *et al.* 2021), and Sri Lanka (0.1 – 0.9 N/m^3; Perera *et al.* 2022). Past investigations have attributed the differences to income level, living standards, and the wide range of potential sources of MPs found in various indoor environments (Perera *et al.* 2022). However, comparison among studies proves challenging due to the lack of standardised protocols for sampling and analysing airborne MPs (Kacprzak and Tijing 2022). Indeed, Xie *et al.* (2022) used similar analytics to our study to investigate the occurrence of airborne MPs > 1 µm in outdoor and indoor locations in Shangai (China) but reported indoor concentrations ranging from 16 to 93 N/m^3. When addressing particles in the breathable range (< 5 µm), state-of-the-art analytical

approaches become crucial. A clear example is the comparison between the study of Xumiao *et al.* (2021), who used Nile Red staining on particles down to 2 µm and found only 0.1 to 0.93 N/m^3, and the study of Xie *et al.* (2022), analysing MPs down to 1 µm with µRaman and reporting an MP concentration approx. 100 times higher. Our findings are in agreement with the latter study but show even higher concentrations (58 – 684 N/m^3). The difference might be explained by the low frequency of the 1 – 10 µm MPs detected by Xie *et al.* (2022), who visually pre-screened particles > 1 µm to submit to chemical characterisation. As previously documented (Primpke *et al.* 2020), this approach is prone to underestimate the smaller particles. Our method overcomes the drawbacks of the studies of Xie *et al.* (2022) by employing a completely automatised strategy, where the random selection of particles involves the entire active area of the sample and is operated by the instrument's software. Accordingly, Schymanski *et al.* (2021) appreciated that randomised strategies applied to µRaman ensure the minimisation of bias and analytical time. Therefore, the analytical protocol of this study may be suitable for the routine chemical analysis of indoor breathable MPs (Duarte *et al.* 2022). As reported by the WHO (WHO 2021), PM_{10} and $PM_{2.5}$ are generally associated with asthma, pulmonary diseases, and even an increase in the mortality rate for long-term exposure. Further investigations need to expand the use of µRaman analysis to include also other organic and inorganic micro- and nanoparticles, such as coatings (Bouchard *et al.* 2009), asbestos fibers (Rinaudo *et al*. 2010), and titan dioxide (Mamedov 2020), which also pose a hazard to human health.

3.4 Microplastic composition and morphology of the indoor air

3.4.1 Polymeric composition

A total of 15 polymers were identified in the analysed samples (Figure 3), with PA clearly dominating the polymer composition (mean 21%), followed by PV (mean 18%), PE (mean 16%), PS (mean 11%), and PEST (mean 8%). The specific sampling locations played a significant role in the MP composition (GLM $p = 7 \cdot 10^{-4}$), while the level of human activity did not significantly influence the polymers present in indoor air (GLM $p = 0.49$).

PA is one of the most common polymers measured in indoor air, together with PE, PEST, and PS (Habibi *et al.* 2022). The sources of airborne MPs in indoor environments can be various and depend on the activities

performed in the considered locations: for PA and PEST, mainly used in synthetic fabrics (Periyasamy *et al.* 2020a), washing machines and tumble dryers are generally considered important emission hotspots (Periyasamy *et al.* 2022b, Kärkkäinen *et al.* 2021). Accordingly, when the activity level increased in the flats (i.e. weekend), where tumble dryers were used, PEST also showed higher frequency values ("new flat": 7.0%, "old flat": 20.7%), as opposed to workdays, when human activity is lower ("new flat": 0%, "old flat": 7.6%). Similarly, a higher PA concentration was recorded in the "old flat" during high activity (35.3% *vs* 10.8% in the low activity period). PS was mainly recorded in the meeting room (mean 13.5%) and two residential locations ("new flat" mean: 12.4%; "old flat" mean: 9.7%), while its presence was scarcer in the workshop (mean 4%). PS is widely utilised in the packaging industry (Block *et al.* 2017) and is an additive in concrete formulations to enhance thermal insulation (Dixit *et al.* 2019). The category "Other" accounted for 36.7% of the polymers identified in the workshop in the workday (i.e. high activity level), a higher percentage compared to the "old flat" (8.2%) and the meeting room (13.7%), but lower than that of the "new flat" (49.9%). Within this polymer cluster, it is worth mentioning PUR (mean 14.5%), EvOH (mean 4.0%), and cellulose acetate (mean 2.9%). PUR is a polymer of choice for several applications in the building, automotive, and furniture industries in the form of coater and sealant (Zia *et al.* 2007), whilst EvOH is employed in heating and cooling piping (Feng *et al.* 2018), and cellulose acetate in textile and yarns (Law 2004). In particular, several polyurethanes used in furniture are also treated with flame retardants, of which almost all are considered harmful (U.S. EPA 2015). As for the other plastic additives of common usage (e.g. organophosphates, phthalates, and bisphenols), these chemicals are released into the surrounding environment due to plastic ageing and have also been detected in the atmosphere (Liu X. *et al.* 2021), which may pose an additional risk to human health alongside airborne MPs (Ageel *et al.* 2022).

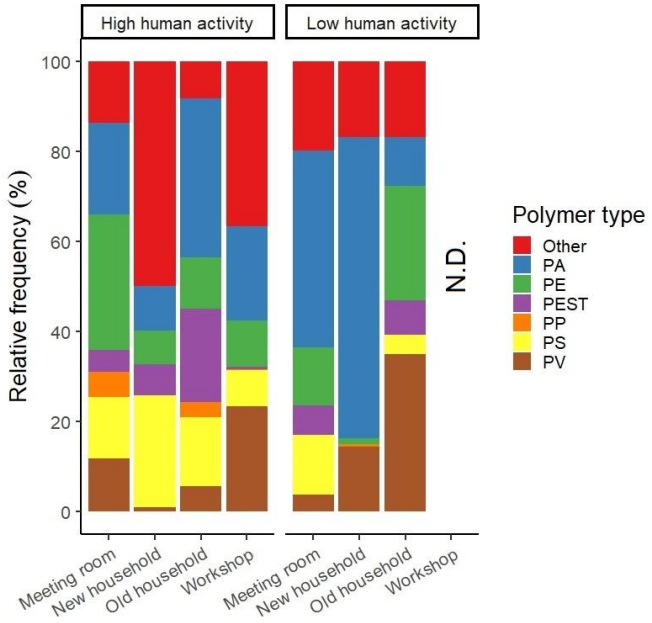

Figure 3. Polymer relative frequency in the investigated indoor locations according to human activity.

3.4.2 Microplastic morphology

The MPs with a length/width ratio > 3 were classified as fibres, while those with a length/width ratio ≤ 3 were classified as fragments (Vianello *et al.* 2019). Length and width for each particle in the visible montage were previously provided by Particle Finder after the morphological analysis. The detected MPs were mainly characterized by irregular fragments (99.4%), with the fibres representing only 0.6% of the total MPs (see also Supplementary Information). These findings contrast most studies investigating MPs in the atmospheric compartment, where fibrous-shaped particles were commonly predominant (Dris *et al.* 2015a, Dris *et al.* 2017b, Jenner *et al.* 2021, Perera *et al.* 2022). Nevertheless, most of these investigations relied on visual and manual pre-sorting of putative MPs, then submitted to chemical identification. These procedures are prone to unavoidable human bias due to the relative ease of recognizing fibers compared to small MP fragments (Song *et al.* 2015).

Airborne MPs ranged in size from 1 to 67.5 µm, with a median of 6.2 µm. When accounting only for particles > 10 µm, the median diameter was 13.6 µm, while the breathable and inhalable fraction (1 – 10

µm), showed a median diameter of 3.2 µm. Most of the MPs were smaller than 10 µm (72.6 %), with the size fraction 1 – 5 µm being predominant (mean 45.2%). In contrast, MPs ≥ 50 µm were very scarce (0.1%) in the indoor samples, most likely because larger MPs may settle to a greater extent than the smaller ones (Zhang *et al.* 2020b). The level of activity significantly influenced the MP size in the indoor air (Kruskal-Wallis p = 0.03); the frequency of inhalable MPs was indeed higher (74.6%) under high activity conditions than during low activity (70.4%). Therefore, the occurrence of inhalable MPs seems inevitable and generally associated with human activity, as already described in previous studies targeting larger airborne MPs (Prata *et al.* 2021b). A comparison of MP size among the different locations also showed a significant difference (Kruskal – Wallis $p = 7.5 \cdot 10^{-11}$), specifically between the two flats (Dunn $p = 4.1 \cdot 10^{-8}$) and the "new flat" and workshop (Dunn $p = 7.1 \cdot 10^{-8}$). The main source of difference among the locations was probably represented by the type of human activity performed, hence the result for the pair "new flat" – workshop. Regarding the pair "old flat" – "new flat", another source of difference may be the ventilation system adopted in these locations (section 3.3).

The 1 – 10 µm MPs fall in the inhalable and breathable range of indoor particulate (Wang T. *et al.* 2021), being able to reach the respiratory tract (PM_{10}) and enter the bloodstream through the lung tissue if smaller than 2.5 µm ($PM_{2.5}$). Larger fibrous MPs can instead accumulate in the lungs (Pauly *et al.* 1997) and eventually cause cancer as a result of long-term exposure, especially in the workers of industrial fields producing synthetic textiles (Wang T. *et al.* 2021). Despite the lack of specialised research on the toxicological effects of inhalable MPs, they are expected to share some common traits with other well-known PMs with carbonaceous composition (Prata 2018a). For instance, Deng *et al.* (2017) demonstrated that oral administration of 20 and 5 µm PS MPs in mice eventually led to accumulation in the liver, kidney, and intestine, probably due to the hydrophobic properties of the particles. However, as Amato-Lourenço *et al.* (2020a) highlighted, most of the toxicological studies published so far employed standard MPs, whose physical and chemical characteristics can be quite different from those of environmental MPs. The usage of standard MPs is justified by the complexity of artificially replicating the processes leading to the generation of secondary MPs in the environment. Hence the risks associated with secondary airborne MPs can be

indirectly inferred from a few studies of occupational medicine (Soutar *et al.* 1980, Pimentel *et al.* 1975), which reported decreased pulmonary function, inflammation, granulomas, and interstitial fibrosis in exposed textile workers. To the best of our knowledge, only Amato-Lourenço *et al.* (2021b) reported the presence of MP fragments between 1.6 – 5.6 µm in human lung tissue using µRaman. Hence our findings on the major frequency of 1 – 5 µm MPs in indoor air are in good accordance with the observations of Amato-Lourenço and co-authors, which indirectly demonstrate the ability of small airborne MPs to overcome the mucociliary clearance mechanisms. Considering the multi-faceted nature of MPs as both pollutants *per se* and vectors for sorbed co-pollutants (transition metals, organic compounds, and pathogenic microorganisms), Rochman *et al.* (2019) proposed to reclassify MPs as a new class of potentially toxic particles needing a multi-disciplinary approach.

3.5 Surgical facemask – reducing the overall exposure but increasing the breathable fraction

Applying a surgical facemask to the inlet of the sampling device led to significantly lower MP concentrations (Kruskal-Wallis $p = 0.03$), ranging from 4 to 196 N/m^3. Figure 4 shows the mean MP concentration (i.e. average of low and high human activity) in the investigated locations for the samples taken without and with the surgical facemask.

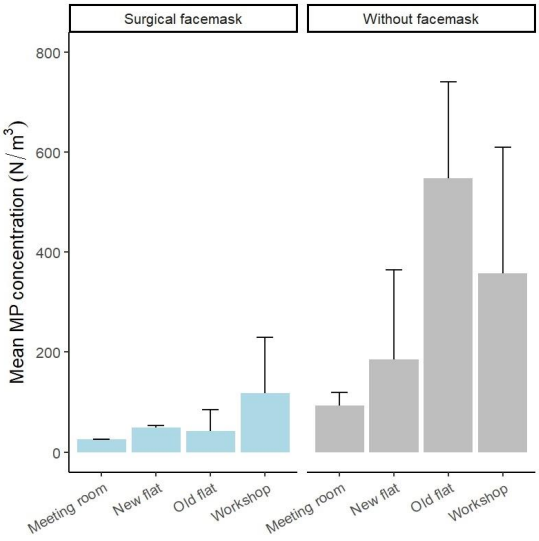

Figure 4. Mean MP concentration (N/m^3) in the investigated indoor locations collected with surgical facemask (blue) and without (grey). The error bars indicate the standard deviation.

Despite the presence of the surgical facemask, MPs were still present. In fact, the surgical facemask reduced the total amount of indoor airborne MPs by selectively filtering out the MP fractions > 5 µm (Figure 5a). This observation is supported by examining the size distributions and comparing the relative frequencies of the lower size classes in the samples collected with and without surgical facemask, respectively (Figure 5a). The median diameter of the MPs found in the indoor air samples (without the facemask) was larger than when the facemask was applied for both the fraction larger than 10 µm (13.6 µm *vs* 12.7 µm, Kruskal-Wallis $p = 3.48 \cdot 10^{-5}$) and the one between 1 and 10 µm (3.2 µm *vs* 2.2 µm, Kruskal-Wallis $p = 1.34 \cdot 10^{-6}$). Moreover, the PCA (Figure 5b) showed that the 1 – 5 µm MP diameter range mostly described the variance of the samples taken with the surgical facemask. This size range was also significantly different when the samples taken without the facemask were compared to those taken with the facemask with regard to the MP diameter (GLM $p = 6.11 \cdot 10^{-14}$). These outcomes indicate that the surgical facemask lacked efficiency towards the 1 – 5 µm MPs, which are suspected to be more threatening to human health (Wieland *et al.* 2022).

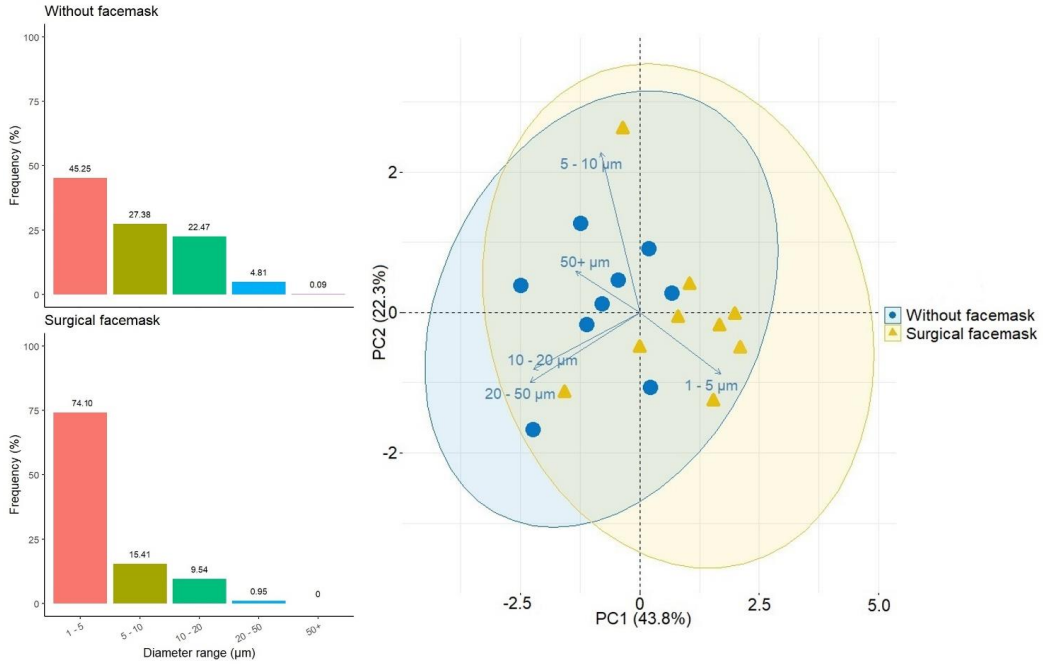

a) *b)*

Figure 5. a) MP relative frequency per diameter range in the investigated samples; b) Principal Component Analysis (PCA) of the MP diameter frequency (scores plot).

Hence the mean MP filtration efficiency of the surgical mask could be estimated for each size range: the lowest value (57.6%) was indeed obtained for the 1 – 5 µm category, whilst for the larger MPs values above 80% were found (5 – 10 µm: 85.4%, 10 – 20 µm: 89.0%, 20 – 50 µm: 94.9%, 50+ µm: 100%). The overall filtration efficiency of the surgical facemask for the indoor airborne MPs was 85.4 ± 3.9%. These results indicate that surgical facemasks can help reduce the exposure to inhalable MPs down to 5 µm, but do not prevent the exposure to breathable MPs (1 – 5 µm MPs). This finding well agrees with the work of Tcharkhtchi *et al.* (2021), who compared the filtration performance of various types of facemasks towards airborne particulate in the micro- and nanometric range and observed that commercially available surgical facemasks limit the penetration of aerosols down to 5 µm, while for smaller particles the efficiency drops to approx. 50%.

3.6 Estimation of the MP human intake from indoor air

The potential MP human intake was estimated for the periods with high activity (i.e. workdays for the meeting room and workshop and weekends for the two flats). Table 1 summarizes the results of MP intake estimation for the overall MP population and the breathable fraction 1 – 5 µm.

Location	**HE_{day} to indoor MPs (N/day)**		**HE_{day} to breathable MPs (1 – 5 µm; N/day)**	
	Without facemask	**Surgical facemask**	**Without facemask**	**Surgical facemask**
Meeting room	352	123	150	67
New flat	4991	753	1915	632
Old flat	6600	67	3222	56
Workshop	1717	190	730	50
Mean ± SD	3415 ± 2881	283 ± 317	1504 ± 1360	201 ± 287

Table 1. Daily human exposure to airborne indoor MPs in the four investigated locations without the facemask and with the surgical facemask (high activity periods).

The values of HE_{day} obtained from the samples without the facemask are significantly higher than those obtained with the surgical mask (Kruskal-Wallis $p = 0.04$), and previously reported in the literature. Vianello *et al.* (2019) estimated HE_{day} up to 272 N/day. Similarly, Cox *et al.* (2020), through a meta-analysis, estimated that the MP human intake from indoor air in the USA was 170 N/day. Soltani *et al.* (2021) reported that approx. 35.3 N/day were inhaled by the inhabitants of Australian flats, which is in agreement with the mean estimation of Torres-Agullo *et al.* (2022) for urban indoor microenvironments (37 N/day). In all these studies, the size limit of the analysed MPs was above 10 µm, hampering the direct comparison with our results. To date, only the work of Xie *et al.* (2022) reported on the human intake of airborne indoor MPs between 1 – 10 µm, obtaining values between 19.6 and 891.6 N/day. Our results provide new insights into human exposure to breathable MPs in indoor environments. We estimated that, on average, a human may intake more than 1500 breathable MPs per day. The use of surgical facemasks in indoor environments, a

routine practice during the COVID-19 pandemic, reduces the overall potential intake (3415 N/day *vs* 283 N/day). Yet, it showed limitations in removing the breathable fraction of airborne MPs (201 N/day, ~71% of the overall potential intake with the surgical facemask).

4. Conclusions

This work expands the current knowledge on indoor airborne MP occurrence by providing novel insights into the breathable fraction of this synthetic particulate. The concentration of indoor airborne MPs down to 1 µm was assessed in four locations (two workplaces and two private apartments) during low and high-activity periods, indicating human activity as a major source of MP pollution in indoor environments. When comparing the activity levels, the median MP concentration increased from 85 ± 317 under low activity conditions to 335 ± 149 N/m^3 at high activity levels, showing that humans are prone to an intake of 3415 ± 2881 N/day during high-activity periods. Further, a simple experiment to test the reduction of MP human exposure using a surgical facemask showed an overall filtration efficiency of 85.4 ± 3.9% for the MPs > 1 µm. However, the MPs in the breathable range of 1 – 5 µm were only partially filtered (57.6%). These additional findings indicate that wearing surgical facemasks indoors would only partially reduce the potential exposure to MPs, considering the limited efficiency in the breathable fraction.

Funding

This work has received funding from the European Union's Framework Programme for Research and Innovation Horizon 2020 under the Marie Skłodowska-Curie Grant Agreement MONPLAS No. 860775, as well as support from the North Atlantic Microplastic Centre (NAMC). The authors declare that they have no conflict of interest.

References

Ageel H.K., Harrad S., Abou-Elwafa Abdallah M., Occurrence, human exposure, and risk of microplastics in the indoor environment, Environ. Sci.: Processes Impacts, 24, 17-31 (2022), DOI: 10.1039/D1EM00301A

Allen S., Allen D., Phoenix V.R., Le Roux G., Jiménez P.D., Simonneau A., Binet S., Galop D., Atmospheric transport and deposition of microplastics in a remote mountain catchment, Nat. Geosci., 12, 339–344 (2019), https://doi.org/10.1038/s41561-019-0335-5

a. Amato-Lourenço L.F., dos Santos Galvão L., de Weger L.A., Hiemstra P.S., Vijver M.G., Mauad T., An emerging class of air pollutants: Potential effects of microplastics to respiratory human health?, Sci. of The Total Environ., 749, 141676 (2020), ISSN 0048-9697, https://doi.org/10.1016/j.scitotenv.2020.141676

b. Amato-Lourenço L.F., Carvalho-Oliveira R., Júnior G.R., dos Santos Galvão L., Ando R.A., Mauad T., Presence of airborne microplastics in human lung tissue, J. of Hazard. Mater., 416, 126124 (2021), ISSN 0304-3894, https://doi.org/10.1016/j.jhazmat.2021.126124

Andrady A.L., Neal M.A., Applications and societal benefits of plastics, Phil. Trans. R. Soc., B, 364, 1977–1984 (2009), http://doi.org/10.1098/rstb.2008.0304

Arthur C., Baker J., E., Proceedings of the International Research Workshop on the Occurrence, Effects, and Fate of Microplastic Marine Debris, September 9-11, 2008, University of Washington Tacoma, Tacoma, WA, USA, International Research Workshop on the Occurrence, Effects, and Fate of Microplastic Marine Debris 2008, 2009, https://repository.library.noaa.gov/view/noaa/2509

Block C., Brands B., Gude T., Packaging Materials 2. Polystyrene for Food Packaging Applications—Updated Version., International Life Sciences Institute (2017)

Bouchard M., Rivenc R., Menke C., Learner T., Micro-FTIR and micro-raman study of paints used by Sam Francis, Preservation Sci., 6, 27-37, 2009, ISSN: 1581-9280

Brahney J., Hallerud M., Heim E., Hahnenberger M., Sukumaran S., Plastic rain in protected areas of the United States, Science, 368, 6496, 1257-1260 (2020), DOI: 10.1126/science.aaz5819

Chen Y., Li X., Zhang X., Zhang Y., Gao W., Wang R., He D., Air conditioner filters become sinks and sources of indoor microplastics fibers, Environ. Pollut., 292, B, 118465 (2022), ISSN 0269-7491, https://doi.org/10.1016/j.envpol.2021.118465

Cox K.D., Covernton G.A., Davies H.L., Dower J.F., Juanes F., Dudas S.E., Correction to Human Consumption of Microplastics, Environ. Sci. Technol., 54, 17, 10974 (2020), https://doi.org/10.1021/acs.est.0c04032

Deng Y., Zhang Y., Lemos B., Ren H., Tissue accumulation of microplastics in mice and biomarker responses suggest widespread health risks of exposure, Sci. Rep. 7, 46687 (2017), https://doi.org/10.1038/srep46687

Dixit A., Pang S.D., Kang S., Moon J., Lightweight structural cement composites with expanded polystyrene (EPS) for enhanced thermal insulation, Cem. and Concr. Compos., 102, 185-197 (2019), ISSN 0958-9465, https://doi.org/10.1016/j.cemconcomp.2019.04.023

a. Dris R., Gasperi J., Rocher V., Saad M., Renault N., Tassin B., Microplastic contamination in an urban area: a case study in Greater Paris, Environ. Chem., 12, 5, 592-599 (2015), https://doi.org/10.1071/EN14167

b. Dris R., Gasperi J., Mirande C., Mandin C., Guerrouache M., Langlois V., Tassin B., A first overview of textile fibers, including microplastics, in indoor and outdoor environments, Environ. Pollut., 221, 453–458 (2017), https://doi.org/10.1016/j.envpol.2016.12.013

Duarte R.M.B.O., Gomes J.F.P., Querol X., Cattaneo A., Bergmans B., Saraga D., Maggos T., Di Gilio A., Rovelli S., Villanueva F., Advanced instrumental approaches for chemical characterization of indoor particulate matter, Appl. Spectrosc. Rev., 57, 8, 705-745 (2022), DOI: 10.1080/05704928.2021.2018596

EN, 1993. EN 481. Workplace Atmospheres. Size Fraction Definitions for Measurement of Airborne Particles, 14 pp.

Eschenbacher W. L., Kreiss K., Lougheed M.D., Pransky G.S., Day B., Castellan R.M., Nylon flock–associated interstitial lung disease, Am. j. of respir. and crit. care med. 159, 6, 2003-2008 (1999)

Fan W., Salmond J.A., Dirks K.N., Sanz P.C., Miskelly G.M., Rindelaub J.D., Evidence and Mass Quantification of Atmospheric Microplastics in a Coastal New Zealand City, Environ. Sci. Technol., 56, 24, 17556–17568 (2022), https://doi.org/10.1021/acs.est.2c05850

Feng J., Li Z., Olah A., Baer E., High oxygen barrier multilayer EVOH/LDPE film/foam, J. of Appl. Polym. Sci., 135, 46425 (2018), https://doi.org/10.1002/app.46425

Field D.T., Green J.L., Bennett R., Jenner L.C., Sadofsky L.R., Chapman E., Loubani M., Rotchell J.M., Microplastics in the surgical environment, Environ. Int., 170, 107630 (2022), ISSN 0160-4120, https://doi.org/10.1016/j.envint.2022.107630

Gasperi J., Wright S.L., Dris R., Collard F., Mandin C., Guerrouache M., Langlois V., Kelly F.J., Tassin B., Microplastics in air: Are we breathing it in?, Curr. Opin. in Environ. Sci. & Health, 1, 1-5 (2018), ISSN 2468-5844, https://doi.org/10.1016/j.coesh.2017.10.002

Gigault J., Halle A., Baudrimont M., Pascal P., Gauffre F., Phi T., Hadri H.E., Grassl B., Reynaud S., Current opinion: What is a nanoplastic?, Environ. Pollut., 235, 1030-1034 (2018), ISSN 0269-7491, https://doi.org/10.1016/j.envpol.2018.01.024

Habibi N., Uddin S., Fowler S.W., Behbehani M., Microplastics in the atmosphere: a review, Environ. Expo. Assess. 1, 6 (2022), 10.20517/jeea.2021.07

Hussein T., Indoor-to-outdoor relationship of aerosol particles inside a naturally ventilated apartment – A comparison between single-parameter analysis and indoor aerosol model simulation, Sci. of The Total Environ., 596–597, 321-330 (2017), ISSN 0048-9697, https://doi.org/10.1016/j.scitotenv.2017.04.045

Isaxon C., Gudmundsson A., Nordin E.Z., Lönnblad L., Dahl A., Wieslander G., Bohgard M., Wierzbicka A., Contribution of indoor-generated particles to residential exposure, Atmos. Environ., 106, 458-466 (2015), ISSN 1352-2310, https://doi.org/10.1016/j.atmosenv.2014.07.053

Jenner L.C., Sadofsky L.R., Danopoulos E., Rotchell J.M., Household indoor microplastics within the Humber region (United Kingdom): Quantification and chemical characterisation of particles present, Atmos. Environ., 259, 118512 (2021), ISSN 1352-2310, https://doi.org/10.1016/j.atmosenv.2021.118512

Kacprzak S., Tijing L.D., Microplastics in indoor environment: Sources, mitigation and fate, J. of Environ. Chem. Eng., 10, 2, 107359 (2022), ISSN 2213-3437, https://doi.org/10.1016/j.jece.2022.107359

Karbalaei S., Hanachi P., Walker T.R., Cole M., Occurrence, sources, human health impacts and mitigation of microplastic pollution, Environ. Sci. Pollut. Res. 25, 36046–36063 (2018), https://doi.org/10.1007/s11356-018-3508-7

Kirstein I.V., Kirmizi S., Wichels A., Garin-Fernandez A., Erler R., Löder M., Gerdts G., Dangerous hitchhikers? Evidence for potentially pathogenic Vibrio spp. on microplastic particles, Mar. Environ. Res., 120, 1-8 (2016), ISSN 0141-1136, https://doi.org/10.1016/j.marenvres.2016.07.004

Kärkkäinen N., Sillanpää M., Quantification of different microplastic fibres discharged from textiles in machine wash and tumble drying. Environ. Sci. Pollut. Res. 28, 16253–16263 (2021), https://doi.org/10.1007/s11356-020-11988-2

Law R.C., Applications of cellulose acetate, Macromol. Symp., 208, 1, 255 – 265 (2004), DOI: 10.1002/masy.200450410

Liu S., Koupriyanov M., Paskaruk D., Fediuk G., Chen Q., Investigation of airborne particle exposure in an office with mixing and displacement ventilation, Sustain. Cities and Soc., 79, 103718 (2022), ISSN 2210-6707, https://doi.org/10.1016/j.scs.2022.103718

Liu X., Zeng X., Dong G., Venier M., Xie O., Yang M., Wu O., Zhao F., Chen D., Plastic Additives in Ambient Fine Particulate Matter in the Pearl River Delta, China: High-Throughput Characterization and Health Implications, Environ. Sci. Technol., 55, 8, 4474–4482 (2021), https://doi.org/10.1021/acs.est.0c08578

Long X., Fu T., Yang X., Tang Y., Zheng Y., Zhu L.,1, Shen H., Ye J., Wang C., Wang T., Li B., Efficient atmospheric transport of microplastics over Asia and adjacent ocean, Environ. Sci. Technol., 56, 10, 6243–6252 (2022), https://doi.org/10.1021/acs.est.1c07825

Mamedov S., Characterization of TiO2 Nanopowders by Raman Spectroscopy, Spectrosc., 35, 2, 41 – 49 (2020)

Memarzadeh F., Jiang Z. Effect of operation room geometry and ventilation system parameter variations on the protection of the surgical site, Proceeding of IAQ, 2004

Miller A., Teirstein A.S., Chuang M., Selikoff I.J., Warshaw R., Changes in pulmonary function in workers exposed to vinyl chloride and polyvinyl chloride, Ann. of the New York Acad. of Sci., 246, 42-52 (1975)

Munno K., De Frond H., O'Donnell B., Rochman C.M., Increasing the Accessibility for Characterizing Microplastics: Introducing New Application-Based and Spectral Libraries of Plastic Particles (SLoPP and SLoPP-E), Anal. Chem., 92, 3, 2443–2451 (2020), https://doi.org/10.1021/acs.analchem.9b03626

Mølgaard B., Viitanen A.-K., Kangas A., Huhtiniemi M., Larsen S.T., Vanhala, E., Hussein T., Boor B.E., Hämeri K., Koivisto, A.J., Exposure to Airborne Particles and Volatile Organic Compounds from Polyurethane Molding, Spray Painting, Lacquering, and Gluing in a Workshop, Int. J. Environ. Res. Public Health, 12, 3756-3773 (2015), https://doi.org/10.3390/ijerph120403756

Pauly J.L., Stegmeier S.J., Allaart H.A., Cheney R.T., Zhang P.J., Mayer A.G., Streck R.J., Inhaled cellulosic and plastic fibers found in human lung tissue, Cancer Epidemiol. Biomarkers Prev., 7, 5, 419–428 (1997)

a. Periyasamy A.P., Viková M., Vik M., Preparation of photochromic isotactic polypropylene filaments: influence of drawing ratio on their optical, thermal and mechanical properties, Text. Res. J. 90, 19–20, 2136–2148 (2020), DOI: 10.1177/0040517520912037

b. Periyasamy A.P., Tehrani-Bagha A., A review on microplastic emission from textile materials and its reduction techniques, Poly. Degrad. Stab. 199, 109901 (2022), ISSN 0141-3910, https://doi.org/10.1016/j.polymdegradstab.2022.109901

Perera K., Ziajahromi S., Nash S.B., Manage P.M., Leusch F.D.L., Airborne Microplastics in Indoor and Outdoor Environments of a Developing Country in South Asia: Abundance, Distribution, Morphology, and Possible Sources, Environ. Sci. Technol. 56, 23, 16676–16685 (2022), https://doi.org/10.1021/acs.est.2c05885

Pimentel J.C., Avila R., Lourenço A.G., Respiratory disease caused by synthetic fibres: a new occupational disease, Thorax, 30, 204-219 (1975)

a. Prata J.C., Airborne microplastics: Consequences to human health?, Environ. Pollut., 234, 115-126 (2018), ISSN 0269-7491, https://doi.org/10.1016/j.envpol.2017.11.043

b. Prata J.C., Castro J.L., da Costa J.P., Cerqueira M., Duarte A.C., Rocha-Santos T., Airborne Microplastics, Handbook of Microplastics in the Environment. Springer, Cham (2021), https://doi.org/10.1007/978-3-030-10618-8_37-2

Primpke S., Cross R.K., Mintenig S.M., Simon M., Vianello A., Gerdts G., Vollertsen J., Toward the Systematic Identification of Microplastics in the Environment: Evaluation of a New Independent Software Tool (siMPle) for Spectroscopic Analysis, Appl. Spectrosc., 74, 9, 1127-1138 (2020), doi:10.1177/0003702820917760

Rahman A., Sarkar A., Yadav O.P., Achari G., Slobodnik J., Potential human health risks due to environmental exposure to nano- and microplastics and knowledge gaps: A scoping review, Sci. of The Tot. Environ., 757, 143872 (2021), ISSN 0048-9697, https://doi.org/10.1016/j.scitotenv.2020.143872

Rahman L., Mallach G., Kulka R., Halappanavar S., Microplastics and nanoplastics science: collecting and characterizing airborne microplastics in fine particulate matter, Nanotoxicol., 15, 9, 1253-1278 (2021), DOI: 10.1080/17435390.2021.2018065

Ramsperger A. F. R. M., Narayana V. K. B., Gross W., Mohanraj J., Thelakkat M., Greiner A., Schmalz H., Kress H., Laforsch C., Environmental exposure enhances the internalisation of microplastic particles into cells, Science Adv., 6, 50 (2020), DOI: 10.1126/sciadv.abd1211

Revell L.E., Kuma P., Le Ru E.C., Somerville W.R.C., Gaw S., Direct radiative effects of airborne microplastics, Nature, 598, 462–467 (2021), https://doi.org/10.1038/s41586-021-03864-x

Rinaudo C., Croce A., Musa M., Fornero E., Allegrina M., Trivero P., Bellis D., Sferch D., Toffalorio F., Veronesi G., Pelosi G., Study of Inorganic Particles, Fibers, and Asbestos Bodies by Variable Pressure Scanning Electron Microscopy with Annexed Energy Dispersive Spectroscopy and Micro-Raman Spectroscopy in Thin Sections of Lung and Pleural Plaque, Appl. Spectrosc., 64, 6, 571-577 (2010), doi:10.1366/000370210791414380

Rochman C.M., Brookson C., Bikker J., Djuric N., Earn A., Bucci K., Athey S., Huntington A., McIlwraith H., Munno K., De Frond H., Kolomijeca A., Erdle L., Grbic J., Bayoumi M., Borrelle S.B., Wu T., Santoro S., Werbowski L.M., Zhu X., Giles R.K., Hamilton B.M., Thaysen C., Kaura A., Klasios N., Ead L., Kim J., Sherlock C., Ho A., Hung, C., Rethinking microplastics as a diverse contaminant suite, Environ. Toxicol. Chem., 38, 703-711 (2019), https://doi.org/10.1002/etc.4371

Ryan P.G., Moloney C.L., Plastic and other artefacts on South African beaches: temporal trends in abundance and composition, South African J. of Science, 86, 450-452 (1990)

Sarigiannis D.A., Gotti A., Karakitsios S.P., Chapter 1 - Indoor Air and Public Health, Management of Emerging Public Health Issues and Risks, Academic Press, 3-29 (2019), ISBN 9780128132906, https://doi.org/10.1016/B978-0-12-813290-6.00001-9

Schmid O., Stoeger T., Surface area is the biologically most effective dose metric for acute nanoparticle toxicity in the lung, J. of Aerosol Sci., 99, 133-143 (2016), ISSN 0021-8502, https://doi.org/10.1016/j.jaerosci.2015.12.006

Schymanski D., Oßmann B.E., Benismail N., Boukerma K., Dallmann G., von der Esch E., Fischer D., Fischer F., Gilliland D., Glas K., Hofmann T., Käppler A., Lacorte S., Marco J., Rakwe EL M., Weisser J., Witzig C., Zambülte N., Ivleva N.P., Analysis of microplastics in drinking water and other clean water samples with micro-Raman and micro-infrared spectroscopy: minimum requirements and best practice guidelines, Anal. Bioanal. Chem. 413, 5969 – 5994 (2021), https://doi.org/10.1007/s00216-021-03498-y

Shao L., Li Y., Jones T., Santosh M., Liu P., Zhang M., Xu L., Li W., Lu J., Yang C., Zhang D., Feng X., BéruBé K., Airborne microplastics: A review of current perspectives and environmental implications, J. of Clean. Prod., 347, 131048 (2022), ISSN 0959-6526, https://doi.org/10.1016/j.jclepro.2022.131048

Silva T., Pokhrel L.R., Dubey B., Tolaymat T.M., Maier K.J., Liu X., Particle size, surface charge and concentration dependent ecotoxicity of three organo-coated silver nanoparticles: Comparison between general linear model-predicted and observed toxicity, Sci. of The Total Environ., 468–469, 968-976 (2014), ISSN 0048-9697, https://doi.org/10.1016/j.scitotenv.2013.09.006

Stabile L., Buonanno G., Frattolillo A., Dell'Isola M., The effect of the ventilation retrofit in a school on CO2, airborne particles, and energy consumptions, Build. and Environ., 156, 1-11 (2019), ISSN 0360-1323, https://doi.org/10.1016/j.buildenv.2019.04.001

Stifelman M., Using doubly-labeled water measurements of human energy expenditure to estimate inhalation rates, Sci. of The Tot. Environ. 373, 2–3, 585-590 (2007), ISSN 0048-9697, https://doi.org/10.1016/j.scitotenv.2006.11.041

Studnicka M. J., Menzinger G., Drlicek M., Maruna H., Neumann M.G., Pneumoconiosis and systemic sclerosis following 10 years of exposure to polyvinyl chloride dust, Thorax, 50, 5, 583-589 (1995)

Soltani N.S., Taylor M.P., Wilson S.P., Quantification and exposure assessment of microplastics in Australian indoor house dust, Environ. Pollut., 283, 117064 (2021), ISSN 0269-7491, https://doi.org/10.1016/j.envpol.2021.117064

Song Y.K., Hong S. H., Jang M., Han G. M., Rani M., Lee J., Shim W.J., A Comparison of Microscopic and Spectroscopic Identification Methods for Analysis of Microplastics in Environmental Samples, Mar. Pollut. Bull., 93, 202– 209 (2015), DOI: 10.1016/j.marpolbul.2015.01.015

Soutar C.A., Copland L.H., Thornley P.E., Hurley J.F., Ottery J., Adams W.G., Bennett B., Epidemiological study of respiratory disease in workers exposed to polyvinylchloride dust, Thorax, 35, 644-652 (1980)

Tcharkhtchi A., Abbasnezhad N., Zarbini Seydani M., Farzaneh Z.S., Shirinbayan M., An overview of filtration efficiency through the masks: Mechanisms of the aerosols penetration, Bioact. Mater., 6, 1, 106-122 (2021), ISSN 2452-199X, https://doi.org/10.1016/j.bioactmat.2020.08.002

Torres-Agullo A., Karanasiou A., Moreno T., Lacorte S., Airborne microplastic particle concentrations and characterization in indoor urban microenvironments, Environ. Pollut., 308, 119707 (2022), ISSN 0269-7491, https://doi.org/10.1016/j.envpol.2022.119707

Uddin S., Fowler S.W., Habibi N., Sajid S., Dupont S., Behbehani M., A Preliminary Assessment of Size-Fractionated Microplastics in Indoor Aerosol—Kuwait's Baseline, Toxics, 10, 71 (2022), https://doi.org/10.3390/toxics10020071

U.S. Environmental Protection Agency. Flame Retardants Used in Flexible Polyurethane Foam: An Alternatives Assessment Update, U.S. EPA Des. Environ. EPA 744-R-, 1–441, EPA 742-R-05-002A (2015), https://doi.org/10.1002/ejoc.201200111

Vethaak A.D., Legler J., Microplastics and human health, Sci., 371, 6530, 672-674 (2021), DOI: 10.1126/science.abe5041

Vianello A., Jensen R.L., Liu L., Vollertsen J., Simulating human exposure to indoor airborne microplastics using a Breathing Thermal Manikin, Sci. Rep., 9, 8670 (2019), https://doi.org/10.1038/s41598-019-45054-w

Wang J., Tan Z., Peng J., Qiu Q., Li M., The behaviors of microplastics in the marine environment, Mar. Environ. Res., 113, 7-17 (2016), ISSN 0141-1136, https://doi.org/10.1016/j.marenvres.2015.10.014

Wang T., Rovira J., Sierra J., Blanco J., Chen S., Mai B., Schuhmacher M., Domingo J., Characterization of airborne particles and cytotoxicity to a human lung cancer cell line in Guangzhou, China, Environ. Res., 196, 110953 (2021), ISSN 0013-9351, https://doi.org/10.1016/j.envres.2021.110953

Wang X., Wei N., Liu K., Zhu L., Li C., Zong C., Li D., Exponential decrease of airborne microplastics: From megacity to open ocean, Sci. of The Total Environ., 849, 157702 (2022), ISSN 0048-9697, https://doi.org/10.1016/j.scitotenv.2022.157702

Warheit D.B., Hart G.A., Hesterberg T.W., Collins J.J., Dyer W.M., Swaen G.M.H., Castranova V., Soiefer A.I., Kennedy G.L. Jr., Potential Pulmonary Effects of Man-Made OrganicFiber (MMOF) Dusts, Crit. Rev. in Toxicol., 31, 6, 697–736 (2001), https://doi.org/10.1080/20014091111965

WHO global air quality guidelines. Particulate matter (PM 2.5 and PM 10), ozone, nitrogen dioxide, sulfur dioxide and carbon monoxide. Geneva: World Health Organization; 2021. Licence: CC BY-NC-SA 3.0 IGO

Wieland S., Balmes A., Bender J., Kitzinger J., Meyer F., Ramsperger A.F.R.M., Roeder F., Tengelmann C., Wimmer B.H., Laforsch C., Kress H., From properties to toxicity: Comparing microplastics to other airborne microparticles, J. of Hazard. Mater., 428, 128151 (2022), ISSN 0304-3894, https://doi.org/10.1016/j.jhazmat.2021.128151

Wright S.L., Levermore J.M., Kelly F.J., Raman Spectral Imaging for the Detection of Inhalable Microplastics in Ambient Particulate Matter Samples, Environ. Sci. Technol., 53, 15, 8947–8956 (2019), https://doi.org/10.1021/acs.est.8b06663

Wu P., Lin S., Cao G., Wu J., Jin H., Wang C., Wong M.H., Yang Z., Cai Z., Absorption, distribution, metabolism, excretion and toxicity of microplastics in the human body and health implications, J. of Hazard. Mater., 437, 129361 (2022), ISSN 0304-3894, https://doi.org/10.1016/j.jhazmat.2022.129361

Xie Y., Li Y., Feng Y., Cheng W., Wang Y., Inhalable microplastics prevails in air: Exploring the size detection limit, Environ. Internatl., 162, 107151 (2022), ISSN 0160-4120, https://doi.org/10.1016/j.envint.2022.107151

Xumiao L., Prata J.C., Alves J.R., Duarte A.C., Rocha-Santos T., Cerqueira M., Airborne microplastics and fibers in indoor residential environments in Aveiro, Portugal, Environ. Adv. 6, 100134 (2021), ISSN 2666-7657, https://doi.org/10.1016/j.envadv.2021.100134

Yao Y., Glamoclija M., Murphy A., Gao Y., Characterization of microplastics in indoor and ambient air in northern New Jersey, Environ. Res., 207, 112142 (2022), ISSN 0013-9351, https://doi.org/10.1016/j.envres.2021.112142

Zhai X., Zheng H., Xu Y., Zhao R., Wang W., Guo H., Characterization and quantification of microplastics in indoor environments, Heliyon, 9, 5, e15901 (2023), ISSN 2405-8440, https://doi.org/10.1016/j.heliyon.2023.e15901

Zhao X., Zhou Y., Liang C., Song J., Yu S., Liao G., Zou P., Tang K.H.D., Wu C., Airborne microplastics: Occurrence, sources, fate, risks and mitigation, Sci. of The Total Environ., 858, 2, 159943 (2023), ISSN 0048-9697, https://doi.org/10.1016/j.scitotenv.2022.159943

a. Zhang Q., Xu E.G., Li J., Chen Q., Ma L., Zeng E.Y., Shi H., A Review of Microplastics in Table Salt, Drinking Water, and Air: Direct Human Exposure, Environ. Sci. Technol., 54, 7, 3740–3751 (2020), https://doi.org/10.1021/acs.est.9b04535

b. Zhang Q., Zhao Y., Du F., Cai H., Wang G., Shi H., Microplastic Fallout in Different Indoor Environments, Environ. Sci. Technol. 2020, 54, 11, 6530–6539 (2020), https://doi.org/10.1021/acs.est.0c00087

Zia M.K., Bhatti H.N., Bhatti J.A., Methods for polyurethane and polyurethane composites, recycling and recovery: A review, React. and Funct. Polym., 67, 8, Pages 675-692 (2007), ISSN 1381-5148, https://doi.org/10.1016/j.reactfunctpolym.2007.05.004

ISSN (online): 2446-1636
ISBN (online): 978-87-7573-623-2

AALBORG UNIVERSITY PRESS